Program and Abstracts

INTERNATIONAL CONFERENCE ON

HYDROGEN EFFECTS ON MATERIAL BEHAVIOR and CORROSION DEFORMATION INTERACTIONS

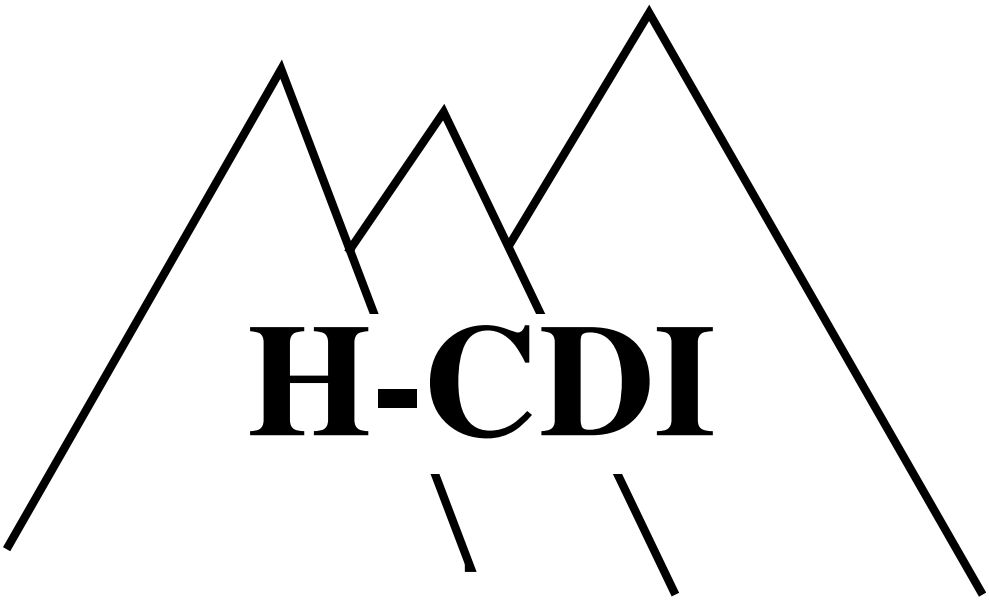

Jackson Lake Lodge, Moran, WY
September 22-26, 2002

International Conference On

HYDROGEN EFFECTS ON MATERIAL BEHAVIOR
and
CORROSION DEFORMATION INTERACTIONS

Jackson Lake Lodge
Moran, Wyoming USA
September 22-26, 2002

Sponsored by

Joint TMS/ASM Environmental Effects Committee, Structural Materials Division, TMS
Environment Sensitive Fracture Working Group, European Federation of Corrosion
National Institute of Standards and Technology
Sandia National Laboratories

Endorsed by

Materials Research Society

Program Committee

Russell Jones, Pacific Northwest National Laboratory
Neville Moody, Sandia National Laboratories
Anthony Thompson, Lawrence Berkeley Laboratory
Thierry Magnin, Ecole des Mines de St. Etienne
Richard Ricker, National Institute of Standards and Technology
Gary Was, University of Michigan

Support Provided by

National Institute of Standards and Technology
Sandia National Laboratories
Structural Materials Division, TMS

Conference Chairs

Neville Moody	Anthony Thompson	Richard Ricker	Gary Was	Thierry Magnin
Sandia National Laboratories	University of California	NIST	University of Michigan	Ecole des Mines de St. Etienne
Livermore, CA 94551-0969	Berkeley, CA 94720	Gaithersburg, MD 20899	Ann Arbor, MI 48109	42023 Saint Etienne France
nrmoody@sandia.gov	awthompson@lbl.gov	richard.ricker@nist.gov	gsw@umich.edu	magnin@emse.fr

CONFERENCE HIGHLIGHTS

Sunday Afternoon, September 22, 2002
1:00 pm Registration Desk Opens

Sunday Evening, September 22, 2002
7:30 pm-10:30 pm Evening Session

Monday Morning, September 23, 2002
8:30 am-12:30 pm Morning Session
One hour break for Poster Session I
9:00 am-10:00 am Accompanying Family and Guests-Morning Coffee

Monday Evening, September 23, 2002
5:00 pm-6:00 pm Welcome Reception
7:30 pm-10:30 pm Evening Session

Tuesday Morning, September 24, 2002
8:30 am-12:30 pm Morning Session

Tuesday Afternoon, September 24, 2002
1:30 pm-5:00 pm Afternoon Session

Tuesday Evening September 24, 2002
6:30 pm-9:00 pm Conference Dinner

Wednesday Morning, September 25, 2002
8:30 am-12:30 pm Morning Session
One hour break for Poster Session II

Wednesday Evening, September 25, 2002
7:30 pm-10:30 pm Evening Session

Thursday Morning, September 26, 2002
8:30 am-12:30 pm Morning Session
One hour break for Poster Session III

Thursday Evening, September 26, 2002
7:30 pm-10:30 pm Evening Session

Conference Program

Sunday Evening
Introduction

7:30 pm-10:30 pm
Session Chairs: N.R. Moody, Sandia National Laboratories, Livermore, CA, USA
A.W. Thompson, Lawrence Berkeley Laboratory, Berkeley, CA, USA

Reflections on Hydrogen Conferences
A.W. Thompson (USA) (Welcome Address)
Mechanisms of Hydrogen Assisted Cracking-A Review
S.P. Lynch (Australia) (Invited)
Hydrogen Assisted Cracking of Quenched and Tempered 4135 Steel in an Hydroxide Solution
É. Verniquet, R. Roberge, S. Lalonde, J.I. Dickson (Canada)
Vacancy Generation in Electrochemical Oxidation of Copper in $NaNO_2$ Solutions and its Role in TGSCC Mechanisms
P. Aaltonen, Y. Yagodzinskyy, O. Tarasenko, H. Hanninen (Finland)
Advanced Materials for hydrogen Storage
G. Thomas (USA)
A Mechanism of the Hydrogen Embrittlement of Cr-Ni Austenitic Steels and Alloys at High Pressures and Temperatures
Yu I. Archakov (Russia)

Monday Morning
Hydrogen Effects on Material Behavior

8:30 am-12:30 pm
Session Chairs: P. Sofronis, University of Illinois, Urbana, IL USA
S.L. Robinson, Sandia National Laboratories, Livermore, CA, USA

Hydrogen Interactions with 2.25Cr and 9Cr Steels
H. Hänninen, Y. Yagodzinskyy, O. Tarasenko, P. Castello J.-P. Schosger (Finland) (Invited)
Probing Hydrogen - Deformation Interactions Using Nanoindentation
D.F. Bahr, K.R. Morasch, C.L. Woodcock, D.P. Field (USA)
Effects of Hydrogen on Slip Character in a Precipitation-Strengthened Alloy
A.W. Thompson, D.C. Nguyen (USA)
Examination of Deformation Microstructures in Hydrogen Embrittled Commercial Alloys
D.S. Gelles, R. Bajaj (USA)

Break for Poster Session I

Effects of Hydrogen Isotopes on the Fracture Toughness Properties of Austenitic Stainless Steel Weldments
M.J. Morgan, S.L. West, M.H. Tosten, G.K. Chapman (USA) (Invited)
Tritium Decay, Irradiation and Hydrogen/Helium Effects on Austenitic Stainless Steels
M.R. Louthan, Jr. (USA)
Effect of Environmental Hydrogen on Tensile Properties of Inconel 690
X.-H. Luo, M. Habashi (China)

Monday Evening
Permeation, Segregation, and Fracture

7:30 pm-10:30 pm
Session Chairs: M. I. Baskes, Los Alamos, National Laboratory, Los Alamos, NM, USA
R. Schwarz, Los Alamos, National Laboratory, Los Alamos, NM, USA

Hydrogen Segregation at Dislocations, Grain- and Phase-Boundaries
R. Kirchheim (Germany) (Invited)
Hydrogen Diffusion and Trapping in Low Alloy High Strength Steels
A.M. Brass (France) (Invited)
Local Hydrogen Uptake in Stationary and Propagating-Real and Model Crack Tips
J.R. Scully, D.G Kolman, G.A. Young, Jr., L.M. Young, R.P. Gangloff (USA) (Invited)
Analyses for the Rate Constants of the Hydrogen Absorption/Evolution Reactions for Both Langmuir and Frumkin Conditions
H.W. Pickering, F. M. Al-Faqeer (USA)

Break

Role of Hydrogen in Stress Corrosion Cracking of Low Strength Al-Mg
R.H. Jones, M.J. Danielson (USA) (Invited)
Hydrogen Effects on Grain Boundary Fracture During SCC in Al-5Mg: Critical Experiments and Atomistic Computer Simulations
D. Tanguy, B. Bayle, T. Magnin (France)
Irreversible Hydrogen Trapping in High-Strength Alloys
B. Pound (USA)

Tuesday Morning
Hydrogen Induced Cracking

8:30 am-12:30 pm
Session Chairs: J.R. Scully, University of Virginia, Charlottesville, VA, USA
D. Eliezer, Ben Gurion University of the Negev, Israel

Hydrogen Embrittlement: Plasticity vs Decohesion Mechanisms
I.M. Robertson (USA) (Invited)
Functions of Microstructures in Delayed Fracture of Martensitic Steels
M. Nagumo, T. Tamaoki, T. Sugawara (Japan)
Structures and Their Effects on Deformation, Fracture and Fatigue-Behavior of Zr-Ti-Ni-Cu-Be Bulk Metallic Glass Alloys
D. Suh, R.H. Dauskardt (USA)
Analysis of Hydrogen Related to Embrittlement of an Al-Zn-Mg-Cu Alloy
J. Okahana, S. Kuramoto, M. Kanno (Japan)

Break

A Perspective on Corrosion and Corrosion Fatigue
R.P. Wei (USA) (Invited)

The Sour Gas Susceptibility of Steels for Oil and Gas Transport
J.L. Albarran, S. Serna, G. Gonzalez, L. Martinez (Mexico)
Diffusion Coefficients and Hydrogen Assisted Crack Growth
M. Pfuff, G.G. Juilfs, W. Dietzel (Germany)
Hydrogen Induced Intergranular Stress Corrosion Cracking in Nickel Based Alloys 600 and 690 Under High Temperature Water/Steam
H.F. Lopez, A. Mehboob, J.L. Albarran, L. Martinez (USA)
Interactions Between Previous Cyclic Deformation and Stress Corrosion Cracking in Cold Drawn Steel
J. Toribio, V. Kharin, E. Ovejero (Spain)

Tuesday Afternoon
Stress Corrosion Cracking

1:30 pm-5:00 pm
Session Chairs: R.P. Gangloff, University of Virginia, Charlottesville, VA, USA
R.H. Jones, Pacific Northwest National Laboratory, Richland, WA,USA

Overview of Corrosion Deformation Interactions During Stress Corrosion Cracking and Fatigue Cracking
T. Magnin, D. Delafosse, B. Bayle, C. Bosch (France) (Keynote)
The Increment of Hydrogen-Induced Corrosion Fatigue Crack Growth per Cycle: Comparing Theory and Experimental Data
S.A. Shipilov (Canada)
A Comparison of Short Fatigue Crack Growth (SFCG) Rates in a Medium Strength Steel Under In-Air and Corrosion Fatigue Loading Conditions
H. Hu, R. Akid (United Kingdom)

Break

IGSCC Behavior of CSL-Related and High Angle Boundaries in Ni-16Cr-9Fe-xC Alloys
B. Alexandreanu, G.S. Was (USA)
Developments in Stress Corrosion of Solid-Solution Alloys
R.C. Newman, J. Deakin, B. Lynch (UK) (Invited)
Modeling the Influence of Crack Path Deviations on the Propagation of Stress Corrosion Cracks
R.E. Ricker (USA)

Wednesday Morning
Hydrogen Interactions

8:30 am-12:30 pm
Session Chairs: R. Kirchhiem, Universitat, Gottingen, Gottingen, Germany
J.A. Brooks, Sandia national Laboratories, Livermore, CA, USA

Thermodynamics of Two-Phase Systems with Coherent Interfaces: Application to Metal-Hydrogen Systems
R.B. Schwarz, A.G. Khachaturyan (USA) (Invited)
Structure Dependence of Hydrogen Effects at Grain Boundaries in an FCC Solid
M.I. Baskes, R.G. Hoagland (USA) (Invited)

The Vibrational, Elastic, and Electronic Contributions to the Chemical Potentials of Hydrogen Isotopes in Palladium
W.G. Wolfer, B. Meyer (USA)
Elastic Properties of Pd-Protium, Pd-Deuterium, and Pd-Tritium Single Crystals
H. Bach, R.B. Schwarz, D. Tuggle (USA)

Break for Poster Session II

Numerical Study of Microstructural Evolution in Low Alloy Cr-Mo Steels During Hydrogen Attack
S.M. Schlogl, E. van der Giessen (The Netherlands)
Migration and Trapping of Hydrogen in Martensitic Steels-Effect of Irradiation and Helium Implantation
P. Jung, Z. Yao, C. Liu (Germany)
Hydrogen Effects on Multi-Vacancy Formation in Alpha-Fe
Y. Tateyama, T. Ohno (Japan)

Wednesday Evening
Hydrides and hydrogen Processing

7:30 pm-10:30 pm
Session Chairs: W.W. Gerberich, University of Minnesota, Minneapolis, MN, USA
B. C. Odegard, Sandia National Laboratories, Livermore, CA, USA

The Effect of Applied Stress on the Accommodation Energy and the Solvi for the Formation and Dissolution of Zirconium Hydride
M.P. Puls, B.W. Leitch, S.-Q. Shi (Canada) (Invited)
Influence of a Hydrided Layer on Fracture of Zircaloy-4 Cladding
R.S. Daum, D.W. Bates, D. A. Koss, A.T. Motta (USA)
Uranium Hydride Nucleation Kinetics: Effects Of Oxide Thickness And Vacuum Outgassing
D.F. Teter, R.J. Hanrahan, Jr., C.J. Wetteland (USA)

Break

Crack Initiation by Delayed Hydride Cracking at Sharp Notches in Zr-2.5 Nb Alloys
S. Sagat, G.W. Newman, D.A. Scarth (Canada)
Hydrogen-Assisted Materials Processing
D. Eliezer, N. Eliaz, D. Zander, D.L. Olson (Israel) (Invited)
Beneficial Effects of Hydrogen as a Temporary Alloying Element in Titanium Alloys: An Overview
F.H. Froes, D. Eliezer, O.N. Senkov, J.J. Qazi (USA) (Invited)

Thursday Morning
Fundamental Effects of Hydrogen in Materials

8:30 am-12:30 pm
Session Chairs: M.R. Louthan, Westinghouse Savannah River Company, Aiken, SC, USA
M. Puls, Atomic Energy of Canada, Mississauga, Ontario, Canada
Crack Tip Hydrogen Damage in High Performance Alloys
R.P. Gangloff, J.R. Scully (USA) (Invited)

Hydrogen-Induced Changes of the Mechanical Properties of Beta-Titanium Alloys—Instrinsic and Extrinsic Effects
H.-J. Christ, K. Prüßner, A. Senemmar, M. Decker (Germany)
Hydrogen Influence on Plastic Deformation of Stable 18Cr-16Ni 10Mn Austenitic Stainless Steel Single Crystals
Y. Yagodzinskyy, O. Tarasenko, H. Hanninen (Finland)
SSRT and Modelling of Hydrogen Assitsed Crack Growth in Super Martensitic Stainless Steels
T. Boellinghaus (Germany)

Break for Poster Session III

Some Recent Advances at Illinois in Hydrogen Induced Shear Localization and Decohesion
P. Sofronis, I.M. Robertson, Y. Liang, D.F. Teter, N. Aravas (USA) (Invited)
Hydrogen Effects on Mechanical Responses of Small Volumes
W.W. Gerberich, N.I. Tymiak, J. Jungk, T. Wyrobek (USA) (Invited)
Dueterium-Induced Interfacial Fracture of Beryllium Films
N.R. Moody, R.A. Causey, D.F. Bahr, K.L. Wilson, W.W. Gerberich (USA)

Thursday Evening
High Temperature Stress Corrosion Cracking

7:30 pm-10:30 pm
Session Chairs: R.E. Ricker, NIST, Gaithersburg, MD, USA
G. Was, University of Michigan, Ann Arbor, MI, USA

Interactions of Hydrogen with Moving Dislocations in Nickel and Nickel Base Alloys-Consequences on the Intergranular Rupture
J. Chêne, A.M. Brass (France) (Invited)
The Effect of Hydrogen on Creep in High Purity Ni-16Cr-9Fe Alloys at 360˚C
D.J. Paraventi, T.M. Angelius, G.S. Was (USA)
Constituitive Deformation Model for Analysis of Stress Corrosion Crack Tip Strain Rates in Ni-Cr-Fe Alloy 600
M.M. Hall, Jr., D.M., Symons (USA)

Break

Some Uses of Slow Strain Rate Testing Under Applied Potential Control in Studying SCC of Materials Used in Nuclear Power Plant
J. Congleton, E.A. Charles (United Kingdom) (Invited)
Hydrogen Dislocation Interactions During Cyclic Plastic Deformation and Static Strain Ageing Tests in Single Crystals and Polycristals of Ni and Its Alloys
C. Bosch, G. Girardin, D. Delafosse, T. Magnin (France)
Oxidation Induced Intergranular Cracking in Nickel Base Alloys in the Temperature Range 400˚C to 600˚C
L. Fournier, B. Capell, T. Magnin, G.S. Was (USA)

Poster Presentations

Poster Session I (Monday)

The Protective Effect of Glassy and Glass Ceramic Coatings in the Processes of the Hydrogen-Steel Interactions at High Temperatures-High Pressures
I. Yu. Artchakov, B.Z. Pevzner, V.G. Konakov, T.D. Alyferenko (Russia)

Effect of the Density of States on the Stacking Fault Energy and Hydrogen Embrittlement of Transition Metals and Alloys
J.A. Lee (USA)

Hydrogen Embrittlement and Mossbauer Effects
J. Vosta, P. Sajdl, O. Schneeweiss, R. Novotny (Czech Republic)

The Effects of Neutron Damage on the Migration Parameters of Hydrogen Isotopes in CVD Silicon Carbide
R.A. Causey, L.L. Snead, T.J. Venhaus, W.R. Wampler (USA)

The Influence of Hydrogen on the Dislocation Velocity in Ni_3Al Single Crystals
C. B. Jiang, H. Li, S. D. Wu, S. Patu (China)

Multi Layer Blister Formation in Structural Materials Due to Hydrogen and Helium Implantation
D. Moreno, D. Eliezer (Israel)

Modeling of Hydrogen Diffusion in Amorphous Alloys
N. Eliaz, D. Fuks, D. Eliezer (Israel)

Visualization of Hydrogen Desorption Process from Ferrite, Pearlite and Graphite by Secondary Ion Mass Spectrometry
K. Takai, Y. Chiba, A. Nozue (Japan)

The Influence of Plastic Strain on the Hydrogen Diffusion in an HSLA Steel
G.G. Juilfs, W. Dietzel, M. Pfuff (Germany)

Quantitative Visualization of Hydrogen Evolved from Steels by Hydrogen Microprint Technique
K. Ichitani, S. Kuramoto, M. Kanno (Japan)

Irreversible Hydrogen Traps in High Strength Steel Weld Metal
C. Lensing, I. Maroef, D.L. Olson (USA)

The Mechanical Instability of Amorphous Metal Alloys Appearing under Hydrogenation
N.E. Skryabina, L.V. Spivak, A.S. Petrov (Russia)

Environmental Factors on Embrittlement of Vitreous Silica Fibers
K. Takai, D. Yamada, A. Nozue (Japan)

Mechanical Stresses and Strains Developing in Thin Y-Films Due to H-Absorption
M. Dornheim, A. Pundt, R. Kirchheim (Germany)

Monitoring of the Distribution and Desorption of Residual Tritium From Radioactive Waste After Detritiation
A.M. Brass, J. Chêne, S. Rosanvallon (France)

Estimation of Internal Hydrogen Pressure in Metal Cavities Based on the Thermodynamics Approach
I. Skrypnyk (Ukraine)

Factors Affecting the Hydrogen Environment Assisted Cracking Resistance of an Al-Zn-Mg-(Cu) Alloy
G.A. Young, J.R. Scully (USA)

Hydrogen Interactions with Aluminum Surfaces
R. Bastasz, J.A. Whaley (USA)

Corrosion Fatigue of Riveted Joints with LY12CZ Aluminum Alloy in 3.5% Sodium Chloride Solution
E-H. Han, B. Zhang, Z.G. Zhang, W. Ke (China)

Hydrogen Embrittlement of Al 2195 Alloy
E.I. Meletis (USA)

The Influence of Grain Boundary Precipitation on the Stress Corrosion Cracking of Al-Li and Al-Li-Cu Alloys
R.E. Ricker, A.K. Vasudevan (USA)

Poster Session II (Wednesday)

Hydrogen Isotope and Microstructure Effects on Deformationand Fracture in 22Cr-13Ni-5Mn
B.P. Somerday, C.H. Cadden, S.L. Robinson (USA)

Materials Testing in High-Pressure Gaseous Hydrogen at Sub-Zero Temperatures
M. Watwood, B. Hurless, M. Jackson, S. Gentz (USA)

Relationship of Laboratory Tests of Rock Bolt SCC to Service Failures
E. Gamboa, A. Atrens (Australia)

Effect of Microstructure and Electrochemical Potential on the SCC Resistance of X-80 Steel in Diluted $NaHCO_3$ Solutions
J.G. Gonzalez-Rodriguez, M. Casales, V.M. Salinas-Bravo, J.L. Albarran, L. Martinez (Mexico)

Numerical Simulation of Hydrogen Effects on Stress Corrosion Crack-Tip Plasticity
D. Delafosse, J. P. Chateau, S. Teysseyre, T. Magnin (France)

Factors Influencing Stress Corrosion Cracking of Mild Steels in Alcoholic Environments
E. Risson, B. Bayle, R. Kefferstein, T. Magnin (France)

Effects of Strain Rate and Hydrogen Trapping Behavior on Fatigue Crack Growth of SA 508C1.3 Pressure Vessel Steel in High Temperature Water
S.G. Lee, I.S. Kim (Korea)

Reproducibility and Repeatability of Tensile and Low Cycle Fatigue Properties in Propulsion Grade Hydrogen
E.J. Vesely, B.N. Bhat, W.B. McPherson, C.E. Grethlein (USA)

Stress Corrosion Cracking and Life Prediction of Austenitic Stainless Steels in Calcium Chloride Solution
H. Leinonen, I. Virkkunen, H. Hanninen (Finland)

Surface Work Hardening and Stress Corrosion Cracking of an Austenitic Stainless Steel
C. Braham, A. Bouzina, J. Lédion (France)

Effect of Nitrogen on the SCC of 316LN Weld Metal
S.N. Soman, V.J. Gadgil, S.N. Malhotra, R. Raman, V.S. Raja, S.D. Kulkarni (India)

Effects of Thermohydrogen Processing on Microstructure and Properties of Uranium Alloys
M.B. Shuai, Y.J. Su, D.M. Lang, Z.H. Wang, P.J. Zhao, S. Wu (China)

Phase Transformations in Ti-6Al-4V-xH Alloys
J.I. Qazi, J. Rahim, O.N. Senkov, S.N. Patankar, F.H. Froes (USA)

Influence of Hydrogen on the Stability in Ti-Nb alloys
D. Zander, B. Kofmann, D. Eliezer, E.Y. Gutmanas, E. Abramov, D. Olson (Israel)

How Helium Affects the Thermodynamics of the Palladium-Tritium System
S.E. Guthrie, W.G. Wolfer (USA)

Improved Thermal Stability by Hydrogenation of Zr-Cu-Ni-Al Metallic Glasses and Quasicrystals
D. Zander, E. Beduli, D. Eliezer, N. Eliaz , U. Köster (Israel)

Effect of Hydrogen on Deformation of Ni in Crack Tip Model
M. Wen, X. Xu, S. Fukuyama, K. Yokogama (Japan)

Effect of Applied Stresses on Hydride Orientation in Titanium
A. Politi, M.I. Luppo, G. Vigna (Argentina)

Hydrogen Effects on a Microalloyed X70 Linepipe Steel
A. Hazarabedian, P. Bruzzoni, R.J. Cordoba, N. Mingol, M. Ortiz, M.I. Luppo, G. Anteri, J. Ovejero-Garcia (Argentina)

Comparison of Hydrogen Effects on the Behavior of C-Mn Steels by Different Methods
J. Sojka, P. Betakova, I. Schindler, L. Hyspecka, M. Sozanska, C. Dagbert, J. Galland, M. Tvrdy (Czech Republic)
Doping Influence on the Kinetics of Hydride Decomposition in Titanium Alloys
LG. Malyshev, V.G. Shamruk (Russia)

Poster Session III (Thursday)
The Investigation of Hydrides in Uranium with Small Angle Neutron Scattering
J.S. Bullock, S. Spooner, R.L. Bridges, G.L. Powell, G.M. Ludtka, J. Barker (USA)
A Mechanistic Model of Helium Retention and Release for Aging Metal Tritides
D.F. Cowgill (USA)
Interactions Between Sodium Alanate Metal-Hydride and Candidate Containment Materials
E.H. Majzoub, B.P. Somerday, S.H. Goods, K.J. Gross (USA)
Microstructure, Stress and Mechanical Properties of Sputtered Rare Earth Metal and Rare Earth Metal Hydride Thin Films
D.P. Adams, N.R. Moody, J.A. Romero, J. Floro, M. Rodriguez (USA)
Hydrogen Assisted Fracture in LENS™ 316 Stainless Steel
B.P. Somerday, J.E. Smugeresky, J.A. Brooks (USA)
Nanomechanical Evaluation of Hydrogen Affected Deformation and Fracture in Stainless Steels
N.I. Tymiak, A. Daugela, J. Jungk, Y. Katz, W.W. Gerberich (USA)
Role of Heat Treating on the Sour Gas Susceptibility of an X-80 Steel
H.F. López J.L. Albarran, L. Martinez (Mexico)
On the Heat Treatment and Microstructure in the Intergranular Stress Corrosion Cracking Response of Alloy 600
A. Aguilar, H.F. Lopez, L. Martinez, J.L. Albarran (Mexico)
Effect of Temperature, Strain Rate and Microstructure on the Tensile Properties of Hydrogen Charged Nickel and Alloy 600
A.M. Brass, J. Chêne (France)
Kinetic Features of Metal Hydride Decomposition in Nonisothermal Conditions
L.G. Malyshev, V.G. Shamruk (Russia)
Thermo-Oxidation Degradation in Cyanate Ester Resins
A. Venkatramanian, Z. Liu, J.P. Lucas (USA)
The Initiation and Propagation of The Stress Corrosion Cracks in High Temperature and High Pressure Conditions
R. Novotny, P. Sajdl, J.Vosta (Check Republic)
Study of Hydrogen Embrittlement Sensibility in Low Alloyed Steels Towards Critical Tests for Classification
B. Bayle, C. Bosch, X. Longaygue, T. Magnin (France)
The Interpretation of Wave Shape Effects During the Corrosion Fatigue of Anodically Polarised Steel in Sea Water
C.J. van der Wekken, M. Janssen (The Netherlands)
Hydrogen Cracking and Stress Corrosion Cracking of Pipeline Steels
D. Le Friant, B. Bayle, T. Magnin (France)
Tensile Behavior of Austenitic Stainless Steels in Hydrogen Atmosphere at Low Temperatures
S. Fukuyama, D. Sun, L. Zhang, M. Wen, K. Yokogawa (Japan)
The Influence of the Surface layer of the Carbon Steel While Its Cycle Deforming on the Hydrogen Absorption and Fatigue Strength
V.A. Slezhkin, S.M. Beloglazov (Russia)

Fatigue Behavior of the High Strength Steel SE702 in Vacuum, Air and NaCl Solution
B. Huneau, J. Mendez (France)

Moisture-Induced Embrittlement of B2-type CoTi Ordered Intermetallics
Y. Kaneno, T. Takasugi (Japan)

Evaluation of Electrolytic Hydrogenation Influence on Fatigue Crack Growth Resistance of High-Strength Steels.
A.I. Balitskii, V.I. Pokhmurskii, O.O. Krohmalny,

Prevention of Hydrogen Embrittlement and Corrosion of Steels in Aqueous Salt Media with SRB by Industrial Organic Additives
S.M. Beloglasov, A.A. Myamina, E.M. Kondrasheva (Russia)

CONFERENCE ABSTRACTS

Sunday Evening, September 22, 2002
Session I: Introduction

Reflections on Hydrogen Conferences. (Keynote) A.W. Thompson, University of California, Berkeley, CA, USA

Mechanisms of Hydrogen Assisted Cracking-A Review. S.P. Lynch
Aeronautical & Maritime Research Laboratory, Melbourne, Australia

This review will outline the present state of knowledge and current controversies concerning mechanisms of hydrogen assisted cracking in non-hydride forming materials such as steels, nickel, aluminium alloys, and intermetallies in hydrogen and aqueous environments. Mechanisms based on (i) hydrogen-enhanced localised plasticity, (ii) hydrogen-induced decohesion, (iii) adsorption-induced localised slip, (iv) corrosion-enhanced plasticity, and (v) other models will be examined in the light of experimental observations and theoretical modelling. The importance of accounting for the metallographic and fractographic observations, such as crystallographic characteristics, crack-arrest markings, dimples on fracture surfaces, etc., will be emphasised. Explanations for the effects of microstructure, strength, temperature, stress-intensity factor, and other variables on susceptibility to hydrogen embrittlement and stress corrosion cracking will also be discussed.

Hydrogen Assisted Cracking of Quenched and Tempered 4135 Steel in an Hydroxide Solution. É. Verniquet, R. Roberge, S. Lalonde, IRÉQ, Varennes, Quebec, Canada, and J.I. Dickson, École Polytechnique, Montreal, Quebec, Canada

The hydrogen-assisted cracking of quenched and tempered SAE-AISI 4135 steel was studied in an aqueous solution of 0.686 mole/*l* KOH and 0.144 mole/*l* of NaOH at applied potentials of –1.1V, -1.2 V and –1.4 V with respect to a saturated calomel electrode. The tempering temperatures employed were 480°C, 580°C and 650°C and the tempering time was 30 minutes.

The curves of the crack propagation velocity versus the stress intensity factor K obtained were three-stage curves, with the second stage corresponding to a plateau. The K value at which continuous cracking started increased with increasing tempering temperature and increased slightly as the applied potential became less cathodic. The stage II or plateau velocity decreased with increasing tempering temperature and decreased as the applied potential became less cathodic. The K value at which stage III began as well as the maximum K value measured during these tests decreased with decreasing tempering temperature and decreased as the applied potential became more cathodic.

The fractographic features during stages I and II were generally a mixture of quasi-cleavage and of "intergranular" cracking. For the two higher tempering temperatures, the intergranular facets could often be clearly observed to correspond to quasi-intergranular cracking following a crack path close to but generally not along the prior austenite grain boundary, with lines often observed indicating both the crack propagation direction and some intermediate positions of the crack front. Although less clear, the cracking also appeared to be quasi-intergranular but closer to the

grain boundary for a tempering temperature of 480°C. For all tempers, stage III corresponded to a change in fractographic features to entirely ductile fracture dimples. For the steel tempered at 480°C, this ductile fracture mode was then followed by cleavage.

Corrosion-fatigue tests in the same environment were carried out on a 4135 steel commercially tempered near 650°C, employing a sinusoidal waveform, R-ratios of 0.1 and 0.5, a cycling frequency of 1 Hz and occasionally of 0.1 Hz and applied potentials of −1.1 V and −1.4 V with respect to a saturated calomel electrode. These corrosion-fatigue tests showed an initially steeper stage II slope than that obtained in air followed by a plateau. The crack propagation curve then joined the stage II curve obtained in air at high ΔK. The plateau crack growth rates were 4-5 times higher for the more cathodic potential. The plateau crack growth rate when transformed into a crack propagation velocity agreed well with the stage II plateau velocity obtained in the static hydrogen-assisted cracking propagation tests for a tempering temperature of 650°C at the same applied potential. The results will be discussed and analyzed.

Vacancy Generation in Electrochemical Oxidation of Copper in $NaNO_2$ Solutions and its Role in TGSCC Mechanisms. P. Aaltonen, Technical Research Centre of Finland (VTT), FIN-02044, Finland, Y. Yagodzinskyy, O. Tarasenko, H. Hanninen, Helsinki University of Technology, Helsinki, Finland

Interaction of copper base metal with the oxide layers growing on its surface under various conditions of electrochemical oxidation in $NaNO_2$ solutions has been studied. It was shown that the process of copper oxidation is accompanied with generation of large amounts of vacancies at the copper-Cu_2O interface, when CuO oxide layer starts to grow on the Cu_2O oxide, which is partially coherent to copper substrate. Diffusive flow of vacancies into the base metal results in significant rearrangement of dislocation substructures, similar to that in irradiation of copper with electrons or neutrons, and also in development of elastic stresses in surface layers of copper substrate.

The influence of electrochemical oxidation on creep rate of copper at various temperatures has also been studied. It was shown that excessive vacancies generated at a stage of CuO oxide layer growth lead to a significant increase in creep rate. The phenomenon of plastic deflection of thin copper strips in their one-sided oxidation has been found and studied in detail. It is shown that deflection is due to plastic relaxation of elastic stresses accompanying the rearrangement of dislocation assemblies, stimulated by vacancy flow in surface layers of copper. The influence of oxidation process on dislocation substructures in surface layers of copper is confirmed by experiments with low-temperature internal friction and TEM observations of surface layers of specimens. OFHC copper and high-purity (99.9999 %) copper were used in the above-mentioned experiments which allowed to obtain information on the influence of oxygen content on the process of generation and transfer of vacancies into the metal, and also on their interaction with dislocation assemblies.

The results are discussed in connection with model development of TGSCC based on electrochemical oxidation of copper. The major influence of vacancies generated in the process of electrochemical oxidation on stress corrosion crack growth is the basis of TGSCC model.

A Mechanism of the Hydrogen Embrittlement of Cr-Ni Austenitic Steels and Alloys at High Pressures and Temperatures. Yu I. Archakov, VNIINeftechim, St.-Petersburg, Russia

The investigations were carried out at the hydrogen pressures of 30-70 MPa at temperatures 500 - 900C. The following materials: 18Cr-10Ni-0.6Ti-0.10C; 18Mn-3Al-0.45C and 15Cr-26Ni-2W-4Mo-0.6Nb-0.08C steels, 20Cr-77Ni-2Ti-0.9Al alloy and nickel (Ni-1) were studied. The concentration of hydrogen in the samples studied was 70-140 ppm.

The kinetics of the hydrogen saturation of the above-mentioned materials under the high pressure and temperature conditions was investigated and the equilibrium concentrations of hydrogen in metals vs experimental conditions were determined. The mechanical tests were developed just after the high-speed cooling of the samples located in autoclaves at hydrogen pressure. The results of the experiments indicated that the hydrogen embrittlement increases with the increment of the nickel concentration in alloys and depends on the content of nickel and hydrogen in metal.

Using the microscopic study of the destruction character at the static and impact loads it was established that in the initial state as well as after the heat influence the intragranular destruction took place. As a rule directly after the hydrogen saturation of the austenitic steels and alloys the destruction on the grain boundaries was determined. The hydrogen resistant austenitic steels after the hydrogen saturation with the following drawback showed the intragranular destruction again. The decarbonizing austenitic steels in that case had the clearly indicated intercrystalline character of destruction. The reversible or irreversible type of the hydrogen influence on steel is in the first place caused by the decrease of the intercrystalline durability of the metal. The decrease in the grain boundary toughness for nickel and nickel-based alloys under the hydrogen influence is stipulated by the high pressure effect of the hydrogen placed in the defects and interstices situated mainly on the grain boundaries, as well as by the existence of the brittle hydride interlayer formed at such conditions. On the basis of the experimental data the mechanism of the hydrogen embrittlement of Cr-Ni steels and nickel-based alloys was proposed.

Monday Morning, September 23, 2002
Session II: Hydrogen Effects on Material Behavior

Hydrogen Interactions with 2.25Cr and 9Cr Steels. H.Hänninen, Y. Yagodzinskyy, O. Tarasenko, Helsinki University of Technology, Finland, P. Castello J.-P. Schosger, Institute for Advanced Materials, Petten, The Netherlands

Interaction of hydrogen with a number of chromium-alloyed steels, which are used or proposed as materials resistant to hydrogen attack at elevated temperatures, has been examined. 2.25Cr-1Mo and 2.25Cr-1Mo-V steels with bainitic microstructure and 9Cr-1Mo-V and 8Cr-2W-V (F82H) steels with tempered lath martensitic microstructure were studied. State of hydrogen was, especially, examined and parameters of its diffusion in crystal lattice of these steels were determined using a low-temperature internal friction (IF) method. Wide multicomponent IF peaks were observed after electrolytic hydrogen charging of both bainitic and martensitic chromium-alloyed steels. The peak extends over a temperature range of 100-400 K and contains, as a rule, four components. The relationship between the intensities of composite IF peak components depends on the value of prior deformation and charging conditions. Detailed analysis of the variation of these composite IF peak components with the frequency of the natural oscillation of the pendulum allowed evaluation of the energies of hydrogen interaction with dislocations and alloying elements and determination of the activation parameters of the elementary diffusive jumps of hydrogen. The effective coefficients of hydrogen diffusion were derived from the variation of high-temperature composite IF peak components caused by the process of thermal desorption of hydrogen from steel. Effective coefficients of hydrogen diffusion were also measured by means of electrochemical permeation experiments with membranes of the studied steels. Finally, the results obtained with different methods are compared and discussed.

Probing Hydrogen - Deformation Interactions Using Nanoindentation. D.F. Bahr, K.R. Morasch, C.L. Woodcock, D.P. Field,Washington State University, Pullman, WA, USA

One of the concerns in the impact of hydrogen on the mechanical properties of materials is the way in which hydrogen acts in conjunction with localized deformation mechanisms. When straining large volumes of material, it is often difficult to make a direct correlation between cross slip and slip band formation. Utilizing sub-μm indentation techniques, which probe small volumes of materials, it is possible to identify both of these deformation mechanisms. Out of plane deformation around a nanoindentation is a result of the strain hardening characteristics of the material, and is largely caused by cross slip of dislocation structures underneath the indenter tip. Additionally, individual slip bands around an indentation can be measured using atomic force microscopy. This study was undertaken to identify the deformation mechanisms around these small scale indentations. A BCC titanium polycrystalline alloy was vacuum annealed and then electrolytically charged with hydrogen to various concentrations. Increasing hydrogen concentrations in the alloy correspond to less out of plane deformation around the indentation, suggesting that cross slip is inhibited in the presence of hydrogen. The hardness of the alloy increases slightly with increasing hydrogen content. The distinctive change in deformation morphology, while only slightly increasing the hardness, which would be consistent with a change in cross slip behavior and the constraints of indentation testing (where a bulk material with one free surface is examined). The number of localized slip steps on the surface was also examined, and found to be primarily a function of crystallographic orientation, as tracked by Orientation Imaging Microscopy. Only a weak correlation between slip step density and hydrogen concentration was identified. The differences in deformation are compared to the bulk fracture behavior, in which increased hydrogen concentration in this alloy leads to extensive

cleavage fracture. These data suggest the reduction of cross slip in BCC alloys due to hydrogen may act to both embrittle and harden the sample.

Effects of Hydrogen on Slip Character in a Precipitation-Strengthened Alloy. A.W. Thompson, D.C. Nguyen, University of California, Berkeley, CA, USA

The slip morphology of the precipitation-strengthened alloy A-286 was examined in both underaged and overaged conditions. The degree of aging was chosen so that materials had about equal yield strengths, but exhibited well-defined dislocation cutting of precipitates in the underaged condition, and by-passing or looping when overaged. It was found that increasing strain resulted in decreasing slip line spacing and an increasing degree of slip waviness, as expected from prior studies. Pre-charging with hydrogen decreased slip line spacing at low strain, but at higher strains had no significant effect. For slip-line waviness, hydrogen increased waviness for underaged material, but had no effect on overaged material. Interpretation of these results is discussed.

Examination of Deformation Microstructures in Hydrogen Embrittled Commercial Alloys. D.S. Gelles, R. Bajaj, Battelle Pacific Northwest National Laboratory, Richland WA, USA

It is rarely possible to generate microstructural understanding of hydrogen embrittlement because experiments must be carefully planned. In an effort to understand the effects of hydrogen on deformation response of Ni-base alloys, tensile specimens were sectioned following deformation and examined by transmission electron microscopy to show slip band propagation across grain boundaries. Alloys included X-750 (in two heats), A625, A690, and A600, as well as EN82 and R127 weldments. Specimens without hydrogen and those with ~60 wppm hydrogen were deformed to between 1% and 4% plastic strain at strain rates of $1x10^{-5}$ or $1x10^{-7}$ s^{-1}. Procedures were developed to show slip band structure on both sides of a grain boundary in stereo. Results demonstrated that the mode of deformation without hydrogen present: slip band formation and propagation across grain boundaries, is not significantly altered by the addition of hydrogen. Nor is the stacking fault energy changed in the simpler alloys, A600 and A690, by the addition of hydrogen. The only clear effect of hydrogen appears to be the development of dislocation "debris" immediately adjacent to carbide precipitates at grain boundaries, where boundaries are intersected by slip bands. Examples of the slip band structure observed across grain boundaries will be demonstrated using anaglyph stereo images.

Effects of Hydrogen Isotopes on the Fracture Toughness Properties of Austenitic Stainless Steel Weldments. M.J. Morgan, S.L. West, M.H. Tosten, G.K. Chapman, Westinghouse Savannah River Company, Aiken, SC, USA

The effects of hydrogen and tritium on the fracture toughness properties of austenitic stainless steel weldments are being investigated. Weldments of two different austenitic stainless steels, Types 304L and 21-6-9, were prepared with weld ferrite contents ranging from 4 to 33%. The ferrite content within the weld was varied by using different filler wires (Types 308L, 309 and 312) during welding. Electron beam welding (without a filler wire) was used to produce the lowest ferrite levels. Welds with low ferrite content (less than 8%) had a microstructure consisting of discontinuous skeletal ferrite present in a predominant austenite matrix. Welds with high ferrite content (more than 20%) had microstructures consisting of nearly continuous skeletal/acicular/cell-like ferrite present in a plate-like and globular austenite matrix. Fracture toughness samples were machined from the welds so that the crack was oriented along the centerline of the weld. J-integral fracture toughness properties were measured at room

temperature before and after an equilibrium exposure to hydrogen (69 MPa) or tritium (35 MPa) gas at 623 K. Tritium-exposed samples are being aged and tested periodically for five years to quantify the effects of increased concentrations of helium-3 from tritium decay. For unexposed steels, weldments containing the discontinuous skeletal ferrite had fracture toughness values two-to-three times higher than the base metal. The discontinuous ferrite phase seemed to act as a barrier to crack propagation. At higher levels, ferrite had a detrimental effect on fracture toughness. For hydrogen-exposed welds, ferrite had a detrimental effect on fracture toughness at all levels. In addition, the fracture path in hydrogen exposed samples changed from dimpled rupture in low-ferrite (< 4%) welds to fracture along the austenite-ferrite interfaces in medium-ferrite (< 12 %) welds to fracture through the ferrite phase in high-ferrite (20-30 %) welds. Although, the fracture toughness tests of the first set of aged tritium-exposed weldments will not be completed until July of 2001, the build-in of helium-3 from tritium decay is expected to cause further reductions in the fracture toughness properties. The results of these tests will be included in the conference presentation and publication.

* The information in this article was developed during the course of work under Contract No. DE-AC09-96SR18500 with the U. S. Department of Energy.

Tritium Decay, Irradiation and Hydrogen/Helium Effects on Austenitic Stainless Steels.
M.R. Louthan, Jr Westinghouse Savannah River Company, Aiken, SC, USA

The deleterious effects of hydrogen on the mechanical properties of austenitic stainless steels tested at room temperature are frequently magnified by the presence of helium. Helium can be introduced into steel by either tritium decay or by implantation during irradiation. Displacement damage, which accompanies irradiation-induced hydrogen/helium implantation, is not generally associated with the tritium decay process. Therefore, the microstructure of steels containing any given level of hydrogen and helium will differ significantly between the tritium-tricked and the irradiated materials. Irradiated materials will contain significantly more traps for the hydrogen and helium atoms. Numerous studies have demonstrated that trapping has major effects on the susceptibility of metals and alloys to hydrogen embrittlement. Additionally, helium-induced degradation in the weldability of Type 304 stainless steel was found to be much greater when the helium was introduced by irradiation.

Evaluation of the combined, and potentially synergistic, effects of hydrogen, helium and displacement damage on the mechanical properties of austenitic stainless steels show that hydrogen absorption and displacement both raise the tensile strength decrease the toughness and limit the ductility of the austenite lattice. The decreases in ductility have been attributed to the pinning or blockage of dislocations and an increased tendency for strain localization or dislocation channeling. The introduction of helium to the lattice causes additional increases in the strength in the tritium-tricked steels but has minimal effect on irradiation-induced strengthening. For example, recent studies with austenitic stainless steels irradiated with high-energy (up to 800MeV) protons and spallation neutrons have demonstrated that the effects of displacement damage on strength are similar, especially at high displacement levels (5 to 10 dpa). Irradiation with these high-energy particle beams

The differences, and similarities, among tritium tricked and spallation neutron irradiated austenitic steels are discussed in terms of trapping. Additionally, the effect of trapping on helium distribution and subsequent release and redistribution during welding is used to explain the difference in the weldability of tritium tricked and irradiated stainless steels.

Effect of Environmental Hydrogen on Tensile Properties of Inconel 690. X.-H. Luo, Chinese Academy of Sciences, Beijing, China and M. Habashi, Ecole Centrale Paris, Paris, France.

To minimize the chromium depletion associated with grain boundary carbide precipitation, Inconel 690 was developed with higher chromium content (up to 30%wt.) to substitute for Inconel 600 used in nuclear power plants. In the past years, many papers have been published about the resistance to intergranular attack (IGA) and stress corrosion cracking (SCC) of Inconel 690, which indicated that Inconel 690 had much better resistance than Inconel 600 alloy. However few studies have been reported on hydrogen embrittlement (HE) resistance of Inconel 690.

In order to understand how environmental hydrogen influences the mechanical properties of Inconel 690 alloy, environment-simulated tensile tests were conducted on this alloy. Three different heat treatment conditions: A) as-received, B) aged at 973K, and C) solution treated at 1323K and then aged at 973K, were involved to identify what role the microstructure would play. The metallography observation showed that, from microstructure A to C, the amounts of carbides both in the matrix and on the grain boundaries increased gradually, and the carbides distribution on the grain boundaries evolved from discrete to semi-continuous, and finally to almost continuous. Thermal activation analysis techniques, such as strain rate change and stress relaxation, were also employed to investigate the effects of environmental hydrogen and microstructure on thermally activated deformation in this alloy. The fracture surfaces were analyzed using SEM.

Tensile results showed that, with YS almost unchanged, environmental hydrogen evidently decreased the UTS and El of the material, especially for heat treated microstructures, suggesting that the hydrogen concentrated on the specimen surface and promoted surface microcracks.

From stress relaxation experiments, it could be seen that, environmental hydrogen led to much higher relaxation rates. Furthermore, hydrogen produced higher strain rates at lower strain levels, and almost had no effect at higher strain levels though the stress relaxation of the specimen tested in hydrogen was faster. The strain rate change experiments showed that an increase in strain rate gave almost the same stress increment at various strain levels. And, hydrogen just increased the stress increment very slightly. Further thermal activation analysis indicated that the area swept out during the thermal activation event evidently depended on the microstructure, hydrogen and the technique applied. It was drastically reduced by environmental hydrogen, especially at low strain levels. Furthermore, with strain or stress increasing, the activation area decreased in the absence of hydrogen but increased in the presence of environmental hydrogen, and then seemed to tend to a common threshold. The results from stress relaxation experiments were more sensitive to microstructure and hydrogen than those from strain rate change experiments.

Conclusion could be drawn that the environmental hydrogen embrittled the alloy 690, especially when the alloy was aged or solution treated and then aged. The fine and homogeneous distribution of carbide precipitates in the matrix and/or on the grain boundaries were responsible for the embrittlement.

Poster Session I

The Protective Effect of Glassy and Glass Ceramic Coatings in the Processes of the Hydrogen-Steel Interactions at High Temperatures-High Pressures. I. Yu. Artchakov, B.Z. Pevzner, V.G. Konakov, Institute of Silicate Chemistry of Russian Academy of Sciences, St. Petersburg, Russia, T.D. Alyferenko All-Russian Scientific Research Institute for Petrochemical Processes, St. Petersburg, Russia

The study of the protective effect of the special high temperature stable glassy and glass-ceramic coatings was carried out for the two steel types: low-carbon and stainless. The steel sample with coating and the unprotected one in the same working volume were exposed at 150 atm hydrogen pressure at temperatures 550-600 °C during 24 hours. The values of hydrogen solubility in steel were determined and the metallographic analysis was carried out for the studied samples. The protective effect of glassy coatings was especially evident in a series of experiments with the model low-carbon steel. The existing of the protective effects was confirmed reliably for the case of stainless steel with glass-ceramic coating. The prospects to use the high temperature stable glassy and glass-ceramic coatings for the protection of stainless steel and engineering materials at high temperatures and hydrogen pressures are discussed.

Effect of the Density of States on the Stacking Fault Energy and Hydrogen Embrittlement of Transition Metals and Alloys. J.A. Lee, NASA-Marshall Space Flight Center, Huntsville, AL, USA

Previously, a quantitative correlation was proposed between the electronic density of states (DOS) at the Fermi level and the hydrogen embrittlement for several transitional metals, binary, ternary and complex alloys. The correlation was based upon the d-band filling and electronic state interactions between hydrogen and metals at the atomic level, which are characterized by the atomic number and electron-atom ratio. The purpose of this paper is to expand the scope of this work by presenting a relationship between the Stacking Fault Energy (SFE) and the DOS for transitional metals and binary alloys such as NiCu, NiCo, NiFe, NiTi, NiCr, PdAg and PdCu. This theory is somewhat contrary to the dislocation transport model for hydrogen embrittlement, which denotes that an increasing susceptibility to hydrogen embrittlement would occur with decreasing SFE, particularly with austenitic stainless steels, since increased slip planarity would optimize hydrogen transport by dislocations to the fracture sites. In this paper, the argument is that metal with a low SFE may increase the slip planarity, but it will not necessary result in increasing susceptibility to hydrogen embrittlement. In contrast, it has been found that the maximum in hydrogen embrittlement does not often coincide with the mininum SFE experimental values for most transition metals and binary alloys. Concerning the Ni-Cr-Fe system, based on an analysis of the free energy and enthalpy, a qualitative relationship was established between the SFE and the reciprocal of the DOS at the Fermi level, which again supports the cohesion model rather than the hydrogen dislocation transport model.

Hydrogen Embrittlement and Mossbauer Effect. J. Vosta, P. Sajdl, O. Schneeweiss, R. Novotny, Institute of Chemical Tech., Prague, Czech Republic

In this study we measured in transmission technique Mossbauer effect on alpha Fe foil. The spectrum was excellent and we used these data for calibration of Mossbauer equipment. After this we putted foil into special electrochemical cell with small narrow reservoir and electrochemically

polarised one part of foil as cathode in acid solution. On this part of foil can take place reaction hydrogen proton or electrical and chemical excited state of hydrogen with the surface of iron and can diffuse into foil. During a few minutes where alpha Fe foil was under cathodic condition, the Mossbauer effect was cancelled. We think that hydrogen pressure diminish or suppress magnetic dipole and electric quadrupole interaction and influence electric dipole moment in the sample. It knows, that width and position of the centre of Mossbauer spectrum depend on the inner pressure in the solid phase and can inform about inner stress in material. This elimination of Mossbauer effect is still investigated.

The Effects of Neutron Damage on the Migration Parameters of Hydrogen Isotopes in CVD Silicon Carbide. R.A. Causey, Sandia National Laboratories, Livermore, CA, USA, L.L. Snead, T.J. Venhaus, W.R. Wampler, Sandia National Laboratories, Albuquerque, NM, USA

Silicon carbide is one of the best permeation barriers available for hydrogen.[1] The hydrogen solubility and permeation appear to be dominated by a small concentration of strong trap sites, perhaps due to dangling bonds at grain boundaries. If radiation damage increases the number of dangling bonds, the transport properties may be altered. In this study, fully dense Morton CVD silicon carbide samples were irradiated at different temperatures in the High Flux Beam Reactor at the Brookhaven National Laboratory. All samples were irradiated for sufficient times and neutron fluxes to generate 1.1 dpa damage while the samples were maintained at temperatures from 373 K up to 1373 K. Because an increase in the concentration of trap sites would increase the apparent solubility, but reduce the effective diffusivity by the same degree, just measuring the permeation rate would not necessarily reveal the change. The steady state permeation rate is not affected by traps but under some conditions, the time delay for onset of permeation depends on the trap concentration. Instead of using a permeation technique, a technique based on concentration profiles was employed. The samples were exposed to deuterium gas at a pressure of 66.5 kPa at temperatures of 973 K and 1073 K for two hours. For these exposure conditions, the deuterium concentration profiles should extend several microns into the silicon carbide samples. After exposure, the samples were analyzed using Nuclear Reaction Analysis (NRA) to determine the concentration profiles. The peak concentration gives the apparent solubility or trap density, and the depth of penetration reveals the apparent diffusivity. The implication of the results for the use of silicon carbide in fission and fusion reactors is discussed.

R.A. Causey, W.R. Wampler, J.R. Ratelle, and J.L. Kaae, "Tritium migration in vapor-deposited beta silicon carbide," J. Nucl. Mater. 203 (1993) 196.

The Influence of Hydrogen on the Dislocation Velocity in Ni_3Al Single Crystals. C.B. Jiang, H. Li, S.D. Wu, S. Patu, Chinese Academy of Sciences, Shenyang, China.

In the microscopic transmission electron microscopy (TEM) *in situ* studies, the effect of solute H enhancing dislocation velocity in different materials in the environmental cell has been directly observed and interpreted. However, attempts to relate these results to macroscopic phenomena have caused controversies because of the special condition in TEM foil. To directly study the effect of hydrogen on the dynamic behavior of dislocation in bulk specimens is becoming necessary to provide a bridge between the macroscopic and microscopic phenomena. In this paper, the effect of high content hydrogen (6.2 at.%, introduced by the high-pressure thermal charging method) on the average dislocation velocities in Ni_3Al (B) single crystals has been investigated by the etch-pit technique. In addition, the effect of hydrogen on the Vickers hardness anisotropy of (001), (110) and (111) surface of this material is also studied. It is found that an obvious strengthening phenomenon results from the introduced hydrogen, which makes the

bending strength increase about 2.5 times. The measurement of the average dislocation velocity of octahedral slips at room temperature shows that the velocity is dramatically decreased by the charged hydrogen and that the tension/compression asymmetry of the dislocation velocity is reversed. To reach the same dislocation velocity of 10^{-6}m/s, the required RSS (resolve shear stress) increases from about 111 MPa to 316 MPa under the tension state and 127 MPa to 214 MPa under the compression state. In the hydrogen-free specimens, the dislocations on the tension side move faster than those on the compression side under the same RSS, but in the hydrogen-charged specimens, the dislocations on the compression side move faster than those on the tension side and the difference is larger.

Detailed observation of the dislocation structure indicates: in the hydrogen-charged specimens, besides the existence of the straight screw dislocations, there are many mixed dislocations and tangled dislocations which are thought to have caused due to the inhibition of motion of the superkinks by the hydrogen solutes. In addition, the same reason also causes a change of the dislocation structures of the Vickers indentation rosette on (001) surface and increase in the Vickers hardness. The shape of the (001) rosette changes from a cross to a square. The disappearance of the rosette arms, which are formed because the motion velocity of edge superkinks is faster than that of the screw parts, is caused due to inhibition of motion of the superkinks too. The hardness increases very much by the effect of hydrogen, which changes from 216 to 387 on (001) plane, 233 to 432 on (110) plane and 233 to 413 on (111) plane. The range of increasing is 79.2%, 85.4% and 77.3% respectively. The anisotropy of the hardness becomes more significant in hydrogen charged Ni_3Al. All the above results provide strong evidence to the strengthening mechanism of hydrogen solutes in metals. Acknowledgements—This work was financially supported by the National Natural Science foundation of China (grant No. 57371003 and 58895156). The authors are grateful for this support.

Multi Layer Blister Formation in Structural Materials Due to Hydrogen and Helium Implantation. D. Moreno, NRCN, Beer-Sheva, Israel, D. Eliezer, Ben Gurion University of the Negev, Beer Sheva, Israel

Blister formation phenomenon is discussed by means of mathematical solution on a uniformly loaded circular plate with clamped edges. Investigations revealed that blister formation depends on the mechanical properties of the alloys and on the near- surface concentration of the implanted gas, which itself contingent on the crystallographic orientation by means of the stopping power of the implanted atoms. The reported model is based on the fact that at certain depths from the surface, the pressure in the cavities approaches the yield stress of the metal. The thickness of this thin cap of the metal depends on the mechanical properties of the specific metal. Once a blister cavity is formed, the deformation of the surface to form a blister cap depends on the build-up of pressure in the cavity contingent due to the implanted dose.

The implanted hydrogen and/or helium concentration needed to build up enough gas pressure to create a blister at a depth which is close to the projected range is higher by 50 times than the gas helium concentration in the cavity. Experimental results on copper and copper alloys, such as the fact that the blisters have burst at the edge of the circular skin, where the maximum stresses are developed, and the fact that at high implantation energy (large projected range) the bursting of the blisters occurs by multi layer caps, support the present model.

Modeling of Hydrogen Diffusion in Amorphous Alloys. N. Eliaz, Tel-Aviv University, Israel, D. Fuks, D. Eliezer, Ben Gurion University of the Negev, Beer-Sheva, Israel

The diffusion coefficient of hydrogen in amorphous alloys has been reported to deviate from Arrhenius law. This deviation was traditionally explained by the existence of various kinds of jumps, or in terms of continuous distributions of activation energies due to different kinds of disorder. In this work, another model was developed which relates this deviation to the temperature dependence of the short-range order (SRO). This model was applied to the Fe-Si-B system. Firstly, the SRO in the amorphous structure was defined on the basis of the radial distribution function (RDF) of amorphous iron and its temperature dependence. Secondly, the mechanism of hydrogen diffusion in amorphous iron was defined. Hydrogen atoms were assumed to form an extremely dilute solid solution, in which they occupy the octahedral interstitial positions in an fcc-like quasi-lattice. Then, the diffusion process of hydrogen atoms was described as the result of their jumps over the sublattice of octahedral sites. The activation energy for this process was calculated by subtracting the energy of a hydrogen atom in the saddle-point from its energy in the interstitial position. For this calculation, the first- and second-nearest neighbor atoms around an octahedral interstice and a saddle-point were defined in terms of their position in the quasi-fcc-lattice. The contributions of all kinds of atoms were then expressed in terms of the appropriate temperature-dependent coordination number in the amorphous structure. Following this procedure, the activation energy for the diffusion process was found to be temperature-dependent, thus reflecting the deviation from Arrhenius law. Thirdly, the Fe-H interatomic interaction potential was calculated. The activation energy and diffusivity of hydrogen in amorphous iron could then be drawn quantitatively. A non-Arrhenius behavior, characterized by a negative curvature of the diffusivity vs. temperature plot, was observed. Finally, the effect of alloying with silicon or boron on the diffusion of hydrogen in amorphous iron was studied. The Fe-H interatomic interaction potential, VFeH, was replaced with the effective potential of the complex, V(Fe,Si)H or V(Fe,B)H. The activation energy for hydrogen diffusion was found to increase significantly as a result of alloying with either silicon or boron. At relatively low concentrations (0.5-1.5 at.%) of the alloying element, silicon and boron had similar influence on the activation energy, although boron increased it slightly more. However, at higher concentrations (4.0-9.5 at.%) of alloying elements an opposite tendency was observed, silicon having a more pronounced effect. This behavior could be explained in terms of the electronic structure (i.e., the effective number of free electrons) of the alloying elements and their mean volume per atom compared to iron.

Visualization of Hydrogen Desorption Process from Ferrite, Pearlite and Graphite by Secondary Ion Mass Spectrometry. K. Takai, Y. Chiba, A. Nozue, Sophia University, Tokyo, Japan

Hydrogen and deuterium distribution in nodular graphite cast iron have been visualized by secondary ion mass spectrometry (SIMS). This paper concerns three main points; visualizing hydrogen distribution immediately after hydrogen occlusion, visualizing hydrogen desorption process from each metallurgical microstructure under various holding times at room temperature, and visualizing hydrogen desorption process from the each microstructure during heating up to 573K. The nodular graphite cast iron was prepared for visualizing hydrogen because it consists of basic microstructures of steels such as ferrite and pearlite. The specimen was occluded hydrogen and deuterium in D_20 and 20 mass % NH_4SCN solution. The amount of hydrogen and the hydrogen exiting states in the specimen were analyzed by thermal desorption spectrometry (TDS). Secondary ion image analysis by SIMS was applied to visualize hydrogen distribution. In SIMS analysis, deuterium ions can be detected with greater sensitivity than hydrogen ions and

measurements can be started in a matter of minutes. TDS analysis shows that the hydrogen thermal desorption rate has two peaks, corresponding to trap activation energies of 5.5 kJ/mol and 56.5 kJ/mol for the lower and higher temperature peaks, respectively. SIMS analysis of the specimen immediately after hydrogen occlusion shows that the hydrogen accumulates in the pearlite and the interfaces between the ferrite and the graphite much more than in the ferrite and the graphite. Secondary ion image analysis therefore makes it possible to compare the distribution of hydrogen amount in the each microstructure. SIMS analysis of the specimen under various holding times at room temperature shows that the hydrogen in the ferrite desorbs much faster than that in the pearlite and the graphite. SIMS analysis of the specimen cooled after heating up to 373K, 473K and 573K shows that the hydrogen desorbs from the ferrite up to 373K, from the pearlite and the interfaces between the ferrite and the graphite up to 473K, and from the pearlite up to 573K. The graphite remains hydrogen after heating up to 573K. We could identify the trapping sites corresponding to the lower temperature peak as the ferrite, the pearlite, and the interfaces between the ferrite and the graphite, and those corresponding to higher temperature peak as the graphite. These SIMS results confirm the location of the trapping sites to be the same as those estimated from the trap activation energy by TDS. Secondary ion image analysis also makes it possible to compare binding force between hydrogen and trapping sites.

The Influence of Plastic Strain on the Hydrogen Diffusion in a HSLA Steel. G.G. Juilfs, W. Dietzel, M. Pfuff, GKSS-Forschungszentrum Geesthacht, Geesthacht, Germany

The influence of plastic strain on the hydrogen diffusion in a low alloyed structural steel (FeE 690T) was investigated using electrochemical permeation experiments. Plastic deformation was introduced into the specimens by either cold rolling or by tensile straining. Specially prepared compact specimens additionally enabled the direct measurement of the hydrogen flux in the highly deformed region ahead of a blunting crack. It could be shown that the diffusion coefficient thus determined depended on the amount of plastic strain and on the overall hydrogen concentration, while the maximum hydrogen flux remained almost unchanged. These observations can be rationalized by taking into account variations in the dislocation density with the dislocations acting as 'sinks' for the diffusable hydrogen atoms.

The permeation data thus obtained can also help to understand the results of previous investigations on the effect of hydrogen on the fracture toughness of the same steel FeE 690T. It is suggested that the influence of various applied deformation rates on the cracking mechanism which had been reported from these earlier tests is associated with the reduced mobility of the hydrogen atoms in the plastic zone of the pre-cracked specimens.

The assumption of the hydrogen transport in the presence of simultaneous monotonic straining being controlled by diffusion could be confirmed by potentiodynamic investigations. In these, the formation of surface films was studied using cyclovoltammetry. It was observed that the nature of the passive layers forming on the specimen surfaces depended on the applied potentials. These affected mainly the hydrogen absorption reaction with the hydrogen entry preferably taking place at 'active sites' on the metal surface.

Quantitative Visualization of Hydrogen Evolved from Steels by Hydrogen Microprint Technique. K. Ichitani, S. Kuramoto, M. Kanno, The University of Tokyo, Japan

The new technique for quantitative visualization of hydrogen evolved from steels was developed. This was accomplished by a combination of hydrogen microprint technique (HMT) for visualizing hydrogen and an electrochemical hydrogen permeation method for measuring

hydrogen flux. This new technique will be applied to researches on hydrogen embrittlement of various metals, because no method has been as simple and powerful as this technique for quantitative analysis of hydrogen distribution in metals.

In this study, normalized 0.85 mass% carbon steel sheets of 1 mm in thickness were used as specimens. For HMT, one side of the specimen was final polished with 0.15 μm alumina paste, and covered with nuclear emulsion containing silver bromide crystals. The other side was mounted on a cathodic charging cell. Then this cell was galvanostatically polarized at a constant charging current. Introduced hydrogen atoms diffused through steel to the surface covered with the emulsion, and reduced silver ions in the silver bromide crystals to metallic silver particles. The specimen was subsequently immersed in a fixing solution to remove remaining silver bromide crystals. Consequently these reduced silver particles indicate the points where hydrogen has been released, and the quantity of evolved hydrogen can be assessed based on the amount of silver particles. These silver particles were observed by SEM, and the amount of silver particles was estimated from X-ray intensity measured by using EDXS. The quantity of hydrogen released from the polished surface was measured independently by using the electrochemical hydrogen permeation method under the same condition of charging with that of HMT. As a result, the quantity of released hydrogen was the same order with that of silver bromide on the surface. In the result of HMT, however, the number of silver particles observed by SEM was much smaller than that expected on the assumption that the efficiency of the reduction of silver ion by hydrogen was unity. Accordingly, it was examined whether nickel plating can increase the sensitivity of HMT, because nickel plating is known to improve sensitivity of the electrochemical hydrogen permeation method. The polished surface of the specimen was electroplated with nickel layer of 50 nm thickness prior to covering with the emulsion, and HMT was conducted in the preceding way. The number of silver particles observed was over ten times as large as that observed on the specimen without nickel plating. HMT was conducted by this nickel plating method under different charging conditions, and it has become apparent that the X-ray intensity of silver increased consistently with the quantity of evolved hydrogen. Thus hydrogen distribution in metals would be quantitatively estimated by this new technique.

Irreversible Hydrogen Traps in High Strength Steel Weld Metal. C. Lensing, I. Maroef, D.L. Olson, Colorado School of Mines, Golden, CO, USA

Effective control of weld diffusible hydrogen content has been achieved with the use of irreversible hydrogen traps in higher strength steel weld deposits. The potential for ferro-addition to the welding consumable to form weld metal inclusions which exhibited irreversible hydrogen trap has been utilized to prevent the hydrogen diffusion or transport to regions with high stress concentrations. Through these interfacial irreversible traps, hydrogen management can be achieved to a level known to reduce the susceptibility of hydrogen cracking. The benefit of yttrium as an irreversible hydrogen trap in the weld metal will be to decrease the diffusible hydrogen content in the weld metal down to appreciable levels around 1 to 2 ml of hydrogen per 100 g weld deposit (or 0.89 to 1.8 ppm of hydrogen). Diffusible hydrogen measurements were performed using the ANSI/AWS gas chromatograph 4.3-93 method and the residual (trapped) hydrogen is measured by the thermal desorption analysis.

The addition of 1600 ppm yttrium in HSLA steel metal cored wire can effectively reduce the weld metal diffusible hydrogen content significantly from 6 to 7 ml H_2/100g weld deposit to 1 to 2 ml H_2/100g weld deposit. The reduction in diffusible hydrogen was verified by the thermal desorption analysis with the evidence of high temperature, high binding energy traps characteristic of irreversible type traps. Yttrium formed two types of irreversible traps, yttrium

oxide and yttrium oxy-sulfide inclusions in the weld metal. However, yttrium oxy-sulfide inclusions is more compositionally complex and tend to agglomerate within the weld metal. From the Kissingers analysis, the trap activation energy was determined for micro-pores, yttrium oxide inclusion, and the complex yttrium oxy-sulfide inclusion and are 58, 78, and 96 kJ/mole respectively.

The weld metal diffusible hydrogen content is affected by variations in welding parameters which in turn affects the heat input i.e. cooling rate, as well as the amount of yttrium, transferred to the weld deposit. The voltage effect seems to be more significant than welding current on the HSLA steel weld metal diffusible hydrogen content. Transition voltage and current for low diffusible hydrogen levels on the order of 1 to 2 ml/100g weld deposit were found to be 30 to 32 volts and 380 to 400 Amperes respectively. The results showed that weld parameters can impact the arc metal transfer mode used in gas metal arc (GMA) welding and the resulting the diffusible hydrogen content. The spray transfer mode promotes more efficient transfer of yttrium in the form of effective yttrium compound traps to the weld pool resulting in less diffusible hydrogen, less than 1 ml/100g weld deposit. Hydrogen desorption analysis shows a higher trapped (residual) hydrogen in the weld metal for spray transfer compared to globular transfer. In the spray mode, the fine metal droplets have a greater ability to react with oxygen to form a large concentration of oxide traps in the smaller size distribution. The influence of oxygen additions to the shielding gas (Ar-0 to 4 %) was also correlated to weld metal hydrogen content

The Mechanical Instability of Amorphous Metal Alloys Appearing Under Hydrogenation.
N.E. Skryabina, L.V. Spivak, A.S. Petrov Perm State University, Perm, Russia

The interaction of hydrogen and deuterium with Fe-, Co- and Ni-based amorphous metal alloys (AMAs) has been investigated. It is shown that hydrogenation of AMAs in the creep mode under loads constituting 0.1-0.3 of the yield stress activates the deformation of alloys. The deformation stops after discontinuance of charging with hydrogen (at any stage of creep). Prolonged hydrogenation leads to the destruction of the alloy. It is important to note that all alloys remained amorphous after hydrogenation as observed from their X-ray diffraction patterns. Another feature that was obtained is a decrease in the shear modulus of the alloys during hydrogenation. By studying the deformational response of the Finemet-type alloy, a previously unknown phenomenon before has been discovered. During charging with hydrogen the alloy loses its carrying power and becomes shapeless with a shear modulus value close to zero. This is one of the reasons of mechanical instability of the alloy under an applied stress field that is a typical feature of liquids. However, it is unusual that the value of its modulus of elasticity does not change significantly, as is characteristic of solids. According to these criteria we call the state that appears after hydrogenation quasi-liquid. 10-15 minutes after charging with hydrogen the alloy reacquires this ability; after 60-80 hours the sample returns to its initial state. Repeating the process of hydrogenation-relaxation several times will cause the sample to destruct. Based on X-ray analysis and X-ray spectroscopy data it was found that hydrogenation of the alloy changes the topological as well as the chemical short-range order. The appearance of the quasi-liquid state in amorphous alloys under the conditions of structural instability and superequilibrium hydrogen concentration is the result of the liquefaction of AMAs that is localized to certain areas of the material. This is one of the reasons that mechanical instability may be observed during a phase transition occurring in an externally applied stress field. Hydrogenation of crystalline materials leads to amorphization of the crystalline matrix but there is no transition to the quasi-liquid state. In case of Fe-based AMAs like Finemet, for which the hydrogen diffusion coefficients are relatively high, the initial absence of short-range order makes the transition to the quasi-liquid state easier.

Environmental Factors on Embrittlement of Vitreous Silica Fibers. K. Takai, D. Yamada, A. Nozue, Sophia University, Tokyo, Japan

Environmental embrittlement factors of vitreous silica fibers for optical communication have been investigated using thermal desorption spectrometry (TDS). The fibers were held in vacuum, in atmosphere, in water, and in hydrogen for two and four weeks. The tensile strength of the fibers in atmosphere, in water, and in hydrogen decreases with increasing holding time under various environments compared with that in vacuum. TDS analyses show that the fibers held in atmosphere and in water occlude H2O (M/e=18) released at the peaks of 100 ˚C, 300 ˚C, and released at the shoulder of 550 ˚C, whereas those held in hydrogen occlude H2 (M/e=2) released at the peak of 200 0C. The water peak of 100 0C corresponds to surface water absorption, that of 300 ˚C corresponds to water trapped at macropore sites, and that of 550 ˚C corresponds to water released from Si-OH bonds. The hydrogen peak of 200 ˚C corresponds to hydrogen molecules trapped in defect structures in SiO2. The hydrogen as well as the water thus causes environmental embrittlement to the vitreous silica fibers.

Mechanical Stresses and Strains Developing in Thin Y-Films Due to H-Absorption. M. Dornheim, A. Pundt, R. Kirchheim, Universität Göttingen, Göttingen, Germany

Results on stress measurements during hydrogen absorption on switchable mirror Y thin films are presented. Hydrogen absorption in a metal is generally accompanied by a large expansion of the host lattice. When the metal is fixed to a substrate, in-plane expansion is not possible and large in-plane stresses as well as large out-of-plane expansions occur. The stresses often are so large that they might result in film damage during cycling. However, in YH_x films the stress and strain development exhibits an interesting behavior that prevents them from this early failure. While for $x < 1.8$ compressive stresses of up to - 0.7 GPa occur, they decrease at higher concentrations $2 < x < 2.6$. Further H-loading in the trihydride phase (g) results in an increase of the compressive stresses compensating the previous decrease. In the case of textured Y-films the di (b) and trihydride (g) end up with the same final stresses and during the switching period stresses are changed moderately only.

Monitoring of the Distribution and Desorption of Residual Tritium From Radioactive Waste After Detritiation. A.M. Brass, J. Chêne, Université Paris-Sud, Orsay, France, S. Rosanvallon, CEA/DRN/DER, St Paul lez Durance, France

Steel detritiation is an important challenge for the waste management of fusion reactors as nuclear waste storage assigns limited tritium contents. The optimization of a detritiation process and the monitoring of the desorption of residual tritium from the waste needs detailed investigations on the role of the materials microstructure on the distribution of residual tritium in the waste and on its desorption rate at the storage temperature. Very sensitive techniques are required as the residual amount of tritium in the waste has to be very low.

The purpose of this study is to characterize the distribution and the desorption rate at room temperature of the residual amount of tritium in an austenitic stainless steel ingot after detritiation treatment. The residual concentration of tritium in the material is less than 10^{-3} ppm. Different heat treatments favoring microstuctural changes in the alloy or the presence of oxide films on the surface were investigated. Autoradiographic observations were performed in order to assess the detritiation efficiency and to look for the role of different microstructural features on hydrogen trapping. The rate of tritium outgassing from selected samples was monitored by liquid scintillation counting. The strong influence of the microstructure on the tritium distribution and

desorption illustrates the role of defects or secondary phases on the trapping of tritium or on short path for hydrogen diffusion. The barrier effect of superficial oxide films is also discussed.

Estimation of Internal Hydrogen Pressure in Metal Cavities Based on the Thermodynamics Approach. I. Skrypnyk, National Academy of Science of the Ukraine, Lviv, Ukraine

The hypothesis concerning the high internal pressure of hydrogen in metal cavities exists already for quite a long time [1, 2]. It is often used to explain the phenomenon of hydrogen embrittlement of steels [3]. The theory of hydrogen attack [3, 4] also utilizes this idea. However, it is difficult to obtain direct (explicit) experimental evidences of this concept. Non-direct estimations, obtained using electronic microscopy [5], gives the pressure level about 29301900 MPa for the void of radius 17.5 nm in aluminum alloy. There is also the theoretical estimation [3, 5] for internal hydrogen pressure in cavities of radius r:

$$p=2*gamma/r-sigma. \quad (1)$$

Here "gamma" is the free surface energy and sigma denotes hydrostatic stresses around the void. This relation is obtained based on the thermodynamic analysis of two-phase-system, gas-liquid, under the suggestion, that the variation of the amount of gaseous substance leads to change in volume and surface area of this phase respectively.

On the other hand, it seems that the pressure values, determined using this approach, are overestimated. According to the above mentioned estimations, metal cannot sustain long-term loading in presence of hydrogen, since it would create extremely high pressure in the micro-voids and, hence, simply tear these cavities apart. In reality, however, metallic structural elements operate in hydrogen environment for 103 to 105 hours, also this period is often considerably reduced comparing to the service life under conditions, when hydrogen is lacking.

Our approach is based on the affirmation that hydrogen extrication from the metal into the void does not cause any substantial change in phase volume. Instead, the gaseous pressure within the void varies. Hence, in the paper the thermodynamic analysis of the two-phase-system, metal-void, with an interphase surface is performed, taking the hydrogen pressure as an independent parameter. The equation of thermodynamic equilibrium derived, basing on the condition of equivalence of first variation of Gibbs potential to zero.

Taking into account the Gibbs adsorption equation and assuming the ideal gas behavior for hydrogen, a relation, that can be used to estimate internal pressure of hydrogen in metal cavities, is derived. For the voids with relatively large radius ($r \sim 10^{-7}$ m) this relation reduces to well-known Sieverts law. In case of microvoids ($r \sim 10^{-9}$ m) it gives an elevated internal pressure of hydrogen. However, the estimated value is by two orders of magnitude lower comparing to the level, predicted by earlier proposed approach (1).

References:
1. Zapfe C.A., Sims G. (1941) Trans. ASME 145, 225-259.
2. Zapfe C.A. (1941) Met. Progr. 39, 6, 802-808.
3. Kolachov B. (1985) Hydrogen embrittlement of metals. Moscow: Metallurgy, (In Russian).
4. Burg M.W.D. van der, Giessen E. van der, Brouwer R.C. (1996) Acta. Mat. 44, 2, 505-518.
5. Kurtasova L. A., Polansky V. (1980) Physico-Chemical Mechanics of Materials, 4, 7-12. (In Russian).

Hydrogen Production, Absorption and Transport During Environment Assisted Cracking of an Al-Zn-Mg-(Cu) Alloy in Humid Air. G.A. Young, J.R. Scully, University of Virginia, Charlottesville, VA, USA

Precipitation hardenable Al-Zn-Mg alloys are susceptible to hydrogen environment-assisted cracking (HEAC) when exposed to aqueous environments. In Al-Zn-Mg-Cu alloys, overaged tempers are used to increase HEAC resistance at the expense of strength but overaging has little benefit in low copper alloys. However, the mechanism or mechanisms by which overaging imparts HEAC resistance is poorly understood. The present research compares hydrogen uptake, diffusion and trapping behavior to stage II crack growth rate in 90% relative humidity (RH) air for both a commercial copper bearing Al-Zn-Mg-Cu alloy (AA 7050) and a low copper variant of this alloy in order to better understand how the factors which affect HEAC resistance are altered by aging. Experimental methods used to evaluate hydrogen concentrations local to a surface and near a crack tip include nuclear reaction analysis (NRA), focused ion beam, secondary ion mass spectroscopy (FIB/SIMS) and thermal desorption spectroscopy (TDS).

Humid air is a very aggressive environment capable of producing near surface (~1 mm) hydrogen concentrations in excess of 10,000 wt. ppm at 90ºC when freshly bared coupons of AA 7050 are exposed to 90ºC, 90% RH air. Hydrogen ingress follows inverse-logarithmic-type kinetics and is equivalent for underaged (HEAC susceptible) and overaged (HEAC resistant) tempers. However, when the native oxide is allowed to form (24 hrs in 25ºC, 40% RH lab air) prior to exposure to 90ºC, 90% RH air, the overaged alloy shows significantly less hydrogen ingress than the underaged alloy. Results show that overaging the copper bearing alloys both inhibits hydrogen ingress from oxide covered surfaces and decreases the apparent hydrogen diffusion rates in the metal. As AA 7050 is aged from underaged to peak aged to an overaged condition, the activation energies for hydrogen diffusion and stage II (K-independent) crack growth increase and the apparent diffusivity of hydrogen and stage II crack growth rate decrease. In the low copper alloy, overaging has little effect on hydrogen diffusion or crack growth kinetics. Comparisons of the apparent activation energies for hydrogen diffusion and for K independent (stage II) crack growth rate in 90% RH air between 25 and 90ºC suggest that hydrogen transport kinetics can account for the decreased crack growth rate of overaged AA 7050 relative to the peak aged temper assuming that cracking occurs when the hydrogen concentration exceeds a critical level over a local distance ahead of the crack tip. This argument is supported by moving line source analyses of diffusion controlled hydrogen uptake.

Hydrogen Interactions with Aluminum Surfaces. R. Bastasz, J.A. Whaley, Sandia National Laboratories, Livermore, CA, USA

We have measured the effects of thermal adsorption and energetic hydrogen bombardment on aluminum surfaces using low-energy ion scattering (LEIS) spectroscopy and secondary-ion mass spectrometry (SIMS). Clean polycrystalline Al and Al(111) surfaces were prepared by sputter cleaning using either Ar or He ions followed by annealing in vacuum (base pressure <100 nPa) to at least 825 K. The surface condition of the samples was monitored using LEIS spectroscopy, which confirmed that the preparation method removed the native oxide layer and, in the case of Al(111), produced an ordered surface. SIMS measurements using a 500 eV H2+ or H3+ primary ion beam showed that significant emission of aluminum hydride secondary ions (AlH+ and AlH2+) occurs when surface hydrogen is present. There was no appreciable difference in the secondary-ion species distribution produced by H2+ or H3+ bombardment. Aluminum hydride ion emission was absent during He ion bombardment. Adsorption of atomic deuterium on clean Al(111) was studied using a thermal deuterium atom source with a flux of about 10^{14} D/cm^2-s and LEIS spectroscopy. Measurements made at an observation angle below the maximum angle

(300) for He scattering from D, showed a weak scattering peak from adsorbed D. It appears that surface Al atoms shadow much of the adsorbed deuterium, indicating that the preferred adsorption site for D on Al(111) is below the topmost Al atom plane.

Corrosion Fatigue of Riveted Joints with LY12CZ Aluminum Alloy in 3.5% Sodium Chloride Solution. E-H. Han, B. Zhang, Z.G. Zhang, W. Ke, The Chinese Academy of Sciences, Shenyang, China

Corrosion and corrosion fatigue (CF) are the most common failure phenomena on aircraft. The riveted joints are often used in airplane from where corrosion damage is often initiated. In order to solve aging aircraft problems, many research works about damage mechanisms have been done. However, the difficult thing is to do the real structural research work under serving condition. And most difficult thing is how to relate the laboratory results and practical behavior of materials and structure. Therefore, to study materials' behavior under the imitating real operating conditions is very useful for the lifetime prediction of aging aircraft.

The CF of riveted joint with LY12CZ aluminum alloy (similar 2024), which is used for fuselage, was performed under 3.5% sodium chloride solutions. The rivet material is LY10. The specimen shape is dog bone and six rivets are in the middle of the specimen with two rows. All processing methods are same with practical in fuselage. In order to comparing, the bare specimens also were used with no any paints. The CF experiments were conducted by EHF-EB10-20L electro-hydraulic servo fatigue machine with stress ratio 0.1, frequency 6Hz and wave shape sinusoidal. Two stress levels (30 MPa and 50 MPa), different pH value (6 and 3) and temperature (18, 25, 40, 60 degree C), and various pre-immersion terms (10, 30, 60, 150 days) were selected to mimic real operation conditions. Fracture surface was observed by optical microscope and scan electron microscope.

Pre-immersion time: Pitting, intergranular corrosion, exfoliation and crevice corrosion are occurred on the riveted specimen. And the corrosion phenomena are more severe with the advance of time. CF life is decreased with the pre-immersion time. At the earlier stage of pre-immersion, CF lifetime is decreased rapidly. For the long term pre-immersion, CF life time also decline but not as obvious as it at the earlier stage. The decreasing curve shape is like the exponential curve. The decrease is more obvious for the lower stress level. However, the CF life of the riveted specimen without pre-immersion under room temperature is longer than that in air under both the relatively high and low stress amplitude. For the coating removed specimen, CF life is always lower than that in air.

Temperature: Under 30 MPa stress amplitude, CF life decreases with temperature increasing and is an exponential function of temperature. Here, pre-immersion in corrosive environment also declines the CF life. Under room temperature, the CF life time of 50 days pre-immersion is only one third of that of unimmersion. Under 60 degree C, CF life of 50 days pre-immersion is about three fourth of that of that of unimmersion which is also about one third of CF life under room temperature and unimmersion approximately. Under higher stress level (50 MPa), CF life also decrease with temperature increasing but the changes are not large as at lower temperature.

pH value: The CF fatigue life under pH 3 is only one fourth of that under pH 6, and is also half of that in air.

In order to understand the mechanisms, the polarization curves under various conditions similar to all experimental were measured. And the SEM was used to recognize the evidences for anodic dissolution, hydrogen embrittlment, crack propagation marks etc. on the fracture surface.

Hydrogen Embrittlement of Al 2195 Alloy. E.I. Meletis, Louisiana State University, Baton Rouge, LA, USA

Aluminum-lithium alloys can be susceptible to environment-assisted cracking (EAC) depending on their composition and aging treatment. Our previous studies have shown that the degree of embrittlement correlates well with the precipitation characteristics of the T1 (Al_2CuLi) phase and the slip behavior. The present evidence suggests that more than likely EAC occurs via a hydrogen embrittlement (HE) mechanism. Recent experiments on Al 2195 (Al-1Li-4Cu-0.12Zr) showed significant susceptibility when the alloy was tensile tested after an alternate immersion stage in NaCl solution. However, it is difficult to assess the embrittlement process in the latter tests since both anodic dissolution and hydrogen uptake can take place. In the present study, the HE behavior of Al 2195 was investigated by using two different ways of introducing hydrogen into the alloy. First, samples were cathodically charged at a constant current density (10 mA/cm^2) in 0.1M NaCl solution (pH=13) for sufficient time to ensure saturation. In the second process, hydrogen was introduced by utilizing a vacuum chamber and using hydrogen plasma under low pressure. After hydrogen pre-charging, specimens were tensile tested under slow strain rate ($7.2x10^{-6}s^{-1}$). The role of the alloy microstructure was assessed by investigating the peak aged and two overage tempers. Fractographic examinations were conducted by SEM to correlate mechanical behavior and fracture surface morphology. TEM studies were carried out to determine microstructural characteristics of the various tempers. The embrittlement process is discussed in view of the previous and new experimental findings.

The Influence of Grain Boundary Precipitation on the Stress Corrosion Cracking of Al-Li and Al-Li-Cu Alloys. R.E. Ricker, A.K. Vasudevan, National Institute of Standards and Technology, Gaithersburg, MD, USA

The stress corrosion cracking behavior of precipitation hardened alloys may depend on a large number of microstructural parameters that vary during fabrication and heat treatment such as grain size, grain boundary solute segregation, matrix precipitate size, grain boundary precipitate size, precipitate free zone size, and matrix slip character. All of these factors vary simultaneously during normal heat treatments. As a result, it is difficult to assess independently the contribution of each microstructural factor to the SCC behavior of an alloy. To enable evaluation of the influence of grain boundary precipitate size distribution on the deformation, fracture, and stress corrosion cracking behavior of Al-Li and Al-Li-Cu alloys independent of these other factors, a series of experiments were designed where the matrix yield strength (and therefore, the matrix precipitate size distribution, etc.) was held constant while the grain boundary precipitate size was systematically varied. The relative SCC resistance of the heat treatment conditions was evaluated by conducting slow strain rate tests and the deformation and fracture behavior of these alloys was evaluated by scanning electron microscopy.

Monday Evening, September 23, 2002
Session III: Permeation

Hydrogen Segregation at Dislocations, Grain- and Phase-Boundaries. R. Kirchheim, Universität Göttingen, Göttingen, Germany

Hydrogen interaction with dislocations and internal interfaces was studied by small angle neutron scattering (SANS) and field ion microscopy (3d atom probe). SANS-measurements on Pd samples containing dislocations with a density of a few 1011 cm^{-2} reveal an additional intensity for a scattering vector of 0.02 to 0.2 $Å^{-1}$ after loading with hydrogen or deuterium. The corresponding net cross section is proportional to the reciprocal scattering vector as expected for line type scattering objects with a superimposed exponential decrease stemming from scattering within the Guinier-regime. This experimental finding is in accordance with a model where extended segregation of H or D within the dilated regions of edge dislocations occurs. In a first order approximation this corresponds to a precipitation of cylindrically shaped hydrides along the dislocation line and can be treated quantitatively yielding radii in agreement with SANS data. Whereas gas volumetric measurements at the same total concentration reveal no difference for the amount of H- and D-segregation, there is a pronounced effective difference in SANS intensities which cannot be explained by the different scattering lengths alone. However, the different sign of the latter quantity in combinations with an expected volume expansion within the hydride/deuteride region provides a reasonable explanation of the intensity difference observed. Knowing the amount of segregated H or D from gas volumetry and the dislocation density from electron microscopy the SANS results can be explained in a self-consistent way. Using our tomographic or 3-dimensional atom probe the spatial distribution of hydrogen could be determined with atomic resolution. This exciting new technique is applied to H-segregation at grain boundaries, metal/oxide-interfaces and multilayers composed of thin metallic films. In the latter case we were able to demonstrate, that hydrogen is accumulated in the metal with the lowest free energy of dissolution. The H-content at the interface is determined by the intermixing of the metals during thin film preparation. During the analysis new metallic surfaces are exposed which act as strong traps for H- and or D-atoms causing hydrogen transport towards the surface and leading to a depletion in deeper regions of the samples. Thus in analogy to SIMS-measurements H-enrichment in surface near regions is observed. This artifact of the analysis can be suppressed by doing the analysis at very low temperatures.

Hydrogen Diffusion and Trapping in Low Alloy High Strength Steels. A.M. Brass, Université Paris-Sud, Orsay, France.

The improved knowledge of the behavior of materials in stress corrosion cracking conditions requires the study of the competing effects of surface phenomena governing the hydrogen absorption and of bulk processes, such as hydrogen trapping on metal defects, lattice diffusion or enhanced dislocation transport, leading to hydrogen accumulation and hydrogen embrittlement. The objective of this paper is to present experimental results on the effect of plastic deformation on the hydrogen absorption, diffusion and trapping in Cr-Mo high strength steels. The influence of stationary dislocations on the hydrogen absorption and transport in Cr-Mo steels exhibiting different trapping caracteristics is investigated as a function of the hydrogen activity, through electrochemical permeation measurements and H concentration analyses. The absorption and diffusion of hydrogen in pure iron and steels exposed to cathodic charging during continuous deformation from the elastic to the plastic domain are studied through electrochemical permeation tests performed during plastic tensile straining. The influence of strain on hydrogen absorption is inferred from the change in the hydrogen discharged current density or potential during cathodic

polarization. The dependence of the permeation flux on strain is discussed with respect to the strain rate and the trapping caracteristics of the steels, with special attention paid to the external hydrogen activity. The net permeability of the steel to hydrogen during dynamic tensile straining is controlled by the relative influence of dynamic trapping or enhanced transport of hydrogen by dislocations, according to the diffusible hydrogen concentration.

Local Hydrogen Uptake in Stationary and Propagating-Real and Model Crack Tips. J.R. Scully, D.G Kolman, G.A. Young, Jr., L.M. Young, R.P. Gangloff, University of Virginia, Charlottesville, VA, USA

A damaging role of hydrogen is postulated in the mechanism for environment-assisted cracking (EAC) of many engineering alloys. Numerous relationships between fracture toughness and diffusible hydrogen content have been developed based on gas phase hydrogen charging and bulk electrochemical charging experiments. However, local crack tip hydrogen concentrations during EAC remain elusive. Therefore, threshold stress intensities as well as crack growth rates remain difficult to predict during EAC. Over 30 years ago, potential-pH diagram analysis demonstrated that the occluded geometry of a crack tip, crevice, or pit could enhance both hydrolytic acidification and promote ohmic potential drop. The resulting hydrogen overpotential created a situation where a high, yet vaguely specified, hydrogen fugacity was thermodynamically assured at an occluded site. The potential and pH of the bulk solution outside the pit or crack precluded such high hydrogen fugacities on external surfaces away from the occluded site. In these cases, hydrogen ingress could occur at the local occluded site without bulk external hydrogen charging. However, near-surface hydrogen concentrations within crack tips and pits have not been extensively quantified. Early attempts to quantify hydrogen concentrations at crack tips and other occluded sites has focused on permeation experiments in bulk analogs of crack tip solutions at appropriate potentials representative of the crack tip or pit bottom. Additionally, expressions governing the relationship between hydrogen production rate and diffusible hydrogen concentration, derived from permeation experiments, were used in combination with scratch-repassivation data. The transient reduction of water kinetics were taken to simulate hydrogen production rates at transiently bare crack tips. Problems with these approaches include the inherent uncertainty concerning local crack solution compositions and hydrogen production rates as well as difficulty in duplicating surface films, near-surface trap state densities, and near-surface alloy compositions. These issues create great difficulty in quantifying exact hydrogen concentrations at crack tips as well as within crevices and pits. Such analysis methods are particularly thwarted in the case of passive film forming alloys where the passive film on the crack flanks serves as a hydrogen permeation barrier.

In this presentation, several newer approaches to quantify local hydrogen production and uptake are reviewed. These methods have allowed us to overcome many of the experimental difficulties inherent to the problem of local crack tip or pit hydrogen analysis in passive film forming alloys. Results will focus on two independent systems (e.g., high strength titanium alloys and precipitation age hardened aluminum alloys) linked together by several common features. These include passive films that serve as hydrogen permeation barriers and very reactive bare metal surfaces that assure high hydrogen production rates. Analyses of electrochemical transients associated with deformation/film rupture/electrochemical reaction events at crack tips have been performed. These tests indicate that crack tip potentials assure high local hydrogen production rates and that a significant fraction of the cathodic reaction supporting film repassivation occurs at the crack tip. Moreover, various hydrogen analysis tools have been applied to either actual or simulated crack tips to examine hydrogen uptake. Thermal desorption has been applied to small straining electrodes in order to examine hydrogen uptake under film rupture conditions simulating

straining crack tips. Crevice scaling laws have been implemented to enable duplication of the occluded site conditions representative of a small pit, crevice, or crack in larger-sized model electrodes. These model pits are more assessable to hydrogen measurements from the standpoint of length scale and analysis volume. Moreover, a variety of hydrogen probes with enhanced combinations of lateral and depth resolution, as well as great sensitivity to hydrogen concentration have been utilized to examine straining electrodes, actual crack tips as well as model crevice and crack tip electrodes. These include focused ion beam/secondary mass spectroscopy, thermal desorption spectroscopy, and nuclear reaction analysis. The results indicate that local crack tip hydrogen concentrations are very high in the vicinity of Al and Ti crack tips even when anodically polarized. Such concentrations would be difficult to predict based on global hydrogen measurements. Moreover, steep hydrogen concentration gradients are seen at crack tips. Moving line source analysis of hydrogen transport in front of non-stationary cracks reveals steep hydrogen concentration gradients that decay rapidly with distance. The implications towards environment assisted crack initiation and growth models are discussed.

Analyses for the Rate Constants of the Hydrogen Absorption/Evolution Reactions for Both Langmuir and Frumkin Conditions. H.W. Pickering and F.M. Al-Faqeer, The Pennsylvania State University, University Park, PA, USA

This paper reviews the progress made using the Iyer-Pickering-Zamanzadeh (IPZ) analyses for determining the important parameters (rate constants, hydrogen coverage on the surface and concentration in the metal, and exchange current density, i_o) of the hydrogen evolution and absorption reactions. The change in these parametric values is being used to understand the role of additives to the electrolyte, e.g., H_2S, in promoting hydrogen absorption into steel. The initial IPZ analysis is a limiting one since it is only applicable to metal/electrolyte systems that undergo Langmuir-type adsorption. This analysis has recently been generalized to systems that undergo Frumkin-type adsorption. The original IPZ analysis has been successfully applied by different groups to steady state permeation data for some Langmuir-type systems, and the generalized IPZ analysis is now being applied to permeation data for Frumkin-type systems. Values of the parameters are not generally available in the literature, but for those that are available, e.g., i_o, the comparisons are good. An alternative analysis has also been developed for determining the rate constants of the hydrogen evolution reaction from the much more widely available (than permeation data) Tafel data of the cathodic polarization curve.

Role of Hydrogen in Stress Corrosion Cracking of Low Strength Al-Mg. R.H. Jones, M.J. Danielson, Pacific Northwest National Laboratory, Richland, WA, USA

There is continuing uncertainty regarding the relative roles of anodic dissolution and H induced crack growth in Al-Mg alloys containing discrete grain boundary β phase particles. Evidence exists for preferential anodic dissolution of the β phase in Al; however, this dissolution cannot account for the total crack extension for grain boundaries with discrete particles. There is also evidence for considerable H generation and uptake during corrosion of Al and A5083 but no direct evidence for H induced crack growth. Results from hydrogen permeation measurements using a Devanathan-Stachurski cell and changes in electric potential drop in the absence of crack growth provide strong evidence for hydrogen uptake during stress corrosion cracking of Al-Mg alloys. The purpose of this paper is to review the data on crack growth of the low-strength aluminum alloy AA5083 and to identify the possible role of H.

Hydrogen Effects on Grain Boundary Fracture During SCC in Al-5Mg: Critical Experiments and Atomistic Computer Simulations. D. Tanguy, B. Bayle, T. Magnin, Ecole Nationale Supérieure des Mines, Saint-Etienne, France

We studied the stress corrosion cracking (SCC) mechanisms of pure Al-5Mg in NaCl 30g/*l*. The alloy has a very limited intergranular Al_3Mg_2 precipitation. It is therefore very resistant to stress enhanced intergranular corrosion which is the classical SCC mechanism. Under these conditions, crack initiation is slow but we showed that fast propagation (500 μm / day) can be promoted if single cracking and solution confinement are favoured. These observations have induced a set of critical experiments, under static and cyclic loading, in a simulated confined medium. Its composition is chosen to favour the production of external hydrogen.

The results are:
The fast crack propagation does not stem from anodic dissolution alone.
Hydrogen is responsible for the loss of mechanical properties of the grain boundaries.
The local plasticity is the key mechanical parameter.
These macroscopic experiments show that intergranular SCC of Al-5Mg is related to an interaction between plasticity, grain boundaries (GB) and hydrogen.

Atomic scale computer simulations are used to study in detail the implication of hydrogen in the GB fracture. We developed a many body interatomic potential of the "glue" type to describe the Al-Mg-H system. The computation is dedicated to intergranular hydrogen trapping to $\sum$=5(310)[001] symmetrical tilt GB. Monte Carlo simulations revealed a spectacular interface "separation" induced by hydrogen segregation. In the interface core, the Al-Al distances are severely stretched out, which can be a plausible cause of the interface loss of cohesion. The numerical simulation allows a detailed analysis of this phenomenon. The "separation" stems from the large density of deep trap sites, called "holes", in the grain boundary. The synthesis of the experiments and the computer simulations is at the origin of a new model for GB fracture at the atomic scale. The model is an attempt to explain how the GB can be embrittled by the combined action of dislocations and hydrogen, no matter their initial structure.

Irreversible Hydrogen Trapping in High-Strength Alloys. B. Pound, Exponent Failure Analysis Associates, Menlo Park, CA, USA

The intrinsic susceptibility of various high-strength alloys to hydrogen embrittlement (HE) was characterized in terms of irreversible trapping. Two groups of alloys were studied: steels (AerMet 100, two 18Ni maraging steels, and AISI 4340 and H11) and precipitation-hardened alloys (A-286, 718, 925, X-750, and 2Be-Cu). Irreversible trapping constants (k) were obtained for these alloys and compared with the susceptibilities to HE determined in other studies. Both groups of alloys exhibited a correlation between k and the observed susceptibility to HE. The order of the k values for the steels inversely paralleled their threshold stress intensities for stress corrosion cracking. Likewise, the k values for the precipitation-hardened alloys were consistent with data for the reduction of notch strength. Calculations based on a model involving spherical traps showed that differences in the trap size and density and the lattice diffusivity can account for the range of k values obtained for the two groups of alloys. Comparison of the k values with the reduction in strength for alloys from both groups showed that the correlation extends across the two groups, which suggests that irreversible trapping plays an important role in determining the intrinsic susceptibility to HE for a broad range of high-strength alloys.

Tuesday Morning, September 24, 2002
Session IV: Hydrogen Induced Cracking

Hydrogen Embrittlement: Plasticity vs Decohesion Mechanisms. I.M. Robertson, University of Illinois, Urbana, IL, USA

The phenomenon of hydrogen embrittlement has been known for over a century and yet there is still controversy over the physical mechanisms that operate. The most common mechanisms include decohesion, stress-induced hydride formation and cleavage, and plasticity enhancement. While there is ample experimental evidence for the latter two, there are no direct measurement of hydrogen reducing the cohesive strength of the solid, which is required by the decohesion mechanism. In this talk, the experimental evidence for the plasticity-based mechanism will be reviewed. In addition, the results of an extensive study of hydrogen effects in a beta-Ti alloy will be presented, and it will be argued that these are consistent with the decohesion mechanism.

Functions of Microstructures in Delayed Fracture of Martensitic Steels. M. Nagumo, T. Tamaoki, T. Sugawara, Waseda University, Tokyo, Japan

The susceptibility to delayed fracture of martensitic steels is sensitive to the microstructures. The functions of microstructures, precipitates and tempered structures, have been examined by means of hydrogen thermal desorption analysis with Mo- and Mo-V containing steels. The amount of hydrogen desorption increased when hydrogen was charged concurrently with loading. The origin of the increment has been assigned to strain-induced point defects. The susceptibility to delayed fracture could be well correlated with the density of the defects. The stability of microstructures under loading is likely to play an essential role on the delayed fracture susceptibility through the formation of vacancy-originated defects.

Interactions of Hydrogen with Amorphous Nano-Structures and Their Effects on Deformation, Fracture and Fatigue-Behavior of Zr-Ti-Ni-Cu-Be Bulk Metallic Glass Alloys. D. Suh, R.H. Dauskardt, Stanford University, Stanford, CA, USA

In recent years, a series of multi-component bulk glass forming alloys have been developed. The Zr-Ti-Ni-Cu-Be alloy system exhibits a range of unique properties including ultrahigh strength (~1.9 GPa), large elastic strains (up to 2 %), and excellent corrosion and wear resistance. They have the potential for a versatile class of new advanced engineering materials and provide opportunities for fundamental studies of metallic glasses. Previous studies of metallic glasses in the form of thin ribbons suggest that they are susceptible to deleterious effects of hydrogen embrittlement. Understanding hydrogen embrittlement in amorphous metals is, however, far from complete compared to the considerable progress that has been achieved in crystalline metals. The objective of the present work is to understand the interactions of hydrogen with the amorphous nano-structure of a Zr-Ti-Ni-Cu-Be bulk metallic glass alloy. A range of mechanical and thermal behavior, including viscoelastic deformation, strength, fracture, fatigue crack growth, glass transition and crystallization kinetics was examined after hydrogen charging. The nano-scale structure of the hydrogen-charged metallic glass was examined using positron annihilation spectroscopy, high-resolution transmission electron microscopy, small-angle X-ray and neutron diffraction, and X-ray photoelectron spectroscopy, to identify the atomic-scale origin of hydrogen interactions with the amorphous microstructure. It was found that hydrogen increased the time scale for structural relaxation in the amorphous microstructure. The sluggish structural relaxation

process caused higher glass transition temperature, retarded crystallization kinetics and increased viscosity. The sluggish atomic rearrangement process is, in turn, believed to suppress stress relaxation at crack tips and hence cause brittle fracture. In contrast, fatigue crack growth was significantly retarded after hydrogen charging. Such conflicting results are interpreted in terms of a mutual competition between degradation of the inherent resistance to crack extension and a reduced crack driving force by crack tip shielding mechanisms. Possible mechanisms to account for the sluggish atomic rearrangement process are discussed in terms of hydrogen interactions with the nano-scale structure of amorphous metals.

Analysis of Hydrogen Related to Embrittlement of an Al-Zn-Mg-Cu Alloy. J. Okahana, S. Kuramoto, M. Kanno, The University of Tokyo, Tokyo, Japan

Behavior of hydrogen has been examined in relation to environmental embrittlement of an Al-Zn-Mg-Cu alloy. High strength aluminum alloys are susceptible to stress corrosion cracking (SCC) and it is known that the cracking occurs even in air. It has been considered that such embrittlement is caused by hydrogen that permeates from the environment, but there has been no direct evidence. In this study, permeated hydrogen was successfully shown by direct analysis in embrittled specimens.

An ingot was made from 99.99% aluminum, 99.9% zinc, 99.9% magnesium, and Al-33%Cu master alloy, homogenized for 24h at 470:C, and then hot-rolled to 7.8 mm in thickness. Round tensile specimens with gage dimensions of 4.0 mm diameter and 10mm length were machined from the hot rolled material. The specimens were solution treated for 1h at 470C, quenched in water, and aged for 24h at 100C. Tensile testing was carried out in laboratory air at an initial strain rate ranging from $1.67W10^{-7}$/s to $1.67W10^{-4}$/s. It was confirmed that embrittlement occurs as strain rate decreased. Observation of fracture surfaces revealed that transgranular fracture was almost overall at an initial strain rate of $1.67W10^{-4}$/s, but ratio of intergranular fracture surface increased with decreasing strain rate. At the lowest strain rate of $1.67W10^{-7}$/s, it was found that the whole fracture surface was intergranular. To show experimentally that hydrogen permeated the specimens from the testing atmosphere, some specimens were pre-deformed in air saturated with heavy water vapor, and gas emission during subsequent deformation and fracture was analyzed using quadrupole mass spectrometer. As a result, deuterium was emitted from the specimen continuously during deformation, which indicated that deuterium permeated deep into pre-deformed specimens. In the case of the specimen pre-exposed for equal time in the unstressed condition to heavy water vapor, deuterium was emitted only before the onset of plastic deformation. This means that, by only pre-exposure, deuterium did not permeate inside of the specimen but existed only near the surface. Therefore, it suggests that dislocation motion accompanied by plastic deformation contributes hydrogen transport into the interior of the material and such hydrogen has brought about embrittlement.

A Perspective on Corrosion and Corrosion Fatigue. R.P. Wei, Lehigh University, Bethlehem, PA, USA

Research on corrosion and corrosion fatigue (aging) of airframe aluminum alloys over the past decade, in connection with aging aircraft, has provided additional insight on their interrelationship and a new perspective on these processes. Corrosion and corrosion fatigue in these alloys operate competitively, and damage evolution is dominated by localized (pitting) corrosion at the beginning and subsequently by corrosion fatigue crack growth. In this presentation, current understanding of the aging of airframe aluminum alloys and its application to application to damage evolution and distribution are briefly

summarized. Mechanistically based modeling of pit growth in terms of the galvanic coupling of constituent particles and the alloy matrix is summarized. Recent observation of an environmentally induced transition of predominant cracking from {001} to {011} is summarized, and the need for a mechanistically based model for fatigue crack growth is discussed. A perspective on the long-standing dichotomy between the S-N and crack growth (dissolution and hydrogen embrittlement) approaches to corrosion fatigue is proffered in the context of these findings.

The Sour Gas Susceptibility of Steels for Oil and Gas Transport. J.L. Albarran, S. Serna, G. Gonzalez, L. Martinez, UNAM, Cuernavaca, Mexico

High strength low alloy (HSLA) pipeline steels have been developed for applications in hydrogen sulfide environments. The major efforts have been focused on the increase in the yield strength, however the microstructure remains as the main factor that modify the susceptibility to sulfide stress corrosion cracking in sour environments. The sulfide stress cracking (SSC) is a mode of degradation that appear when a hydrogen sulfide environment is present combined with a local state of stress. Most SSC failures are directly related to hydrogen embrittlement (HE) as a result of hydrogen generation and permeation into the crack tip regions. Nascent hydrogen is generated as a product of the corrosion reaction by which a sulfide film forms on the surface of the steel as it is exposed to wet hydrogen sulfide environment. In this work, the role of the yield strength was investigated (steels type API 5L grades X-52, X-65, and X-80) in order to correlate the susceptibility to sour environments.

The environments selected were solutions of NaCl (5% and 3 wt ppm.), saturated with CO_2 and H_2S, and CO_2 without H_2S. In order to correlate the electrochemical behavior with the crack rate, the samples were studied using linear polarization resistance and cyclic polarization in an instrumented vessel at 500C and a pressure of 200 kPa. The susceptibility to SSC was investigated using LEFM compact samples (MWOL specimens), loaded in all cases to 95% of each yield strength. The steel with higher resistance are prone to hydrogen embrittlement produced by anodic dissolution. However, the steel with lower resistance shows a marked corrosion in the fracture surfaces exposed to the environment. In all cases the solution with 3 wt. ppm of NaCl shows the lower corrosion rate, and there is no evidence of crack growth, shows dissolution bulbs.

The Influence of Plastic Strain on the Hydrogen Diffusion in a HSLA Steel: Simulation of Effective Diffusion Coefficients and Hydrogen Assisted Crack Growth. M. Pfuff, G.G. Juilfs, W. Dietzel, GKSS-Forschungszentrum Geesthacht, Geesthacht, Germany

The permeation of hydrogen through thin foils of a low alloyed structural steel (FeE 690T) which had been plastically deformed to various degrees was treated by the transport model proposed by Krom et al. for simulating the hydrogen distribution near a blunting crack. In this model it is assumed that hydrogen atoms diffusing through lattice sites are partially trapped by trap sites due to plastic deformation. The occupancy of traps is determined using the assumption of thermodynamical equilibrium and turns out to depend on the concentration of hydrogen in lattice sites and on the binding energy of hydrogen atoms to the trap sites. The hydrogen distribution within the foil was calculated as a function of the trap density by numerically solving a non-linear diffusion equation which explicitly depends on the trap density. By use of the time lag method effective diffusion coefficients were determined for different loading histories from the flux of hydrogen atoms through the foils. Good agreement was found between the numerical simulation and the experimental data over the whole range of plastic strain levels tested when assuming that

the trap density is related to the plastic strain by a simple power law. Values of the trap density were derived from these results for different degrees of plastic deformation.

A discrepancy between experimental data and simulation was observed when the slope of the measured permeation current as a function of time was compared with the slope of the simulated flux of hydrogen atoms. This difference vanished when changing the boundary condition for the hydrogen concentration at the cathodic side of the foil. By assuming that hydrogen entry preferably takes place at `active sites` which are stochastically distributed across the metal surface a good agreement between measured and calculated curves was obtained.

The trap diffusion model was also used to explain the results of previous investigations on the influence of hydrogen on crack growth in the same steel FeE 690T. Here, it is assumed that hydrogen atoms diffusing from the crack tip into the plastic zone reduce the local strain to failure. Based on this assumption and on the relationship between trap density and plastic strain obtained from the permeation experiments the crack growth rate was calculated as a function of the applied deformation rate again yielding good agreement with the experimental data.

Hydrogen Induced Intergranular Stress Corrosion Cracking in Nickel Based Alloys 600 and 690 Under High Temperature Water/Steam. H.F. Lopez, A. Mehboob, University of Wisconsin-Milwaukee, Milwaukee, WI, USA, J.L. Albarran, L. Martinez, Instituto Mexicano del Petroleo, Col. San Bartolo Atepehuacan, Mexico.

Intergranular stress corrosion cracking (IGSCC) of Inconel alloys 600 and 690 was investigated in the temperature range of 320-420°C in deaerated hydrogen supersaturated steam. Crack growth rates were measured in-situ in the above alloys using modified wedge-opening-load (M-WOL) linear elastic fracture specimens under constant displacement conditions. Applied stress intensity factors (K_I) of 60 and 80 MPa-$m^{1/2}$ were used in measuring the rates of crack growth. The alloys were tested in the as-received condition, and after annealing at 930°C, followed by air cooling. This heat treatment was expected to result in predominant intergranular carbide precipitation, which makes the alloys susceptible to IGSCC. Crack propagation in these alloys along the grain boundaries was examined taking into account the potential for the development of methane bubbles and their linkage just ahead of the crack tip. Discussion of the kinetics of the crack growth rates combined with the microstructural evaluations provides validity to the above-mentioned model.

Interactions Between Previous Cyclic Deformation and Stress Corrosion Cracking in Cold Drawn Steel. J. Toribio, V. Kharin, E. Ovejero, University of Salamanca, Zamora, Spain

Cold drawn eutectoid steels are high-strength materials used as constituents of prestressed concrete structures in civil engineering, and these materials are anisotropic in the matter of fracture in air and stress corrosion cracking. The reason is the manufacturing process by cold drawing which produces a marked orientation of the pearlitic microstructure of the steel at the levels of pearlitic colonies and lamellae, inducing strength anisotropy. This work describes experimental evidence of mixed-mode stress-corrosion cracking in cold drawn eutectoid steel and discusses the interactions between the previous cyclic deformation by fatigue pre-cracking and the posterior stress corrosion cracking process itself.

The material used in the study was a high-strength pearlitic steel in the form of cold-drawn prestressing wire supplied from commercial stock. The experimental programme included slow strain rate tests performed on transversely pre-cracked rods immersed in aqueous environment.

The tests were carried out at two constant electrochemical potentials E = -1200 mV SCE (cathodic), so the mechanism of environment-sensitive fracture was hydrogen assisted cracking (HAC) and E = -600 mV SCE (anodic), so the mechanism of environment-sensitive fracture was localised anodic dissolution (LAD) or pure stress-corrosion cracking.

The main result of the stress-corrosion cracking tests (HAC and LAD) is a special fracture profile associated with the anisotropic behaviour of the cold drawn steel wire. In HAC, cracking from the tip of the mode I fatigue pre-crack propagates at an angle about 80: to its plane, thus producing early mixed mode propagation. In LAD, cracking from the tip of the mode I fatigue pre-crack develops initially in mode I and later at an angle about 80: to its plane, (mixed mode growth). In both HAC and LAD, another crack embryo (a second kink) exists symmetrically to the pre-crack, i.e., the phenomenon is initially crack branching (two crack embryos) and finally crack deflection, i.e., only one of them becomes the final fracture path.

The experimental fact explained above is explained by analyzing the role of fatigue pre-cracking on the posterior stress-corrosion cracking initiation. To this end, finite deformation analysis of a plane strain crack subjected to mode I loading under small scale yielding was performed and different continuum mechanics variables analyzed throughout the pre-loading route, in particular the hydrostatic stress as the variable governing hydrogen transport by diffusion, the equivalent plastic strain as a measure of mechanical damage and the equivalent plastic strain rate as the variable governing hydrogen transport by dislocation movement.

Results of the computational elastoplastic analysis of stress-strain evolution in the vicinity of the crack tip subjected to fatigue and subsequent rising loading are consistent with the experimental fact of anisotropic cracking behaviour of prestressing steel in corrosive environment. It can explain (if coupled with the inherent anisotropy associated with the oriented microstructure of the steel) why crack branching (very early in the case of HAC) takes place at a deflection angle in relation to mode I crack extension.

Tuesday Afternoon, September 24, 2002
Session V: Stress Corrosion Cracking

Overview of Corrosion Deformation Interactions During Stress Corrosion Cracking and Fatigue Cracking. (Keynote) T. Magnin, D. Delafosse, B. Bayle, C. Bosch, Ecole des Mines de Saint-Etienne, Saint-Etienne, France

The objective of this keynote lecture is to show some critical corrosion-deformation interactions which can be taken into account to model stress corrosion cracking and corrosion fatigue.

- Non exhaustive examples of effects of plasticity on electrochemical reactions and of effects of electrochemical reactions on plasticity will be first given, through critical experiments.
- Then stress corrosion cracking tests on Al-Mg alloys and C-Mn steels will be presented to show that damage is mainly related to dynamic straining (slow strain rate tests, creep tests…) and not directly to the applied stress amplitude. Consequences for the type of tests necessary to classify the SCC resistance will be then precised.
- The third part will show how to introduce the local CDI inside classical stress corrosion cracking mechanisms and models. A particular emphasis will be made on hydrogen - dislocation interactions and on vacancies (produced by the anodic dissolution) - dislocation interactions at stress corrosion crack tip. Moreover hydrogen – dislocation interactions at the vicinity of grain boundaries will be also taken into account. Numerical simulations at both the dislocation scale

and the atomic level will be presented to model such local CDI and their consequences on SCC damage.

- Solutions to prevent SCC damage will be proposed in terms of modifications of local CDI.
- Finally, the interest of such approaches on quantitative modelisation of SCC damage and connected critical tests for materials selection will be presented

The Increment of Hydrogen-Induced Corrosion Fatigue Crack Growth per Cycle: Comparing Theory and Experimental Data. S.A. Shipilov, The University of Calgary, Calgary, Alberta, Canada

Many theoretical models have been proposed in discussion of the fatigue crack growth (FCG) phenomenon. Most of these models are based on considering the elastic-plastic fields in the immediate vicinity of a fatigue crack tip. The basic postulation of these models is that the FCG rate is controlled by the small plastically deformed region ahead of the crack usually referred to as the plastic zone, and is based on Rice's suggestion that two types of plastic zones can be at the tip of a fatigue crack. These are a monotonic plastic zone and a cyclic plastic zone. Most models do not account for the significant accelerating effect of environmental factors on FCG rates, possibly because the small scale on which crack growth increments per cycle take place makes it difficult to do so.

In this paper, a comparison was made between hydrogen-induced corrosion FCG rates and critical distances ahead of the growing crack. This comparison was made by using experimental results based on the corrosion FCG behavior of two high-strength low-alloy steels, two titanium alloys, and a magnesium alloy. The critical distances included the distance to the location of maximum triaxial stress ahead of the crack, the sizes of cyclic and monotonic plastic zones and the depths of hydrogen penetration due to lattice diffusion and dislocation sweeping. Hydrogen-induced corrosion FCG rates were presented as macroscopically averaged increments of crack growth per cycle. Critical distances ahead of the crack were calculated from the equations of continuum mechanics of solids.

A Comparison of Short Fatigue Crack Growth (SFCG) Rates in a Medium Strength Steel Under In-Air and Corrosion Fatigue Lading Conditions. H. Hu, Beijing Institute of Technology, Beijing, China. and R. Akid, Sheffield Hallam University, Sheffield, United Kingdom.

An evaluation of the influence of the environment on the fatigue properties of an offshore structural steel has been carried out. Smooth shallow hour-glass specimens have been tested to evaluate the fatigue response (*S - N* curve) and fatigue crack growth rate under constant amplitude loading with a stress ratio of 0.1 in both air and 3.5% NaCl solution. Cathodic polarisation at -950 mV/SCE was also applied for a number of corrosion fatigue tests. The generation and growth behaviour of cracks are investigated through successive observation of plastic replicas taken from the surface of the specimens at selected intervals. Fatigue cracks initiate mostly at defects such as inclusions in air, corrosion pits in 3.5%NaCl solution or artificial seawater under freely corroding conditions and surface defects and polishing micro-scratches under applied cathodic polarisation. The reduction in fatigue endurance caused by the presence of the corrosive environment can be partially recovered through cathodic polarisation.

IGSCC Behavior of CSL-Related and High Angle Boundaries in Ni-16Cr-9Fe-xC Alloys. B. Alexandreanu, G.S. Was, University of Michigan, Ann Arbor, MI, USA

Susceptibility to intergranular stress corrosion cracking in Ni-16Cr-9Fe-xC alloys in 360°C primary water is reduced with increasing fraction of special grain boundaries, i.e. coincident site lattice boundaries (CSLB) and low angle boundaries. The objective of this paper is to analyze the improved cracking behavior of the CSL-related as opposed to random high angle grain boundaries (HAB) from a corrosion-deformation viewpoint. The hypothesis for this work is that the IGSCC of Ni-16Cr-9Fe-xC alloys in a primary water environment occurs as a result of grain boundary deformation, particularly sliding. First, the viability of the proposed model is discussed in light of the slip oxidation model for IGSCC. Second, the difference in deformation behavior of the two main types of boundaries (HAB vs. CSLB) is documented by a series of experiments. Nanoindenter-based experiments show that for equally deformed samples, a higher CSLB fraction results in an increased average hardness. Further, hardening is greater near CSLBs than near HABs. This result suggests that recovery in HABs occurs more easily than in CSLBs. The increased recovery rates at HABs over CSLBs were also probed directly via TEM observation to show that dislocation recovery occurs more quickly in HABs than in CSLBs. Experiments are in progress to assess the sliding behavior of both CSLB and HAB types of boundaries as a result of plastic straining in 360°C Ar. A correlation between grain boundary sliding and IGSCC will be made by straining in primary water at 360°C.

Developments in Stress Corrosion of Solid-Solution Alloys. R.C. Newman, J. Deakin , B. Lynch, UMIST, Manchester, UK

There are persuasive similarities in the aqueous stress corrosion behavior of alloys such as α-brass and Au-Ag or Au-Cu. These similarities are almost certainly due to a common role of de-alloying : selective dissolution of one or more alloying elements from the solid solution. For the gold alloys, the correlation between de-alloying and SCC is easily demonstrable, although there is considerable disagreement as to the exact role of the de-alloyed material in crack growth. The present authors are amongst those who believe there is a fast substrate fracture event nucleated by the nanoporous de-alloyed layer, a process often referred to as film-induced cleavage.

For iron and nickel base alloys, such as austenitic stainless steels, the compositional dependence of SCC is quite analogous to that of noble-metal alloys, but the evidence for de-alloying processes during SCC is much less direct. One problem is that the most noble element is nickel, which is only slightly less noble than iron, and tends to dissolve at a certain rate, with corresponding evolution of hydrogen, in the acidic environment of a crack. One is thus looking for a de-alloyed layer that is in a steady state, forming at one interface and dissolving at the other, and moreover oxidizes rapidly in air upon removal from the cracking medium. There are also geometrical difficulties in applying a de-alloying model to SCC of austenitic stainless steel, chiefly that 8 or 9% nickel is not enough to form a connected porous structure upon removal of all the iron and chromium. It was speculated earlier, on the basis of some rather sparse surface analytical data, that the de-alloyed layer formed in an acidic chloride electrolyte was actually an alloy of Fe and Ni, which would alleviate the space-filling difficulty and possibly allow the formation of a strong porous network.

We now have information for austenitic stainless steel in a completely different electrolyte (strong NaOH solution) that demonstrates the feasibility of our earlier speculations on the nature of de-alloyed layers in stainless steel. There is a strong tendency for de-alloying to arrest, at least

temporarily, at the point where the porous layer has approximately 50 at.% residual iron as well as nickel, the chromium being entirely oxidized. Such a composition, for a 304SS type of alloy, implies a roughly 20% space filling layer, which from studies of gold alloys we know can form a connected porous structure (consistent with the continuum 3D percolation threshold which is about 16%). This structure can then play its role in crack growth, which in most cases will be to alter profoundly the deformation of the substrate and/or inject a microcrack that does not stop at the substrate-layer interface.

Recent studies of de-alloying and SCC in Monels (Ni-Cu alloys) will also be discussed, as will the current state of theory on the micro-mechanics of such systems.

Modeling the Influence of Crack Path Deviations on the Propagation of Stress Corrosion Cracks. R.E. Ricker, National Institute of Standards and Technology, Gaithersburg, MD, USA

Stress corrosion cracks typically nucleate at a stress concentration in the surface and propagate away from the surface on a plane perpendicular to the applied stress. While this is a good macroscopic description of crack propagation, on a microscopic scale, crack tips regularly deviate from this ideal orientation due to deviations in the preferred microstructural paths for crack propagation. These crack path deviations can be influenced by grain boundary size, shape, and crystallographic texture and may or may not have a significant influence on the accuracy of crack propagation rate measurements or the predictions of propagation rate models. This paper examines the effects that crack path deviations can have on measuring and modeling stress corrosion crack propagation by developing a technique for quantifying these deviations and estimating the difference between the measured and the true rate of crack tip propagation. Then, this technique is used to examine the influence of changes in microstructure and sample orientation on the rate of stress corrosion crack propagation.

Wednesday Morning, September 25, 2002
Session VI: Hydrogen Interactions

Thermodynamics of Two-Phase Systems with Coherent Interfaces: Application to Metal-Hydrogen Systems. R.B. Schwarz, Los Alamos National Laboratory, Los Alamos, NM, USA, A.G. Khachaturyan, Rutgers University, Piscataway, NJ, USA

A theory is developed for the coherent decomposition of an interstitial solid solution into two coherent phases of different interstitial concentration. It is shown that the coherency strain changes the conventional thermodynamics for the phase transformation by generating a macroscopic energy barrier between the transforming phases. If the system is free to exchange interstitials with an external source, two-phase coexistence is impossible because the two phases are separated by a macroscopic energy barrier that cannot be surmounted by thermal fluctuations. This barrier splits the phase-transition temperature (pressure) into two temperatures (pressures), one during cooling (increase of pressure) and another during heating (decrease of pressure). As a result, the system looses ergodicity, a fundamental requirement of Gibbs thermodynamics. The theory is applied to the decomposition of metal/hydrogen systems and explain quantitatively the ubiquitous hysteresis in the 'plateaux' of the pressure-composition isotherms and the critical pressure-composition point for the disappearance of the hysteresis.

Structure Dependence of Hydrogen Effects at Grain Boundaries in an FCC Solid. M.I. Baskes, R.G. Hoagland, Los Alamos National Laboratory, Los Alamos, NM, USA

A grain boundary may be identified by five macroscopic variables, three that define the relative orientation of the two grains and two more that define the orientation of the local boundary plane (the tangent plane), and by two microscopic variables that define the in-plane translation of one grain relative to the other. Such variables define a periodic structure, although the period may be large in some cases. However, these variables, per se, provide no details about the atomic structure of the boundary. Indeed, the atomic structure can vary dramatically over the boundary ranging from locations where the structure is close-packed to regions of very low coordination. Such variations appear even in so-called special boundaries, boundaries that have particularly low energies. Furthermore, in many boundaries multiple configurations can occur. Therefore, interactions between the grain boundary and point defects and dislocations may also vary dramatically over the boundary.

This paper explores aspects of interactions between various boundary structures and interstitial hydrogen in nickel via Monte Carlo and molecular statics using the Embedded Atom Method. It was found that grain boundaries that are structurally and energetically very different can trap similar amounts of hydrogen. In addition the transition from bulk dominated hydrogen solubility to grain boundary dominated hydrogen solubility is strongly temperature dependent in nickel. It is expected that other fcc materials that dissolve hydrogen endothermically will display similar behavior.

The Vibrational, Elastic, and Electronic Contributions to the Chemical Potentials of Hydrogen Isotopes in Palladium. W.G. Wolfer, B. Meyer, Lawrence Livermore National Laboratory, Livermore, CA, USA

The phase diagrams of Pd-H, Pd-D, and Pd-T have been measured fairly accurately for all three hydrogen isotopes, and the equations of state of the hydrogen, deuterium, and tritium gas are also well known. This offers a unique opportunity to evaluate the vibrational, the elastic , and the

electronic contributions to the excess chemical potentials of the three isotopes in a metal hydride system which can be modeled as a lattice gas.

The vibrational contributions are evaluated with an Einstein oscillator model, and it is assumed to be the only contribution which depends on the mass of the isotope. The elastic contribution is derived from the Eshelby inclusion model assuming elastic isotropy. It is evaluated with measured data for the bulk modulus of palladium hydrides and for the partial molar volume of hydrogen.

The remaining electronic contribution is then determined by fitting the model to the measured PCT data. The sum of the electronic and elastic contribution is indeed found to be the same for all three isotope systems. Furthermore, the electronic contribution is also independent of temperature when the temperature dependencies for the bulk modulus and the partial molar volume are taken into account when computing the elastic contribution.
The self-consistency achieved strongly supports the lattice gas model for the palladium hydrogen systems.

Elastic Properties of Pd-Protium, Pd-Deuterium, and Pd-Tritium Single Crystals. H. Bach, R.B. Schwarz, D. Tuggle, Los Alamos National Laboratory, Los Alamos, NM, USA

An ultrasonic spectroscopy technique is used to measure the three independent elastic constants of Pd-H, Pd-D, and Pd-T as a function of hydrogen (protium), deuterium and tritium concentration, respectively. These measurements are the first elastic constant data for the beta-phase Pd-tritium. We noticed that for the Pd-H and Pd-D crystals, the shear constants c44 and c'=(c11-c12)/2 , both change with decreasing hydrogen content. But, whereas c44 increases monotonically with decreasing hydrogen, c' increases within the beta phase, has a sharp break upon reaching the beta-(alpha+beta) boundary, and then decreases linearly with decreasing hydrogen content within the two-phase (alpha+beta) region. We attribute this behavior to dipolar relaxations occurring near the surface of the alpha inclusions in the beta matrix, which TEM has revealed have lenticular shape oriented along <110> crystallographic planes. These changes are similar in Pd-protium and Pd-deuterium. In Pd-tritium, one has an additional effect due to the formation of ^{3}He by the radioactive decay of the tritium. The effect gives a clear signature in c' (not in c44). We then use the elastic constant measurements of Pd-T crystals as a function of tritium content and aging time (i.e. ^{3}He content) to propose a model for the atomic distribution of ^{3}He in Pd-tritide at low ^{3}He concentrations. The data suggests that the ^{3}He atoms attract tritium vacancies, since this decreases the elastic strain in the crystal. Each pair introduces an elastic dipole in the crystal, and we are able to use the elastic constant measurements to deduce the anisotropy of the elastic dipoles.

Numerical Study of Microstructural Evolution in Low Alloy Cr-Mo Steels During Hydrogen Attack. S.M. Schlogl, E. Van der Giessen, University of Groningen, Groningen, The Netherlands

Low alloy Cr-1Mo steels are a standard material for reactors used in the petro-chemical industries. In case of hydrocracking or hydrotreating applications, the material of the reactor is exposed to a high hydrogen pressure and to elevated temperatures. It is this combination that is responsible for the material degradation process called hydrogen attack (HA). During HA, carbon, present in the steel, and hydrogen, originating from the gas atmosphere inside the reactor, form methane molecules. These molecules are captured in cavities which have nucleated at the grain boundaries. Due to the presence of methane and hydrogen molecules, the cavities are

internally pressurized. Consequently, the cavities grow and coalesce which finally results in intergranular fracture.

The lifetime of a reactor is mainly determined by the rate of growth of the cavities, which is very sensitive to the level of the methane pressure. Several interacting processes are involved in building up the methane pressure, including diffusion of C and of the metal atoms, dissolution of carbides and reaction of C with H to methane. A detailed study of the coupled processes involved in hydrogen attack requires a combination of continuum mechanics with solid solution thermodynamics, kinetics and chemistry. This paper is concerned with a first attempt of developing a numerical model that combines these ingredients.

First, a microstructural model is presented which takes into account these processes within the framework of a multi-component, multi-phase continuum description. The numerical model is developed for microstructures built up by a ferritic matrix and carbides such as M_7C_3, $M_{23}C_6$, M_6C and M_2C. We start with a relatively simple version, which is a one-dimensional model where the spatial arrangement of the carbides is not taken into account. We apply it to predict the microstructural evolution, the resulting methane pressure, the growth of cavities and failure times in low alloy Cr-Mo steels during hydrogen exposure. The simulations show that cavity growth and methane generation are strongly coupled, thus falsifying previous decoupled approaches to hydrogen attack, where the methane pressure was taken to be constant during exposure.

The results confirm that it is pertinent to treat the coupled processes within a second, more sophisticated model, where the carbides and the matrix are discretized. We will address the first steps in our development of a finite element code for this model. As a first step, we model diffusion of C and metal atoms in the solid solution ferrite and then model the chemical reaction with the help of special interface elements.

Migration and Trapping of Hydrogen in Martensitic Steels-Effect of Irradiation and Helium Implantation. P. Jung, Z. Yao, C. Liu, IFF, Jülich Germany

In future fusion reactors or spallation neutron sources structural materials experience severe displacement damage and compositional changes by nuclear transmutations. The latter produce large amounts of the light elements hydrogen and helium which may be retained and affect the properties of the materials. Migration and retention of hydrogen in martensitic stainless steels which are major candidates for structural materials in both devices were investigated by permeation and desorption experiments.

In a first set of experiments permeability and diffusivity of hydrogen was derived from stationary and transient gas permeation measurements. The results were evaluated in terms of a saturable-trap-model. Included were investigations on pre-irradiated specimens which showed decreasing permeation as well as diffusion of H_2 with increasing dose.

In a second experiment, permeation of deuterium was measured under simultaneous proton irradiation, showing enhancement of permeation by irradiation which was tentatively explained by enhanced permeation of ionized gas.

Thirdly diffusion of protons was measured which were implanted to various depths. The results were in gave good agreement with diffusion H_2-gas in pre-irradiated material.

Desorption of deuterium was measured on thermally loaded specimens of different thickness after quenching. Specimens pre-irradiated to various displacement doses or specimens implanted with helium showed significant enhancement of deuterium retention compared to virgin material, indicating strong trapping by irradiation defects. Some of the helium implanted specimens were subsequently annealed to investigate the effect of formation of helium bubbles on hydrogen retention. The results are compared to deuterium desorption from cold worked pure iron.

Hydrogen Effects on Multi-vacancy Formation in α-Fe. Y. Tateyama, T. Ohno, National Research Institutes for Metals, Ibaraki, Japan

Hydrogen effects on initial crack formation and crack propagation have been still one of the most important problems in hydrogen embrittlement in Fe-based structural materials. Several mechanisms for the effects such as lattice decohesion theory or enhancement of dislocation mobility have been already proposed, and furthermore there are some studies indicating the role of vacancy-hydrogen complexes. However, they are not conclusive yet, because experimental observation of H is very difficult mainly due to the low solubility into α-Fe. In order to settle which mechanism is most predominant, it is essential to clarify hydrogen states in α-Fe from microscopic viewpoints. Thus we perform first-principles investigations of hydrogen state in alpha-Fe with a proper super-cell reproducing the low solubility situation. In this work, we especially focus on the vacancy-hydrogen system in pure alpha-Fe and present the hydrogen effects on the vacancy formation and clusterization.

Concerning monovacancy-hydrogen complexes in α-Fe, it is believed that monovacancy trapping six H atoms inside ($VacH_6$) is the most stable. However, our calculations indicate that the monovacancy is most stable by trapping two H atoms at ambient condition ($VacH_2$), and the $VacH_6$ is energetically unfavorable compared to the monovacancy without H. Investigation of the electronic states and hydrogen positions in the $VacH_n$ (n=1-7) complexes indicates that the stability is mainly dominated by the hybridization between H 1s and Fe 3d dangling orbitals, and the repulsion between negatively charged H atoms in the monovacancy. This suggests that the previous calculations by effective medium theory, which strongly support the $VacH_6$ stability, will be insufficient to describe this system, because the theory intrinsically deals with embedding energy of H into delocalized Fe 4s states as the dominant effect. It is also found that the monovacancy formation energy decreases by about 30! Trapping of two H atoms leads to 10^{12} times increase of vacancy concentration at room temperature.

These results also provide a new insight for the vacancy clusterization. If the $VacH_6$ is the most stable, their clusterization is expected to be unfavorable due to the decrease of hydrogen sites in the vacancy cluster and the occupation of interstitial sites with higher energy by surplus H. This situation, however, does not occur in the case of $VacH_2$. Our calculation of binding energy of the two $VacH_2$s into Vac_2H_4 clearly denotes that this vacancy clusterization is energetically favorable. The multi-vacancy formation by the $VacH_2$ clusterization is also shown to be preferable by a simple energy model deduced from the present first-principles investigation of mono- and di-vacancies.

The present study clarifies that H can significantly affect the vacancy formation and clusterization, and implies large possibility of multi-vacancy contribution to the microscopic fracture mechanism. By comparing the lattice decohesion theory with the present results and taking the relation between vacancies and dislocation motions into consideration, we discuss possible mechanisms for the hydrogen embrittlement in α-Fe.

Poster Session II

Hydrogen Isotope and Microstructure Effects on Deformationand Fracture in 22Cr-13Ni-5Mn. B.P. Somerday, C.H. Cadden, S.L. Robinson, Sandia National Laboratories, Livermore, CA, USA

This study examines hydrogen-assisted fracture in the nitrogen-strengthened, austenitic stainless steel 22Cr-13Ni-5Mn (22-13-5) emphasizing the role of second-phase particles. In addition, the effects of tritium and decay helium on fracture of 22-13-5 are characterized. Forged, tritium precharged-and-aged 22-13-5 exhibited substantial yield strength increases due to helium bubble pinning of dislocations and significant tritium compatibility as evidenced by the retention of ductility and some microvoid fracture. The strain hardening properties and appearance of microvoid fracture suggest that significant dislocation activity was retained despite the high helium content, whereas in other austenitic steels helium bubble pinning of dislocations usually promotes deformation dominated by twinning. Formation of grain-boundary s phase at 800°C degraded the fracture resistance of modern 22-13-5 alloys. The detrimental effect of σ phase was observed for both air-melted 22-13-5 as well as electroslag remelted 22-13-5. Hydrogen reduced the fracture resistance of 22-13-5 for all heat-treatment conditions examined: solution heat treated (SHT), SHT+1000°C/8 hr, and SHT+800°C/24 hr. Measured reduction of area was lower in hydrogen-charged 22-13-5 compared to the uncharged conditions, but fracture occurred by microvoid processes in all cases.

Supported by the U.S. Dept. of Energy under contract # DE-AC04-94AL85000

Materials Testing in High-Pressure Gaseous Hydrogen at Sub-Zero Temperatures. M. Watwood, B. Hurless, M. Jackson, IIT Research Institute, MFSC, AL, S. Gentz, MFSC, AL, USA

Improved material testing methods are required to generate design data for aerospace propulsion systems that must operate successfully at temperatures and stresses unknown to previous generations. Traditionally, these tests were conducted under either high-pressure/high-temperature or ambient-pressure cryogenic conditions, in the belief that the embrittlement effect of high-pressure hydrogen gas would not occur at subzero temperatures. This paper will examine hydrogen embrittlement at temperatures as low as –93°C (-200°F). The authors will discuss advanced test methods and equipment modifications used to examine high- and low-cycle fatigue, fracture toughness, and tensile properties in high-pressure hydrogen at subzero temperatures.

Relationship of Laboratory Tests of Rock Bolt SCC to Service Failures. E. Gamboa, A. Atrens, University of Queensland, Brisbane, Australia

The stress corrosion cracking of rock bolts has been explored using Linearly Increasing Stress Tests (LIST). In LIST testing, a sample is exposed to the environment of interest and the stress is slowly increased until failure. A potential drop technique is used to determine the initiation stress for stress corrosion cracking. SEM examination of the fracture surfaces is used to help identify the fracture mechanism. Rock bolt steel subjected to LIST testing in air show ductile failure and a dimple rupture failure surface. In contrast, rock bolt steel subjected to LIST testing in a dilute sulphate/chloride solution showed subcritical crack growth followed by brittle fracture. SCC initiates at stresses well below the yield stress. Analyses of rock bolts that have failed in service have indicated similar failures.

Effect of Microstructure and Electrochemical Potential on the SCC Resistance of X-80 Steel in Diluted $NaHCO_3$ Solutions. J.G. Gonzalez-Rodriguez, M. Casales, V.M. Salinas-Bravo, J.L. Albarran, L. Martinez, Univ. Aut. del Edo. de Morelos, Cuernavaca , Mexico

The effect of heat treatment and both anodic and cathodic potentials on the stress corrosion cracking of X-80 pipeline steel has been investigated using the slow strain rate testing technique. The heat treatments included the as-received condition, water-quenched, quenched and tempered, and water-sprayed and the solution tested was 0.01M $NaHCO_3$ at room temperature. The results indicated that the steel most susceptible was the quenched one, and the least susceptible was the as-received one. When an anodic potential was applied, the SCC susceptibility increased, whereas a cathodic potential decreased it in all cases. The results are discussed in terms of hydrogen embrittlement assisted anodic dissolution.

Numerical Simulation of Hydrogen Effects on Stress Corrosion Crack-Tip Plasticity. D. Delafosse, J.P. Chateau, S. Teysseyre, T. Magnin, ENS Mines de Saint-Etienne, Saint Etienne, France

This paper presents a numerical simulation method aimed at investigating and quantifying the elementary mechanisms invoked in the Corrosion Enhanced Plasticity Model (CEPM) for the transgranular Stress Corrosion Crack (SCC) propagation in fcc alloys. The basic equations for the coupling between stress and hydrogen diffusion are presented. A numerical simulation method is proposed. It is based on the stress-modified diffusion equation and on a discretisation of the hydrogen concentration field. The simulation scheme is applied to elementary dislocation configurations in order to compute the influence of solute hydrogen on dislocation interactions. A simple general expression is derived for the hydrogen screening effect on the pair interactions between co-planar dislocations. This expression is used to investigate the influence of diffusing hydrogen on the cross-slip probability of screw dislocations. It is compared to recent experimental results on fatigued single crystal containing hydrogen.

The simulation scheme is further developed to study the crack / hydrogen / dislocation interactions at an SCC crack tip. The study of the equilibrium configuration of dislocation pile-ups is of particular interest to assess the fracture mechanism proposed by the CEPM. Another important issue is the effect of a cathodic hydrogen discharge on the activity of dislocation sources at the SCC crack tip. A study of both effects is carried out on a model system (monocrystalline 316L stainless steel in boiling $MgCl_2$), and it is shown how quantitative parameters can be derived from this approach. We also investigate the possibility of applying this approach to industrial – grade high nitrogen austenitic stainless steels. The effect of the high nitrogen content is modelled by the introduction of a friction stress and it is shown how this a microstructural feature alters the behaviour of the crack-pile-up system, thus enabling a semi-quantitative interpretation of macroscopic experimental results in terms of elementary mechanisms.

Factors Influencing Stress Corrosion Cracking of Mild Steels in Alcoholic Environments. E. Risson, B. Bayle, Ecole des Mines de St Etienne, St Etienne, France, R. Kefferstein, SOLLAC CRPC Site de Fos, Fos sur Mer, France, T. Magnin Ecole des Mines de St Etienne, St Etienne, France

Different cases of stress corrosion cracking (SCC) have been observed in the last few years on mild steel structures that were in contact with methanol. In early 1992, SCC phenomenon was highlighted by SOLLAC, on carbon steel tanks used for the storage of petroleum gas liquefied

(P.G.L.). Methanol is in fact widely used in industry and acts as a moisture scavenger in propane gas tank. Cracks are located in the lower part of the cistern, within a zone bathed with methanol. They are detected quickly (7 to 14 months) during storage on park before use. Therefore it is important to identify the cracking mechanism and the damaging factors in order to improve steel SCC resistance. Cracking mechanism was studied by means of slow strain rate tests both with smooth and pre-notched specimens at free and cathodic potentials. The electrochemical potential and the metallurgical variables (microstructure, texture) markedly affect the cracking path. Depending on these factors, either intergranular, transgranular or cleavage-like cracking is observed.

There is strong experimental evidence that the SCC mechanism is governed by the localized dissolution stage, promoting hydrogen-related effects. The latter are responsible for crack advance. Both static and cyclic loading test conditions were carried out intending to identify the reasons for the cistern failure. The role of dynamic loading and "micro-creep" at the crack tip were then highlighted. A cracking mechanism is proposed that takes into account dissolution (influence of carbides), hydrogen effects and microstructure. Study of the SCC mechanism revealed the importance of both the metallurgical variables and the electrochemical behaviour of the steels in the methanol environment to promote cistern failure. Finally it was possible to outline a ranking test and to propose new specifications for industrial applications.

Effects of Strain Rate and Hydrogen Trapping Behavior on Fatigue Crack Growth of SA 508C1.3 Pressure Vessel Steel in High Temperature Water. S.G. Lee, I.S. Kim, Korea Advanced Institute of Science and Technology, Taejon, Korea

Corrosion fatigue tests were performed in 288°C oxygenated water with varied loading frequencies to explain the onset of brittle crack propagation. The crack growth rate was increased with decreasing frequency until a critical frequency. The strain rate effects on the crack growth rate was investigated by means of da/dt vs. d_/dt curves. At intermediate range, there was a transient point corresponding to the onset of dynamic strain aging, where an abrupt increase in the crack growth rate was observed. Above the transient point, small size particles enhanced brittle cracks while only large size particles enhanced brittle cracks below the transient. The sectioned area of the fatigued specimen showed that microcracks were formed by strain localization along slip bands in the crack tip yielding zone. Further, in tensile tests there was a tensile ductility loss in dynamic strain aging region at 288°C due to highly localized deformation and yet predominantly ductile in nature with souse quasi-cleaved area when the specimen was precharged by hydrogen. The tensile results of precharged specimen showed that strain induced hydrogen trapping was more favorable at interface of particle and matrix and the trapping sites more enhanced in the dynamic strain aging region. From these results, it is suggested that environmentally assisted crack (EAC) may be enhanced at a specific strain rate, and that EAC may be related to interactions of hydrogen with oxide, film arid to the Luders band movement with a high strain gradient at inclusion/matrix interface.

Reproducibility and Repeatability of Tensile and Low Cycle Fatigue Properties in Propulsion Grade Hydrogen. E.J. Vesely, B.N. Bhat, W.B. McPherson, C.E. Grethlein IIT Research Institute, Huntsville, AL, USA

Hydrogen has the potential of increased use in the future as an environmentally friendly fuel. It has, however, shown a tendency to embrittle some materials. To be used in a safe manner and to exploit its full potential, it will be necessary to develop a database of material properties for this highly beneficial gas. The tests needed to produce this data are extremely costly to perform. In

earlier work, it was found that a hydrogen tensile test was more than 30 times the cost of a standard air test, while a hydrogen-environment low cycle fatigue test, by comparison, was 40 times it conventional counterpart. Moreover, there is presently a lack of universal test methods to ensure standardized data within the hydrogen community. Each of the industries that work with hydrogen (aerospace, petroleum, fuel cells, etc.) perform tests using their own laboratory-developed methods, thus making cross-comparisons of material property data highly questionable. It is extremely important that data generated in a hydrogen environment be done to a standard that reduces variance to a minimum and allows for direct comparison of test results from different laboratories. This assures that all data generated can be used to further our understanding of the hydrogen effects and to make sure components/products designed to be used in hydrogen are the safest and most efficient possible.

This paper will review the results of two round-robin programs conducted by NASA-MSFC. These two programs examined the reproducibility and repeatability of tensile and low-cycle fatigue testing in high-pressure hydrogen environments. The studies showed that even using the tightest controls available from current commercial standards, the reproducibility (between different laboratories) and repeatability (within a laboratory) of these tests had 5 times the variability present in standard ambient air tests. The paper will conclude by detailing a program that will allow the development of improved test methods that will lead to lower variability in the generation of mechanical property data in the future.

Stress Corrosion Cracking and Life Prediction of Austenitic Stainless Steels in Calcium Chloride Solution. H. Leinonen, VTT Manufacturing Technology, I. Virkkunen, H. Hanninen, Helsinki University of Technology, Helsinki, Finland

Stress corrosion cracking (SCC) susceptibility of austenitic AISI 304L, AISI 304 and AISI 316L stainless steels in 50% $CaCl_2$ solution at 373 K (100°C) under open-circuit corrosion potential and cathodic polarization conditions was studied using the constant load method. The stages of SCC were monitored by acoustic emission (AE). In the early phase of the tests the AE activity was high consisting of low amplitude impulses. In the steady state phase the AE activity was low and towards the end of the test it increased with the increased amplitude of the impulses. Several preliminary experiments were necessary to optimize and calibrate the AE instrumentation and testing configuration in order to take into account the other AE sources active during SCC experiments. AE allowed a good correlation between AE signals and SCC damage. Especially, the activity of AE signals increased in the early stage of the SCC experiment under constant load condition corresponding the changes in the measured steady state strain rates of the specimen. On the other hand, the steady state strain rate obtained from the corrosion elongation curve (elongation vs time curve) showed a linear function of time to failure. This means that the steady state strain rate can be applied as a parameter for prediction of time to failure and crack growth. Based on creep measurements in a non-corrosive environment, the influence of environment on steady state strain rate was more than fivefold. The primary fracture mode was transgranular stress corrosion cracking at small crack length. The fracture mode changed to intergranular stress corrosion cracking when the K-value reached a certain limit.

A new model can explain and describe the observed phenomena of SCC. The rate determining step in stress corrosion cracking is the generation of vacancies by selective dissolution. This step was characterized by low AE activity. The effects of electrochemical polarization on creep are caused by the changes in the vacancy injection from the oxide film interface to the base metal. Cathodic polarization resulted in the decreasing creep strain rate by reducing the oxidation rate suppressing thus the generation of vacancies, which made creep and strain localization more

difficult. Vacancies generated by corrosion are consumed by dislocation climb which enhances creep, but later agglomeration of vacancies under applied stress results in cleavage-like stress corrosion cracking or intergranular stress corrosion cracking depending on the loading conditions.

Surface Work Hardening and Stress Corrosion Cracking of an Austenitic Stainless Steel. C. Braham, A. Bouzina, J. Lédion, CNRS ESA, Paris, France

The influence of material work hardening on stress corrosion cracking still remains a controversial subject. The aim of the present study is to quantify the effect of work hardening on the stress corrosion cracking behaviour of an austenitic stainless steel type AISI 316L. Classical tests under applied loading were conducted in a boiling (117°C) 30% magnesium chloride aqueous solution. Particular attention was given to the preparation of the surfaces. The referential specimen was obtained through a mill annealed treatment and the surface was prepared by electrochemical polishing in order to obtain a material without work hardening and residual stresses. Three surface states were studied: machined (turned), polished using abrasive paper and shot peened. Residual stress corrosion cracking tests were carried out in a 44% magnesium chloride solution at boiling temperature (154°C). X ray diffraction provided the thickness of the work hardening layer and the stress distribution in depth for each specimen. Using the same technique, the stress distribution during the tensile loading was determined. A variation of residual stress distribution is observed even for a weak loading. On the shot peened surface the compressive stress was modified. This was confirmed by corrosion tests which led some cracks in the material: the most hardened specimen (shot peened) cracked first.

The assumption given by the authors is that, in work hardenable materials like the AISI 316L SS, the plastic deformation of the surface changes the material behaviour. A numerical simulation, with a finite element method showed how to take into account surface work hardening of material. The tensile specimen could be considered as a material consisting of thin layers with a high elastic yield and a bulk region with large deformation. This explains why the high compressed surface by shot peening can easily be changed into tension under a weak loading and makes stress corrosion cracking possible.

Effect of Nitrogen on the SCC of 316LN Weld Metal. S.N. Soman, M.S. University, Vadodara, India, V.J. Gadgil, University of Twente, Enschede, The Netherlands, S.N. Malhotra, M.S. University, Vadodara, India, R. Raman, V.S. Raja, S.D. Kulkarni, Indian Institute of Technology Bombay, Mumbai, India

Austenitic stainless steels containing nitrogen find extensive application in the industry because of improved corrosion resistance and higher mechanical strength. Nitrogen has beneficial effect on localised corrosion like pitting, crevice and intergranular corrosion. It is also reported that nitrogen reduces resistance to stress corrosion cracking (SCC). During fusion welding of the nitrogen bearing stainless steels, nitrogen has to be introduced in the weld metal to maintain similar levels of nitrogen in the base metal and the weld metal. This can be achieved by using nitrogen containing filler metal. A second possibility is to introduce nitrides or other sources of nitrogen to the flux. A third method is to add nitrogen to the shielding gas in gas tungsten arc welding (GTAW) or gas metal arc welding (GMAW). During welding nitrogen in the shielding gas is taken up by the molten weld pool. This is dependent on the thermodynamic equilibrium conditions in the arc plasma and molten weld pool. It is well known that small variations in nitrogen content can influence the corrosion behavior of the weld. In this investigation the effect of nitrogen content in the weld metal on the SCC behavior of GTAW welds of 316LN stainless steel was investigated. Filler metal used for the welds was 316L. The nitrogen content of the

shielding gas argon was changed using a gas mixer. After welding, the nitrogen content of the weld metal was analyzed using melting and vacuum extraction method in a Leybold Heraeus NOA 2003 instrument. The susceptibility to SCC was evaluated using slow strain rate tests (SSRT) in 1 N HCl. Tests were carried out at a strain rate of 5×10^{-6}. Time-to-failure was considered as the indication of susceptibility to SCC. Results of SSRT tests are presented. Results of SSRT tests in air are used for comparison as nitrogen also influences mechanical strength. The fractures were investigated using a Hitachi S-800 scanning electron microscope. The fractographic features are discussed with respect to the mechanism of SCC failure. Influence of nitrogen on the SCC susceptibility of GTAW welds is discussed.

Effects of Thermohydrogen Processing on Microstructure and Properties of Uranium Alloys. M.B. Shuai, Y.J. Su, D.M. Lang, Z.H. Wang, P.J. Zhao, S. Wu, China Academy of Engineering Physics, Mianyang, China

The application of thermohydrogen processing (THP), that consists of using hydrogen as a temporary alloying element to modify the microstructures and improve final mechanical and corrosion properties of several uranium alloys, was presented. It was found that after thermohydrogen processing, a refinement in the microstructure with less nonmetallic element impurities, more pure phase constituent and more fine grain was achieved. The microstructural refinement led to an improved ductility, without large loss of strength, and significantly improved corrosion property. Some possible mechanisms of the effects of THP on the microstructures and mechanical/corrosion properties of uranium alloys were proposed.

Phase Transformations in Ti-6Al-4V-xH Alloys. J.I. Qazi, J. Rahim, O.N. Senkov, S.N. Patankar, F.H. Froes, University of Idaho, Moscow, ID, USA

Ti-6Al-4V alloy specimens containing 0, 10, 20 and 30 at.% hydrogen were prepared. Microstructures, phases and phase transformations were then determined in the temperature range of 20 to 1000°C using optical microscopy, transmission electron microscopy, X-ray diffraction and microhardness measurements. Alloying with hydrogen was achieved by exposure of specimens to different hydrogen partial pressures at 780°C. Increasing the hydrogen content from 0 to 30 at.% lowered the beta transus temperature of the alloy from 1005°C to 815°C, significantly slowed down the kinetics of beta-to-alpha transformation and led to formation of orthorhombic martensite instead of hexagonal martensite in quenched specimens. A hydride phase was also detected in the specimens containing 20 to 30 at.% hydrogen. The martensite decomposition behavior and beta phase time-temperature-transformation (TTT) diagrams were determined for different hydrogen concentrations.

Influence of Hydrogen on the β-phase Stability in Ti-Nb Alloys. D. Zander, B. Kofmann, D. Eliezer, Ben Gurion University of the Negev, Beer-Sheva, Israel, E.Y. Gutmanas, Technion, Haifa, Israel, D. Olson, Colorado School of Mines, Golden, CO, USA

The use of hydrogen as a temporary alloying element can strongly enhance fabrication of Ti-based alloys for example due to lower stresses and/or lower temperatures. In addition in refractory metals or alloys hydrogen has a large potential to promote superplasticity. It is known that in bcc metals, e.g. in iron, hydrogen enhances plasticity, since segregation of hydrogen at dislocations lowers their stress field. Furthermore hydrogen-assisted processing can lead to refined microstructures with improved mechanical properties. Until now some work has been conducted on processing and mechanical behavior of Ti-Nb alloys, but very little is known on the microstructural changes associated with hydrogen-assisted metal forming and transformation

mechanism. The objective point of our present research is to investigate in detail the influence of hydrogen on the phase stability in Ti-Nb (20-45 wt.% Nb) alloys.

Hydrogen charging was performed electrochemically in a 2:1 glycerin-phosphoric acid electrolyte. The influence of hydrogen on Ti-Nb (20-45 wt.% Nb) was studied by means of DSC, TDA and microhardness test; the microstructure was investigated by x-ray diffraction, SEM as well as TEM. Hydrogenation of Ti-Nb was found to exhibit a significant effect on the microhardness. Hydrogen influences strongly the slip mechanism in the bcc-phase and assists in lowering the deformation energy. So the hydrogen influence on the mechanism of plastic deformation of Ti-Nb is of considerable interest. The observed microstructural investigations are expected to provide significant conclusions on the microstructural mechanism how hydrogen enhances the plasticity of bcc alloys. Furthermore the influence of deformation on the hydrogen absorption and desorption behavior as well as microstructural transformations will be discussed in detail.

How Helium Affects the Thermodynamics of the Palladium-Tritium System. S.E. Guthrie, W. G. Wolfer, Lawrence Livermore National Laboratory, Livermore, CA, USA

The decay of tritium generates helium, which is stored in the solid in the form of highly pressurized bubbles. The presence of these bubbles in palladium tritides changes the PCT phase boundaries in two ways. First, the plateau pressures are reduced with increasing helium content. Second, the difference between the plateau pressures in absorption and desorption is diminished, thereby resulting in a smaller hysteresis loop as more helium accumulates. Combining a lattice gas model for the metal hydride system with a model for the hydrostatic stress generated by the helium bubbles, plateau pressure are predicted to decline in agreement with the experimental data. The shrinkage of the hysteresis loop is attributed to the dramatic hardening of the palladium matrix by the helium bubbles. The agreement of model results with the experimental observations lends strong support to both the lattice gas model for the hydride phase transition, and to the mechanism for helium bubble growth by dislocation loop punching.

Improved Thermal Stability by Hydrogenation of Zr-Cu-Ni-Al Metallic Glasses and Quasicrystals. D. Zander, E. Beduli, D. Eliezer, Ben Gurion University of the Negev, Beer-Sheva, Israel, N. Eliaz, Tel-Aviv University, Israel, U. Köster, University of Dortmund, Dortmund, Germany

Zr-Cu-Ni-Al exhibits one of the best glass forming alloys known. In a narrow concentration range, however, annealing above the glass transition temperature leads to the formation of quasicrystals in $Zr_{69.5}Cu_{12}Ni_{11}Al_{7.5}$. The high number of potential interstitial sites suitable for hydrogen and the favorable hydrogen-metal chemistry make glassy and quasicrystalline Zr-Cu-Ni-Al candidates for hydrogen storage applications. Zr-based as well as Ti-based quasicrystals were observed to store hydrogen up to a content close to the best crystalline storage materials. The objective of this paper is to present our recent results on the positive effect of hydrogen absorption on thermal stability of glassy $Zr_{69.5}Cu_{12}Ni_{11}Al_{7.5}$.

Hydrogen charging was performed electrochemically in a 2:1 glycerin-phosphoric acid electrolyte. Absorption kinetics and storage capacity were found to be far better for the partially quasicrystalline than for the amorphous phase. Only partial desorption of hydrogen was observed by TDA at about 500°C of glassy or quasicrystalline Zr-Cu-Ni-Al. Since hydrogen desorption seems to be hindered by a surface barrier, the hydrogen remains in the Zr-based alloys thus influencing their thermal stability. Such effects of hydrogen were studied by DSC, TDA and

microstructural investigations. At low hydrogen concentration ($H/M \leq 0.05$) the absorption of hydrogen causes a significant increase in the thermal stability of the amorphous phase; at high hydrogen contents ($H/M \geq 0.9$) the formation of ε - ZrH_{2-x} and δ - ZrH_2 was revealed. It is concluded that hydrogen can be used to control the thermal stability and crystallization process of Zr-based amorphous alloys. The micromechanism of the decomposition during annealing of hydrogenated Zr-based metallic glasses or quasicrystals are discussed in detail.

Effect of Hydrogen on Deformation of Ni in Crack Tip Model. M. Wen, X. Xu, S. Fukuyama and K. Yokogama, National Institute of Advanced Industria, Hiroshima, Japan

Hydrogen embrittlement (HE) has been a serious problem for nickel and nickel-based alloys used for high-temperature devices. Although many experimental studies have been carried out, the influence of hydrogen on the mechanical properties is very complicated, and thus, definite HE mechanisms of nickel have not been established yet. By using computer simulations together with the embedded atom method (EAM), the above processes can be discussed at the atomistic level. Recently, the simulations of hydrogen-induced fracture, dislocation dynamics influenced by hydrogen, and the segregation of hydrogen in the lattice defects have been studied to clarify the HE process of nickel, however, almost all simulations are conducted in the two dimensional (2D) models and the effect of hydrogen on the plasticity around a crack tip is still unclear.
In this study, a large-scale 3D crack tip model of one million nickel atoms, whose size is visible by transmission electron microscopy, was used in the simulation. Molecular dynamics (MD) simulations with the EAM were carried out to study the uniaxial tensile processes of single crystals of nickel at room temperature. The details of the deformation in the specimen were identified by a new method of the deformation analysis originally developed by the authors. The influence of hydrogen was studied by pre-charging a different number of hydrogen atoms into the model with various distributions before simulation to avoid simulating the long time process of diffusion that cannot be achieved by the conventional MD. HE was most serious in the specimen hydrogen-charged in the notched area, in which hydrogen localized dislocation emission at the crack tip to induce a fracture macroscopically on the (100) pre-crack plane perpendicular to the tensile direction. The crack tip opening angle decreased with increasing hydrogen content. At low hydrogen content, although extensive plastic deformation was observed by the motion of dislocations, the deformation was localized in the notched area. At high hydrogen content, hydrogen induced microvoid formation due to bond breaking of the seriously weakened metallic bonds near the crack tip, and a significant reduction in the ductility of the specimen was observed. Fracture occurred after the subsequent microvoid growth and linkage. The emission of dislocations from the crack tip and the crack propagation were localized at the earlier stage of deformation in the specimen hydrogen-charged around the crack tip. Hydrogen slightly localized dislocation emission at the crack tip at the beginning of plastic deformation, but did not affect deformation afterwards in the specimen hydrogen-charged homogeneously in the upper part of the specimen, where deformation takes place. Slip deformation mainly along the two slip planes was observed in the specimen hydrogen-charged along the slip planes intersecting the crack tip. Failure along the slip planes was observed finally, which is in accordance with the observations of the TEM foils. On the basis above simulations, the present results support the hydrogen-enhanced decohesion mechanism with localized deformation and brittle fracture depending on the hydrogen content and distribution. The effect of model size on the deformation behavior was also discussed.

Effect of Applied Stresses on the Hydrides Orientation in Titanium. A. Politi, M.I. Luppo, G. Vigna, C.N.E.A-U.A, Buenos Aires, Argentina

Titanium and its alloys can be embrittled by hydride precipitation, especially when they are oriented perpendicularly to the applied tensile stress. It is well known that the hydrides precipitate as needles or microscopic plates with certain habit planes and fixed crystallographic orientation relationships with the matrix. This study shows that titanium hydrides in unstressed Ti commercial grade with large grains precipitate mainly as thin plates over prismatic planes. After determination of crystallographic orientation of large grains (divergent beam x-ray techniques), they were observed using optical microscopy. These observations showed an important coincidence between macroscopic and microscopic habit planes of hydrides. Coincidentally in TEM large hydrides and, in several cases, microscopic hydrides with low stacking angle were observed.

Successive hydride precipitation tests with constant load applied during the cooling process were conducted to study the redistribution in hydrides orientation. When the material was heated up to 553 K and then slowly cooled applying a constant load when the temperature reached 533 K, applied stress higher than 20 MPa showed important hydrides reorientation. Firstly, the relative frequency of precipitated hydrides in perpendicular planes to tensile axe was increased. Secondly, the increase was notably marked when the orthogonal plane corresponded to a prismatic plane

Hydrogen Effects on a Microalloyed X70 Linepipe Steel. A. Hazarabedian, P. Bruzzoni, R.J. Cordoba, N. Mingol, M. Ortiz, M.I. Luppo, G. Anteri, J. Ovejero-Garcia. Comision Nacional de Energia Atomica, Buenos Aires, Argentina

The hydrogen induced cracking, hydrogen embrittlement and hydrogen permeation of an API X70 linepipe steel have been studied. The microstructural characterization of this steel by optical, electron scanning microscopy showed a very fine mixed acicular - equiaxed ferritic structure, and spheroidal carbides. Mn segregation was detected at the half plate thickness by electron microanalysis. Texture analysis by X ray showed fiber texture {100}<uvw> with the strongest component {100}<100> at surface and a strongest texture with {100}<100>, {511}<114> and {223}<110> components in the middle section. Precipitation in this region was characterized by transmission electron microscopy and microanalysis.

Hydrogen permeation experiments showed strong trapping. The apparent diffusion coefficient at 303 K is 470 to 770 times lower than the diffusion coefficient of pure, annealed iron. The trap density is related to the amount of segregation at the half plate thickness plane.

Tested hydrogen induced cracking specimens, (by immersion in hydrogen sulfide saturated solution A, NACE standard TM0298) showed extended blistering, indicated by an elevated ultrasonic attenuation rate, up to 70%. Blisters were located only at the half plate thickness plane. This is attributed to the enhanced H entry at this place where segregation and modified sulfides are present, and to the presence of Ti-Nb (C, N) particles located in this region. To prove this, additional hydrogen induced cracking test were performed, by cathodic charging over the whole specimen surface or by immersion in hydrogen sulfide and masking the lateral faces the specimen, avoiding the exposition of the segregation region to the solution. In two both tests, specimens did not present cracks or blisters.

Hydrogen assisted cracking was evaluated by conventional tensile test of hydrogen pre-charged and hydrogen free specimens. Hydrogen embrittlement was acceptable: 18% loss of area

reduction, compared to H free specimens. Delamination was present in non hydrogen charged tensile specimens at the same section were blister occurs. Delamination is related to the texture and segregation of that section and is driven by the stress component normal to the tensile axis that appears after necking. H containing samples did not present this phenomenon. Interrupted tests in non charged specimens, proved that the delamination secondary fracture took place at the very late fracture process, not before 68% of deformation measured by reduction of area. A priori, H must benefit delamination. However, H containing specimens fail at a lower area reduction than the one needed to delaminate the non H containing samples. This gives lower triaxiality and lower normal stress at delaminating plane during necking, and delamination does not develop. Fracture in H containing samples was ductile with fragile spots consisting of cuasi-cleavage facets radiating from sulfides and, in lower amount, from Ti-Nb (C, N) particles.

Slow stress rate test in hydrogen sulfide (Solution A) resulted in a hydrogen embrittlement index similar to the obtained by the conventional test. In this case the brittle regions on the fracture surface were only present at the specimen surface.

Comparison of Hydrogen Effects on the Behavior of C-Mn Steels by Different Methods. J. Sojka, P. Betakova, I. Schindler, L. Hyspecka, M. Sozanska, Technical University, Ostrava, Czech Republic, C. Dagbert, J. Galland, Ecole Centrale, Paris, France, M. Tvrdy, Vítkovice, Ostrava Czech Republic

Effects of hydrogen were studied on the behavior of plates manufactured from A516Gr70 steel or from similar ones. Resistance of steels to hydrogen was tested in accordance to NACE TM 0284 procedure and also performing tensile tests. Tensile specimens were taken in three distinct plate orientations (longitudinal, transversal and through-thickness) and electrolytically hydrogen charged prior to tensile tests. The studied steels differed mainly in their microstructure (heat treatment) and in the nature and quantity of non-metallic inclusions.

In case of NACE tests (without applied stress) the resistance of steels to hydrogen induced cracking improved significantly if quenching and tempering or at least "high temperature" normalizing (at 1000C) were applied. Segregation bands in the mid-thickness of the plates, enriched especially in manganese, represented predominant sites for hydrogen induced cracking. The role of non-metallic inclusions seemed to be less important but it could not be neglected. Even for the larger elongated manganese sulfides, very often no cracks initiated around them. Nevertheless, the resistance of steels to hydrogen induced cracking increased for steels containing smaller and less elongated inclusions.

Tensile tests performed on previously electrolytically charged specimens did not confirm the beneficial role of quenching and tempering or "high temperature" normalizing. The degree of hydrogen embrittlement was more or less identical for all performed heat treatments. For any heat treatment hydrogen provoked a strong anisotropy of mechanical properties that was not observed in the initial state. Non-metallic inclusions (elongated manganese sulfides or globular oxides) represented the only sites for the crack initiation in case of tensile tests. Additional laboratory rolling proved that the degree of hydrogen provoked damage depended strongly on the geometric characteristics (size and shape) of non-metallic inclusions.

The obtained results are discussed in terms of hydrogen-deformation interactions and in relation to the microstructure characteristics of the steels (especially those of segregation bands and non-metallic inclusions).

Doping Influence on the Kinetics of Hydride Decomposition in Titanium Alloys. L.G. Malyshev, V.G. Shamruk (Russia)

The questions dealing with hydride stability, including their thermal decomposition, cover a wide circle of problems both of scientific, and practical character. Some of them are solved within the framework of the thermodynamic approach which allows us to determine meanings of thermodynamic potentials and to analyze their change at various transformations occurring in hydride systems. At the same time, kinetic features of metal - hydrogen systems behavior are considerably less investigated.

In the present paper the thermal decomposition of titanium hydrides doped with aluminum, molybdenum and vanadium was investigated. As the objects of research some hydrides of binary titanium alloys, i.e. titanium - aluminum, titanium - molybdenum, titanium - vanadium with the impurities contents of 2, 4 and 6 mass.% were taken. In order to discover the peculiarities in hydrides decomposition a method based on registration of hydrogen quantity, allocated from a sample in conditions of temperature linear change was offered.

The experiments which have been carried out on titanium hydride, showed, that the curve of hydrogen allocation has a superposition of two peaks – a large peak with a maximum near 500°C and a smaller peak, which has a maximum near 550°C. Their existence was explained by the titanium -hydrogen phase diagram. It was found that aluminium doping in titanium changes the curve shape. The peak near 500°C disappears but an additional high-temperature “tail” on a hydrogen flow curve was discovered. It can be interpreted as result of superposition of two peaks, which maxima are near 620°C and 690°C correspondently. Vanadium doping in titanium makes the process of hydrides decomposition more complicated. The most intersting feature is the appearance of a new low-temperature peak near 400°C, which size is increasing with vanadium content growth. Molybdenum doping in titanium allows shows an interesting phenomenon connected to peak "splitting" which takes place near 500°C. Its size increases with increasing of molybdenum content in the alloys

Effect of Hydrogen on the Hardness and Tensile Properties of Pure Copper. A.S. El-Amoush, Al-Balqa Applied University, Tafila Applied University College, Tafila, Jordan

The effect of hydrogen on the Hardness and Tensile Properties of pure copper was investigated after experiments conducted on specimens that hydrogen charged under different cathodic charging conditions. Cathodic hydrogen charging was found to reduce the ductility and ultimate tensile strength of the copper. These parameters are decreased with increasing the current density and charging time. Microhardness measurements revealed that the introduction of hydrogen caused hardening on the surface of copper. The severity of the hardened region increased with either cathodic current density or charging time. Further charging increased the depth of the hardened region of copper. Ageing after charging can result in either complete or partial recovery of hardness, depending on the charging conditions.

Wednesday Evening, September 25, 2002
Session VII: Hydrides and Hydrogen Processing

The Effect of Applied Stress on the Accommodation Energy and the Solvi for the Formation and Dissolution of Zirconium Hydride. M.P. Puls, Atomic Energy of Canada, LTD, Mississauga, Ontario, Canada, B. W. Leitch, Atomic Energy of Canada LTD, Chalk River, Ontario, Canada, S.-Q. Shi, The Hong Kong Polytechnic University, Hung Hom, Kowloon, Hong Kong

Using a finite element model, the elastic-plastic accommodation energy of a plate-shaped hydride precipitate in a zirconium alloy matrix is calculated as a function of externally applied loads. The calculations are based on a previously developed approach in which the starting point of the calculation of the accommodation energy for hydride dissolution is the elastic-plastically formed hydride. Expressions are provided showing how the hydrogen solvi are affected by the accommodation energy for hydride precipitation and dissolution when the solid is subjected to different combinations of external stress or there exists a region of high stress in the material, such as at a crack under tensile loading. The calculations of the accommodation energy show that only a deviatoric stress affects the accommodation energy. However, the effect is not large for the range of yield stress values of practical interest. This means that solvi relations derived experimentally in unstressed solids can be used to a good approximation determine the conditions at which hydrides will precipitate at, for instance, crack tips.

Influence of a Hydrided Layer on Fracture of Zircaloy-4 Cladding. R.S. Daum, Argonne National Laboratory, Argonne, IL, USA, D.W. Bates, D.A. Koss, A.T. Motta, Pennsylvania State University, University Park, PA, USA

During operation of nuclear power reactors, irradiated Zircaloy™-4 cladding tubes contain circumferentially oriented hydrides concentrated in a layer near the outer surface of the cladding. This study has investigated the effect of such a hydride layer or "rim" located near the outer surface of the cladding tube on the failure of *unirradiated* Zircaloy-4 cladding tubes. Utilizing plane-strain ring-stretch tests with the maximum principal stress along the circumferential or hoop direction, we examined the influence of a hydride rim on the failure of Zircaloy-4 cladding at both room temperature and 300°C. Fracture is found to be sensitive to hydride-rim thickness such that cladding tubes with a hydride-rim thickness >140 μm (≈700 wtppm total hydrogen) exhibit brittle behavior, while cladding tubes with a rim thickness <90 μm (≈600 wtppm) remain ductile. The mechanism of failure is identified as strain-induced sequence of micro-crack initiation within the hydride rim, linkage of micro-cracks to form a long (surface) crack, and subsequent failure of the cladding wall due to either a shear instability or ductile crack growth.

Uranium Hydride Nucleation Kinetics: Effects Of Oxide Thickness And Vacuum Outgassing. D.F. Teter, R.J. Hanrahan, Jr., C.J. Wetteland, Los Alamos National Laboratory, Los Alamos, NM, USA

The kinetics of bulk uranium hydride formation have been extensively studied. However, the nucleation kinetics on oxidized specimens has not been specifically measured as a function of oxide thickness. In most kinetics measurements, steps are usually taken to minimize the oxide film thickness so that the reaction kinetics being measured are for the hydrogen gas/uranium metal system. Specimens may be mechanically abraded or pre-hydrided to remove most of the

oxide before exposing to hydrogen gas. Some previous studies activate the surface by exposing the uranium to temperatures ranging from 200°C to 630°C under vacuum before exposing to hydrogen gas. This may affect the character of the oxide, for example changing its stoichiometry or absorbed species content (such as hydroxyls).

In the present study, the hydriding kinetics of oxidized uranium rods was studied to investigate the effects of oxide film thickness and vacuum outgassing on the nucleation of hydride pits. A constant volume Sievert's type apparatus was used to measure the hydrogen reaction rates using ultra-high purity hydrogen (99.9995%). Vacuum outgassing was investigated using thermal desorption mass spectroscopy. Four main conclusions can be drawn from this work: the initiation time for nucleating hydride pits increases with increasing oxide film thickness the maximum hydriding rate increases as the oxide film thickness decreases as the oxide film thickness increases, the density of pits decreases and the average pit size increases the nucleation kinetics of uranium hydride is strongly increased by vacuum outgassing and is believed to be a result of removing impurities from the oxide film, namely CO_2. These conclusions can be explained by considering the diffusion of hydrogen through the oxide layer, giving rise to longer initiation times in samples with thicker oxide films. Also, oxide films with impurities can have slower hydrogen diffusion rates so that when the impurities are removed the reaction will initiate almost immediately.

Crack Initiation by Delayed Hydride Cracking at Sharp Notches in Zr-2.5 Nb Alloys. S. Sagat, Atomic Energy of Canada Limited, Chalk River, Ontario, Canada, G. W. Newman, Ontario Power Generation, Toronto, Ontario, Canada, and D.A. Scarth, Kinectrics Inc., Toronto, Ontario, Canada

Cold-worked Zr-2.5Nb alloys containing hydrogen isotopes are subject to a crack initiation and growth mechanism called Delayed Hydride Cracking (DHC). Usually DHC is not possible unless the material contains flaws at which hydrides could form and cause crack initiation. A model has previously been developed to determine whether DHC initiation would occur at blunt flaws. In the earlier work, the model was validated through an experimental test program on specimens with blunt notches ($\geq 100\ \mu$m root radius). The work presented in this paper examines whether this model can be extended to sharper flaws (with a root radius of $\approx 15\ \mu$m). Specimens were prepared from pre-irradiated material, to which hydrogen was added electrolytically to a concentration of 37 wt. ppm. Twenty-four specimens were tested at effective stress intensity factors, K_I, of 7, 8, 9, and 10 MPa$\sqrt{m}$ following a temperature cycle. The combination of the hydrogen isotope concentration and the temperature cycle was such that "hydride ratcheting" occurred, which means that the notch tip hydrides did not dissolve, but grew in size with every cycle. The effect of creep relaxation on crack initiation was also studied on another group of twenty-four specimens, by including a creep-hold, under load, prior to regular testing. The creep-hold consisted of holding the specimens under load at 300°C for 1,000 hours. In both groups, four specimens, two each at 7 and 10 MPa$\sqrt{m}$, were removed for metallographic examination during testing to determine the hydride distributions and sizes beneath the notches. The failures of specimens were recorded as a function of the number of cycles and the load level. In the final analysis, the results are compared with the model predictions.

Hydrogen-Assisted Metal Processing. D. Eliezer, Ben-Gurion University of the Negev, Beer-Sheva, Israel, N. Eliaz, Tel-Aviv University, Israel, D. Zander, Ben-Gurion University of the Negev, Beer-Sheva, Israel, D.L. Olson Colorado School of Mines, Golden, CO, USA

The physical, chemical and metallurgical phenomena that can be utilized to assist in metal processing will be reviewed. With a fundamental understanding of hydrogen behavior in metals and alloys, the use of hydrogen can achieve advances in metal processing and enhance alloy properties. Various processing approaches utilizing hydrogen will be described including thermohydrogen processing, hydrogen decrepitation, hydrogenation-decomposition-desorption-recombination, hydrogen-induced amorphization, hydrogen-promoted microstructure refinement, hydrogen-assisted metal hot forming, and hydrogen-enhanced alloy properties. The advantages of direct ore reduction with hydrogen, hot forming of hydrogen-saturated metals and alloys, hydrogen-enhancing magnetic and thermal expansion properties, temporary hydrogen alloying to promote amorphization, grain refinement, superplasticity and the use of hydrogen in plasma processing of materials will be described. A mechanistic understanding of the role of hydrogen assisted forming of metals will be discussed in detail.

Beneficial Effects of Hydrogen as a Temporary Alloying Element in Titanium Alloys: An Overview. F.H. Froes, University of Idaho, Moscow, ID, USA, D. Eliezer, Ben Gurion University of the Negev, Beer Sheva, Israel, O.N. Senkov, UES, Inc., Dayton, OH, USA, J.J. Qazi, University of Idaho, Moscow, ID, USA

Use of hydrogen as a temporary alloying element in titanium alloys (thermohydrogen processing, THP) is an attractive method for enhancing processability including working, machining, powder production, sintering, compaction, etc., and also for controlling microstructure and thereby improving final mechanical properties. In the case of near net shapes it is the only method for significant microstructural modification. It allows energy saving in processing final products by improving the workability. In the present paper, the status of the methods and applications of THP of titanium alloys are reviewed. The effect of hydrogen alloying on the phase composition, formation of metastable phases and kinetics of the phase decomposition is described. The effect of hydrogen on hot and cold workability, composite- and powder-metallurgy-product processing, and microstructure modification of wrought and cast conventional alloys and intermetallics, including production of nanocrystalline structures is reviewed.

Thursday Morning, September 26, 2002
Session VIII: Fundamental Effects of Hydrogen in Materials

Crack Tip Hydrogen Damage in High Performance Alloys. R.P. Gangloff and J.R. Scully, University of Virginia, Charlottesville, VA, USA.

Modern high performance alloys have been developed with outstanding strength and fracture toughness; however, hydrogen embrittlement continues to be an Achilles heel. This inadequacy is due to a persisting lack of understanding of time-dependent crack-tip chemical processes as well as the interaction of H with stress, plastic strain, and microstructural traps in the crack tip process zone. Advances are hindered by the complex nature of these factors over the small length scale relevant to the crack tip in a high strength alloy. Occurrences of severe internal and hydrogen environment embrittlement (IHE and HEE) are demonstrated by recent characterizations of cracking in ultra-high strength steel, α-hardened β-Ti alloys, Widmanstätten α/β-Ti alloys, and 7000-series aluminum alloys. For example, H-precharging of AerMet™ 100 steel and β/α Ti alloys such as Ti-15V-3Cr and Ti-7Mo-5Fe-1.5Al degrades the threshold stress intensity (K_{TH}) for transgranular IHE to as low as 10% of the plane strain fracture toughness. Intergranular and transgranular forms of HEE are produced at low K_{TH} and high growth rates (da/dt) when Ti alloys such as β/a Ti-3Al-8V-6Cr-4Mo-4Zr and a/b Ti-6Al-2Sn-2Mo-2Cr-2Zr, and aluminum alloys such as AA7050-T6 and T-7, are stressed actively in aqueous chloride solution.

Predictive models based on micromechanics and H-trapping must be improved to better capture the details of crack tip processes. The location of the fracture process zone (FPZ), and hence the kinetics of cracking, depend on crack-tip surface-H concentration for HEE and the strengths of H-trap sites within the process zone for IHE. The crack stress distribution, determined by tip location in the microstructure and opening shape, interactively governs fracture sites. Considering HEE, the FPZ is within 1 μm of the crack tip. Qualitative analyses of da/dt and the dK/dt dependence of K_{TH} support this conclusion. Widely divergent rates are consistent with differences in trap-modified H diffusivity, provided that diffusion is localized within 1 μm ahead of the crack tip. Further support for a near-tip process zone in HEE is provided by an ultra-high concentration of H measured on the crack-wake surface, as well as observed crack tips that are substantially sharper than predicted by a continuum-mechanics blunting model. Crack sharpness is pronounced for growth along an interface or grain boundary, and may be governed by the mechanics of elastic-plastically dissimilar grains or phases. Considering IHE, the kinetics of cracking are governed by redistribution of H from low/moderate strength traps to the crack tip stress field. This diffusion distance is short, of order 5 μm, for a complex microstructure and strong-stress gradient. The retention of H at dense-intragranular traps can shield grain boundaries from H damage, but TG IHE occurs. IHE at very high rates suggests that H trapping can be sufficiently strong to promote embrittlement without H redistribution. While trapping is characterized effectively by thermal desorption spectroscopy, evidence of the mechanism for the embrittling effect(s) of H at various microstructural sites remains elusive in spite of high-resolution observations. Collectively, these results establish the nature of process zone H accumulation and damage that must be understood to enable new models of IHE and HEE, as well as H-resistant high strength alloys.

Hydrogen-Induced Changes of the Mechanical Properties of Beta-Titanium Alloys- Instrinsic and Extrinsic Effects. H.-J. Christ, K. Prüßner, A. Senemmar, M. Decker, Universität Siegen, Siegen, Germany

Beta-titanium alloys are very promising candidate materials for many structural applications in aviation, marine technique and medicine, since they combine low density with high strength and excellent corrosion resistance. As opposed to the more commonly used alpha and alpha+beta titanium alloys, they show a high hydrogen solubility leading to a rather low susceptibility to hydrogen embrittlement. Conflicting opinions exist in the literature on the way in which hydrogen influences the mechanical properties of beta-titanium alloys. This can be attributed to the beta-stabilizing effect of hydrogen in these materials leading to major changes in the microstructure as a result of hydrogen charging. The resulting (extrinsic) effect of hydrogen on the mechanical properties can possibly cover up the direct (intrinsic) influences.

The objective of the study presented was (i) to quantitatively characterize kinetics and thermodynamics of the interaction of hydrogen with beta-titanium alloys and (ii) to determine the influence of hydrogen on monotonic and cyclic mechanical properties taking the superposition of intrinsic and extrinsic effects into account. The investigations were carried out for three commercial beta-titanium alloys with graduated stability of the beta phase. Hydrogen diffusion coefficients were determined as a function of temperature and heat treatment condition. For this purpose, the hydrogen concentration profiles in rods were analyzed after annealing. The initial hydrogen step profile was established by electrochemical hydrogen charging of one half of these samples. Furthermore, gravimetric and volumetric studies provided information on the rate of hydrogen uptake and the equilibrium conditions (i.e. hydrogen solubility).

The application of this data enabled a reproducible charging of the alloys with hydrogen from the gas phase up to predefined hydrogen concentrations in the range from 2 to 8 at.%. In order to separate intrinsic and extrinsic effects the charging was carried out during one step of the two-step heat treatment of the meta-stable beta-titanium alloys, while the other step was performed in vacuum. Monotonic tensile tests, total-strain controlled fatigue experiments, fatigue crack propagation measurements and Charpy impact tests were applied in order to determine the effect of hydrogen concentration in combination with the way of heat treatment. The corresponding microstructure was studied by electron microscopy (SEM and TEM) and X-ray diffraction.

The results on the single-phase beta conditions represent the intrinsic hydrogen effect. Monotonic and cyclic strength increases at the expense of ductility with increasing hydrogen concentration. The brittle to ductile transition temperature shifts to higher values and the fatigue crack propagation threshold value decreases. The microstructure of the meta-stable, usually two-phase beta-titanium alloys is strongly affected by hydrogen, though the extend of this effect depends not only on the hydrogen concentration but also on the temperature of charging. This microstructural influence (extrinsic effect) changes the mechanical properties in the opposite direction as compared to the intrinsic hydrogen effect. Therefore, hydrogen can curiously lead to an enhanced ductility. Moreover, hydrogen can purposefully be used for an optimization of the mechanical properties of beta-titanium alloys.

Hydrogen Influence on Plastic Deformation of Stable 18Cr-16Ni 10Mn Austenitic Stainless Steel Single Crystals. Y. Yagodzinskyy, O. Tarasenko and H. Hanninen, Helsinki University of Technology, Helsinki, Finland and Institute for Advanced Materials, Petten, The Netherlands

The influence of hydrogen on the plastic deformation of stable 18Cr-16Ni-l0Mn austenitic stainless steel has been studied. Dog-bone specimens cut along [111], [110] and [100] directions

of single crystals were subjected to uniaxial tension in the initial state and after electrolytic hydrogen charging. The main attention was paid to the influence of hydrogen on the details of the multistage stress-strain curve, that is on the values of stresses and strains at which the transitions between various stages occur. Mechanical testing of single crystals in the initial state and after electrolytic hydrogen charging was carried out at different strain rates. Some of the single crystal samples were strained to certain values of strain, and then the dislocation structures were studied in detail by TEM and SEM. Hydrogen influence on formation of dislocation structures and morphology, as well as shear bands on the surface of specimens were determined for different stages of deformation. Furthermore, studies on hydrogen influence on generation of vacancies, and on initiation and development of plastic instabilities at large strains were performed.

The results are analysed based on the ideas on hydrogen-enhanced vacancy generation during plastic deformation of metals, and resulting increase of the non-conservative component of plastic flow. The results of the mechanical tests are discussed based on the phenomenon of hydrogen enhanced localised plasticity (HELP). Concepts for theoretical description of uniform plastic flow of hydrogen-charged metals are formulated. Role of hydrogen-initiated vacancies in nucleation and development of the initial stages of hydrogen embrittlement is discussed.

SSRT and Modelling of Hydrogen Assitsed Crack Growth in Super Martensitic Stainless Steels. T. Boellinghaus, Federal Institute for Materials Research and Testing, Berlin, Germany

Supermartensitic stainless steels are increasingly applied as cost effective alternative pipeline materials not only for flowlines in North Sea oil and gas fields. The steels are exposed to sour service conditions providing a potential risk for hydrogen assisted cracking. The cracking resistance of supermartensitic stainless steels has extensively been studied, but up to the present predominantly by standard test procedures which do not yield very detailed information about the cracking mechanisms. In order to obtain closer insight into the cracking behaviour of supermartensitic stainless steels, slow strain rate tests (SSRT) have been performed. By such procedure, two fracture sequences have been identified dependent on pH and hydrogen sulfide level. At low pH and high hydrogen sulfide levels, the surface of the materials is activated and hydrogen is taken up during black sulfide formation at the surface. At higher pH, the steels are subjected to localized corrosion and hydrogen cracking starts from the inside of pits, due to respective pH and potential drops. Additionally, the fracture mode was found to be significantly dependent on the hydrogen concentration and allows a tentative reflection of cracking mechanisms. It is also shown that strain rates exhibiting any and also complete hydrogen degradation of supermartensitic steels can be determined by respective time-strain-fracture (TSF) diagrams.

In order to establish procedures for prediction of the cracking resistance of components, a quantitative approach for finite element modeling of hydrogen assisted cracking has been developed. The model is based on the three local influences, microstructure, mechanical load and hydrogen concentration. By comparison with the results of the slow strain rate tests the model has been verified and clearly reflects those experimental results. Exemplified by a supermartensitic stainless steel with a typical chemical composition, the present contribution provides an overview of the fracture sequences and modes and demonstrates the links to consistent and quantitative numerical modeling of hydrogen assisted cracking.

Some Recent Advances at Illinois in Hydrogen Induced Shear Localization and Decohesion. P. Sofronis, I.M. Robertson, Y. Liang, D.F. Teter, University of Illinois at Urbana-Champaign, Urbana, IL, USA and N. Aravas, University of Thessaly, Volos, Greece

Despite extensive study over a century, a complete mechanistic understanding of the hydrogen induced degradation of engineering materials has yet to be achieved. Our current understanding leads to the recognition that there is no single mechanism causing hydrogen embrittlement. Of the many suggestions, three mechanisms appear to be viable: stress-induced hydride formation and cleavage, hydrogen enhanced localized plasticity (HELP), and hydrogen-induced decohesion.

According to the HELP mechanism, hydrogen-induced premature failures in non-hydride forming systems result from hydrogen induced plastic instability which leads to hydrogen assisted localized ductile rupture processes. The underlying principle in HELP is that hydrogen shields the elastic interactions between microstructural defects thereby enhancing dislocation mobility in regions of high hydrogen concentration. However, there is no model linking the experimental behavior at the microscale (enhanced dislocation mobility) to that at the macroscale (shear localization). In this work, experimental observations on hydrogen enhanced dislocation mobility and lattice dilatation are used to describe the macroscopic flow characteristics and constitutive response of materials as modified by the presence of hydrogen. The techniques of solid mechanics are then employed to analyze the conditions under which the hydrogen effect at the microscale can lead to plastic flow localization at the macroscale. It will be demonstrated that hydrogen induces loss of ellipticity in the governing equations of the macroscopic elastoplastic material behavior. This loss of ellipticity is identified with the onset of shear localization of the plastic flow.

The decohesion theory is based on the postulate that solute hydrogen decreases the force required to separate the crystal along a crystallographic plane, grain boundary or a particle/matrix interface. While this mechanism may be applicable to some cases of hydrogen-induced intergranular fracture, it has also been used to explain cleavage failure in systems (Fe, steels, Ni alloys, Al alloys etc.) with low bulk hydrogen concentrations, which is improbable. One exception appears to be the beta-titanium alloy, Timetal 21S. This alloy has a high hydrogen solubility and shows an abrupt loss of ductility at hydrogen concentrations exceeding about 18 at.%. As no hydrides were detected along the fracture surfaces or ahead of advancing cracks the stress-induced hydride mechanism can be eliminated. The HELP mechanism can also be eliminated for although hydrogen did enhance the dislocation velocity, this effect increases with hydrogen pressure which would produce a continuous but not an abrupt decrease of ductility. Mechanical properties tests showed that solute hydrogen reduced the yield strength in the ductile regime and decreased the fracture stress in the brittle regime. Although these results do not establish that hydrogen reduces the cohesive strength of the alloy, the decohesion mechanism provides the only consistent explanation for all the experimental observations.

Hydrogen Effects on Mechanical Responses of Small Volumes. W.W. Gerberich, N.I. Tymiak, J. Jungk, T. Wyrobek, University of Minnesota, Minneapolis, MN, USA

Available hardness and thin film fracture data as affected by hydrogen at the film substrate interface are reviewed. At the nanometer scale, it appears that hydrogen can increase the yield point load near the surface of stainless steels by nearly a factor of three. Additionally, it appears to reduce the resistance to interfacial delamination of Cu films from silicon substrates by about a factor of two. Based upon additional observations of small volumes without hydrogen, interfacial toughness appears to vary with a length scale to the 1/2 power while hardness at nanoscale depths may vary with a length scale to the 2/3 power. In both, there is reason to believe that the volume

of surface ratio is an appropriate length scale in the nanometer range. Regarding film fracture, this strongly suggests that even in small volumes the volume/surface ratio is truncated by the hydrogen mechanism. Note that this ratio, as a length scale, could be diminished by hydrogen either causing brittle fracture, as in a cleavage or intergranular process, or by localizing fracture, as in a highly localized plastic rupture. The picture is complicated by the hardness in small volumes increasing with hydrogen additions. This strongly suggests that either in the baseline flow stress is increased even more rapidly than might be anticipated from near-surface hardness measurements or a different scaling law is required for fracture as opposed to deformation. These effects will be further explored with recent nanoindentation experiments.

Dueterium-Induced Interfacial Fracture of Beryllium Films. N.R. Moody, R.A. Causey, K.L. Wilson,, Sandia National Laboratories, Livermore, CA, USA, D.F. Bahr, Washington State University, Pullman, WA, USA, W.W. Gerberich, University of Minnesota, Minneapolis, MN, USA

Beryllium is a prime candidate material in the design of the International Thermonuclear Experimental Reactor (ITER) where it is proposed for use in components exposed to the hot tritium plasma. It has excellent thermal conductivity and a lower affinity for tritium than other candidate materials. However, Causey and Walsh showed in a simulation of potential reactions, where tritium was replaced by deuterium, that deposition of energetic deuterium ions with beryllium atoms can lead to formation of films that delaminate and blister. In this work, we characterized the size and shape of the blisters that formed during deposition of beryllium and deuterium and of blisters induced during nanoindentation of deuterium-free films using Atomic Force Microscopy. Mechanics-based models were then combined with these measurements to determine residual stresses and interfacial fracture energies in both film systems. This analysis showed that deuterium induced high compressive residual stresses in these films. These stresses drove delamination and blister formation. More importantly, the results showed that deuterium significantly lowered the interfacial fracture strength of beryllium films.

R. A. Causey and D. S. Walsh, J. Nuclear Materials, 254 (1998) 84.

Poster Session III

The Investigation of Hydrides in Uranium with Small Angle Neutron Scattering. J.S. Bullock, S. Spooner, R.L. Bridges, G.L. Powell, G.M. Ludtka, J. Barker, Oak Ridge National Laboratories, Oak Ridge, TN, USA

Small Angle Neutron Scattering (SANS) is shown to be an effective method for detecting the presence of hydrogen-bearing precipitates in uranium. These precipitates are consistent with the phase diagram of the uranium-hydrogen system and relate to loss of tensile ductility with hydrogen content in uranium[1]. High purity polycrystalline samples of depleted uranium were given several hydrogenation treatments which included extended exposures to hydrogen gas at different pressures at 630°C and at 850°C followed by a water quench or a slow cooling in vacuum (hydrogen gas activity near zero). All samples exhibited neutron scattering, and the scattering intensity was in proportion to the expected levels of hydrogen content (0.0, 1.4, and 14 μg/g). While the scattering signal was strong, the shape of the scattering curve indicated that much of the population of scattering objects were of relatively large size. Only by use of a very high angular resolution SANS technique was it possible to make estimates of the major diameter of the scattering objects. For the time being, a structural model based on ellipsoidal objects

having a log-normal distribution can be made to fit the scattering curves. This analysis permits an estimate of the volume fraction and mean size of the "hydride" precipitates in uranium.

[1]G. L. Powell, "The Relationship Between Strain Rate, Hydrogen Content, and Tensile Ductility of Uranium," Hydrogen Effects on Material Behavior, A. W. Thompson and N. R. Moody, eds., TMS, Warrendale, PA, 355-361 (1996).

A Mechanistic Model of Helium Retention and Release for Aging Metal Tritides. D.F. Cowgill, Sandia National Laboratories, Livermore CA, USA

Helium generated in tritium-containing components alters their structural integrity and performance. We have developed a mechanistic model of aging metal tritides which can quantitatively account for He retention and release, material swelling, and PCT shifts, along with TEM and NMR data on He bubble evolution. The model is based on observations that He is trapped in high-pressure nano-bubbles from a very early age [1]. Bubble nucleation occurs by He self-trapping [2] and by trapping at lattice defects. Bubble growth is determined by the He supply volume consistent with the nucleated distribution. NMR [3] and swelling [4] measurements show that bubble pressures and bubble expansion follow the dislocation loop punching mechanism [5] and that the bubble density distribution generated at early age remains unchanged until the onset of accelerated release. We currently have two mechanisms for this release: (i) interbubble fracture using Evan's formulation [6] for implanted materials and (ii) bubble coalescence by stress-directed bubble growth. A 1D code incorporating these mechanisms shows how bubble distributions evolve near surfaces and how nucleation parameters affect the release characteristics. It implies that extended defects like grain boundaries can also produce significant effects for fine-grained films. The model is also used to examine modifications to the bubble distribution caused by environmental transients.

[1]G.J. Thomas and J.M. Mintz, J. Nucl. Mater. 116 (1983) 336.
[2]W.D. Wilson, C.L. Bisson, and M.I. Baskes, Phys. Rev. B24 (1981) 5616.
[3]G.C. Abell and D.F. Cowgill, Phys. Rev. B44 (1991) 4178.
[4]T. Schober et al. Phys. Rev. B31 (1985) 7109.
[5]G.W. Greenwood et al., J. Nucl. Mater. 4 (1959) 305.
[6]J.H. Evans, J. Nucl. Mater. 76-77 (1978) 228.

Interactions Between Sodium Alanate Metal-Hydride and Candidate Containment Materials. E.H. Majzoub, B.P. Somerday, S.H. Goods, K.J. Gross, Sandia National Laboratories, Livermore, CA, USA

This study investigates property changes in alloys selected to contain recyclable sodium alanate metal-hydrides. With a theoretical 5.6 wt. % capacity to store and release hydrogen, sodium alanates are approaching the application horizon. The decomposition process involves the following two-step reaction: $NaAlH_4$ --> 1/3 Na_3AlH_6 + 2/3 Al + H_2 --> NaH + Al + 3/2 H_2. The first and second stage decompositions release 3.7 and 1.9 wt. % of hydrogen, respectively. While the kinetics and thermodynamics of hydriding have been addressed, application of these materials for hydrogen storage and cycling requires understanding of interactions with candidate containment materials. Because good thermal conductivity and low density of the containment vessel is required for service, Al alloys are obvious candidates for this application. However, re-hydriding requires elemental Al which may be leached from vessel walls containing Al. Properties of the Al containment material may be degraded by surface pitting or hydrogen uptake. To assess the effects of these interactions, tensile tests were conducted on smooth specimens of 6061-T6 and 5083 Al exposed to sodium alanate for 80 desorption-absorption cycles at 400K.

Cu-coated 6061-T6 was similarly exposed to assess the efficacy of Cu as a permeation barrier, and 304L stainless steel is included to determine if non-Al materials are more inert. Results are compared to two sets of control specimens including one set exposed to hydrogen gas at equivalent pressures and temperatures, and a second set in inert gas with equivalent thermal exposure.

Microstructure, Stress and Mechanical Properties of Sputtered Rare Earth Metal and Rare Earth Metal Hydride Thin Films. D.P. Adams, N.R. Moody, J.A. Romero, J. Floro, M. Rodriguez, Sandia National Laboratories, Albuquerque, NM, USA

The microstructure, stress and mechanical properties of rare earth metal and rare earth metal hydride thin films deposited by ion beam sputtering is investigated. Metal hydride thin films are currently of interest for miniature fuel cells, down-hole oil logging devices and switchable mirrors, and control of stress in this material system potentially benefits device reliability and performance. In this presentation, the development of Er and ErH_x microstructure is investigated as a function of the growth parameters including growth temperature, substrate orientation and sputter gas. This includes a study of texture development on a number of different substrates such as single crystal $Al2O_3$, polycrystalline Mo, and amorphous SiO_x. The structure developed at different stages of growth is correlated with changes in stress measured in-situ. A multi-beam wafer curvature sensor allows for sensitive measurements of intrinsic and extrinsic stress. The earliest stages of growth (<10 nm) reveal morphological effects on stress. At larger thicknesses continuous films have high compressive stresses - most likely a consequence of low sputtering pressures. The effects of growth temperature are analyzed by depositing a series of films at Tg's between 30 and 500C. While little interaction with substrates occurs at low growth temperatures, possible intermixing of rare earth metals with substrates containing oxygen has a large effect on intrinsic stress. Interestingly, strain energy plays a large role in metal hydride phase formation.

Hydrogen Assisted Fracture in LENS™ 316 Stainless Steel. B.P. Somerday, J.E. Smugeresky, and J.A. Brooks, Sandia National Laboratories, Livermore, CA, USA

The objective of this study is to characterize hydrogen-assisted fracture in 316 stainless steel fabricated using Laser Engineered Net Shaping (LENS™). Fracture resistance was measured from smooth tensile specimens that were thermally charged with solute hydrogen. Results for LENS™ 316 are compared to those for wrought, annealed 316 as well as LENS™ 304L. Hydrogen charging decreased the reduction of area in LENS™ 316 by about 50%. Hydrogen-assisted fracture in LENS™ 316 was localized near interlayer boundaries. The microstructural mechanism for near-interlayer boundary fracture was not determined, however, δ-ferrite likely played a primary role. Hydrogen-assisted fracture in LENS™ 316 was more pronounced compared to wrought, annealed 316 but was less severe compared to LENS™ 304L. Interlayer boundaries in LENS™ 316 exacerbated hydrogen-assisted fracture compared to wrought 316. Aligned δ-ferrite near interlayer boundaries as well as planar slip or martensite formation promoted more severe hydrogen-assisted fracture in LENS™ 304L compared to LENS™ 316.

Supported by the U.S. Dept. of Energy under contract # DE-AC04-94AL85000

Nanomechanical Evaluation of Hydrogen Affected Deformation and Fracture in Stainless Steels. N.I. Tymiak, A. Daugela, J. Jungk, Y. Katz, W.W. Gerberich, Hysitron, Inc., Minneapolis MN, USA

Hydrogen effects on elastic-plastic deformation and fracture initiation have been evaluated under normal and sliding contact in 316 stainless steel. Acoustic emission monitoring with a recently developed sensor incorporated into an indenter tip enabled greatly increased resolution in detection of plasticity and fracture events under contact loading. As determined from the indentation curves, electrochemical hydrogen charging resulted in yield points being elevated up to 150-550% increasing with increasing charging time and current density. With sufficient time, load at the plasticity onset returned to the non-charged value implying hydrogen outgassing. The above results suggest hydrogen induced impediment on both dislocation nucleation and motion. Measurements of the load-displacement slopes after yield initiation indicated that charging induced increased rates of strain hardening. As based on unloading slope analysis, hydrogen charging resulted in up to 20% increase in the apparent Young's modulus. Gradual decrease of the apparent modulus down to its initial value occurred in approximately 30 min. During the same time interval, the yield point decreased to its stationary value. AFM measures of the nanoscratch traces revealed increased propensity to cracking following hydrogen charging. Overall results support hydrogen enhanced hardening and decreased cohesion along grain boundaries.

Role of Heat Treating on the Sour Gas Susceptibility of an X-80 Steel. H.F. López University of Wisconsin-Milwaukee, Milwaukee, WI, USA, J.L. Albarran, Instituto de Fisica, Morelos, Mexico, and L. Martinez, Instituto Mexicano del Petroleo, San Bartolo Atepehuacan, Mexico.

In this work, the role of the resultant microstructure of an API X-80 steel modified through various heat treatments was investigated by exposure to a H_2S saturated aqueous NACE solution. It was found that for similar corrosive environments and applied stress intensity factors, crack growth in LEFM compact specimens is strongly influenced by the heat condition. In the as-received alloy, crack growth was controlled by metal dissolution of the crack tip region in contact with the corrosive environment, with crack growth rates of the order of $1/W\ (da/dt) = 8.3 \times 10^{-4}\ h^{-1}$. In the martensitic condition, the rate of crack propagation was relatively fast ($1/W\ (da/dt) = 4.5 \times 10^{-2}\ h^{-1}$) indicating severe hydrogen embrittlement. Crack arrest events were found to occur in water sprayed and quenched and tempered specimens, with threshold stress intensity values (K_{ISSC}) of 26 MPa $m^{1/2}$ and 32 MPa $m^{1/2}$, respectively. Apparently, in the water sprayed condition, numerous microcracks developed in the crack tip plastic zone. Crack growth occurred by linking of microcracks which were able to reach the main crack tip. In particular, preferential microcrack growth occurred across carbide regions but their growth was severely limited in the ferritic matrix. Quenching and tempering resulted in a tempered martensite microstructure characterized by a fine distribution of Nb and Ti containing carbides. In this case, the crack path was predominantly intergranular and discontinuous in nature. Apparently, the fine carbide distribution effectively reduced the harmful effects of hydrogen by providing numerous sites for hydrogen trapping. As a result, the crack was highly tortuous with numerous bifurcations along ferrite grain boundaries. In addition, it was found that large globular calcium sulfide-calcium aluminate inclusions promote the development of transgranular cracks, or intergranular fissuring/cavitation in the case of small inclusions and carbides.

On the Heat Treatment and Microstructure in the Intergranular Stress Corrosion Cracking Response of Alloy 600. A. Aguilar, H.F. Lopez, L. Martinez, J.L. Albarran, Centro de Ciencias Fisicas, Cuernavaca, Mexico

The grain boundaries segregation and precipitation has been recognized as a major parameter controlling the susceptibility of alloy 600 to intergranular stress corrosion cracking (ISCC). In this work, the role of heat treatment and the microstructure produced was investigated, in order to analyze the susceptibility of alloy 600 to ISCC induced in steam generators. The samples were heat treated and quenched in a range of 600-1100°C and compared with the mill annealed treatment at 925°C, the microstructure was characterized using SEM-EDX, TEM. Polarization curves and susceptibility to intergranular corrosion in boiling acid solution were used to measure the corrosion rate. The crack growth was measured using the potential drop technique in modified wedge opening displacement samples immersed in an instrumented vessel at temperatures between 200-350°C, containing solutions of 0.1 M NaCl, 0.1 M $NaHCO_3$ saturated with H_2 at 200kPa. The samples quenched at 800°C shows a wide precipitation of $M_{23}C_6$ carbides, preferentially in grain boundaries with a few transgranular precipitation. The other samples shows a mixture of M_7C_3 and $M_{23}C_6$ precipitates widespread in matrix and grain boundaries. This heat treatment show the lower crack growth rate and corrosion rate, the higher performance is related to the microstructure and the grain boundaries composition. Also, the cracking pattern is strongly affected shifted from complete intergranular to transgranular.

Effect of Temperature, Strain Rate and Microstructure on the Tensile Properties of Hydrogen Charged Nickel and Alloy 600. A.M. Brass, J. Chêne, Université Paris-Sud, Orsay, France

The hydrogen embrittlement (HE) susceptibility of nickel and Alloy 600 has been shown to be strongly dependent on the microstructure of the material but such a dependence is not fully understood. In order to relate these strong microstructural effects to the stress and strain-induced hydrogen motion and redistribution in the alloy different microstructures of Alloy 600 were investigated including: mill annealed, large grain recrystallized, cold worked and sensitized ; pure nickel was used for comparison purpose. Different techniques including electrochemical permeation, SIMS analysis and thermodesorption were used to investigate the microstructural dependence of hydrogen diffusion and trapping in Alloy 600. The tensile properties of hydrogen charged samples were measured in a wide range of temperature (77K to 573K) and strain rate (10^{-6} to 10^{-1} s^{-1}) to investigate the possible role of hydrogen-dislocation interactions on the tensile properties. SEM allowed to characterize the influence of microstructure on the extent of hydrogen induced intergranular cracking and EBSD measurements were performed to correlate the preferential intergranular crack initiation sites observed on the surface to the grain boundaries desorientation.

The results support the existence of a mechanism of strain induced redistribution of hydrogen responsible for the intergranular rupture. The various H.E sensitivity of the different microstructures is discussed in the light of a mechanism involving the dislocation sweeping of hydrogen and a concentration built-up at grain boundaries.

Kinetic Features of Metal Hydride Decomposition in Nonisothermal Conditions. L.G.Malyshev, V.G.Shamruk, The Urals State Technical University, Ekaterinburg, Russia

Questions deal with the features of hydride thermal decomposition cover a wide circle of problems both of scientific and practical character. Thus the kinetic analysis of degasation process, accompanying by hydride disintegration, become of the special interest. It makes

possible to estimate directly a number of the important characteristics of hydride systems, heat of hydride dissociation, in particular

The process of hydrogen allocation during the thermal decomposition of metal hydrides goes through several stages. At the first stage there is a disintegration of hydride as a chemical composition, i.e. the hydrogen occurs in the dissolved condition. The second stage deals with hydrogen diffusion to the sample surface, and at the third stage it desorption takes place. The originality of the situation is the fact that each of these stages can limit the process of hydrogen allocation that requires a creation of methods of their correct description. In order to investigate peculiarities of hydrides thermal decomposition a method based on registration of hydrogen allocation from a sample in conditions of temperature linear change was offered.

The complexity of the theoretical analysis (in the frames of the model offered) of hydride decomposition process and diffusion of hydrogen in metal deal with the temperature changes during process, i.e. it makes impossible the application of the known methods used for the decision of the appropriate isothermal tasks. We carried out some theoretical analysis of this situation in the assumption, that a supervising stage of this process is either speed of hydride decomposition, or diffusion of the dissolved hydrogen. In the first case the reaction of the first order was analyzed. The law of hydride temperature changing was determined. The calculations showed, that the mass of gas allocated at the moment of time, appropriate to given temperature, could be determined. Entering a function which characterizes the amount of hydrogen allocated during an interval of time. The analysis showed that the dependence of hydrogen flow vs. temperature during hydride decomposition in a mode of linear heating has an asymmetric peak, which position and width is determined by parameters of hydride decomposition process and speed of heating also. The result obtained has an important practical meaning. It testifies that the method offered gives essentially new opportunity for studying of hydride properties. The given approach, from our point of view, can be applied in nitrides and carbides of metals studies with success if someone use a gravimetery method combined with a mode of sample linear heating. The similar analysis were carried out in assumption that the speed of process is limited by the diffusion of hydrogen in a sample volume.

Thermo-Oxidation Degradation in Cyanate Ester Resins. A. Venkatramanian, Z. Liu, J.P. Lucas, Michigan State University, East Lansing, MI, USA.

This study reveals the effects of thermal aging and moisture absorption on the mechanical and physical properties of cyanate ester (CE) and siloxane modified cyanate ester (SMCE) polymers. Thermal aging was conducted on these polymers in an air and in an argon environment at temperatures of 60, 80, and 100°C in order to assess susceptibility to thermo-oxidation, since thermo-oxidation can degrade properties of some polymers. Also, the properties of polymers can be degraded by absorption of moisture, which can pose significant problems in CE and SMCE. Spectrographic techniques such as, fourier transform infrared spectroscopy (FTIR) and x-ray photoelectron spectroscopy (XPS) were employed to evaluate and interpret changes observed in the physical properties. Other analysis techniques such as differential scanning calorimeter (DSC) and thermal mechanical analysis were also employed to ascertain the environmental-induced changes in the properties of these materials. Thermal aging of CE and SMCE revealed noticeable differences in the FTIR and XPS spectra in air at elevated temperatures. FTIR analysis revealed the formation of carbonyl groups as well as other significant spectral changes due to the thermal aging. XPS spectroscopy showed an increase in surface concentration of oxygen with thermal aging for between the two polymers. The spectral differences were manifested by observations showing that cyanate ester polymer tended to gain weight when aged in air at elevated temperatures ranging from 60°C - 100°C due to thermo-oxidation up to 1200 h.

However, siloxane-modified cyanate ester showed essentially no weight gain when aged at the similar temperatures, thus suggesting that thermo-oxidation did not occur for this material. Whereas, thermo-oxidation occurred in CE polymer when thermally aged in ambient air, neither CE nor SMCE resins showed a propensity to oxidize during thermal aging in an inert gas atmosphere, argon. Differential scanning calorimeter tests showed that the glass transition temperature of CE remained virtually unchanged even after aging in air for an extend period. The flexural strength of cyanate ester was reduced by 20% after thermal aging in air for ~ 1000 hours. Microhardness results obtained by using a Vickers indenter showed an increase in the hardness of CE but showed no change in the microhardness of SMCE polymers when aged in air. Nanoindentation mechanical microprobe results showed a change in the elastic modulus of CE compared to SMCE with thermal aging in air.

The Initiation and Propagation of The Stress Corrosion Cracks in High Temperature and High Pressure Conditions. R. Novotny, P. Sajdl, J.Vosta, IChT, Prague, Czech Republic

The work represents a study of environmentally assisted cracking in high temperature and high pressure conditions by means of Rising Displacement Tests. It appeared that the crucial part of RDT was crack initiation point definition. The aim of these experiments was threshold stress intensity factor K_{ISCC} determination respectively threshold value of J integral J_{SCC}, crack growth kinetics determination by means of ACPD technique and evaluation of the influence of various displacement rates on tests results. We tested three kinds of materials: reactor pressure steel 15ChNMFA and austenitic stainless steels A316H and 08Ch18N12T in various environments that means primary circuit solution VVER 1000 (15Ch2NMFA) and water solution with defined Cl- concentration (100mg/l in case of A316H and 08Ch18N12T material). We used ACPD technique at crack initiation and propagation observation. The all tested specimens were evaluated by optical microscope and SEM after experiment.

It was found that reactor pressure steel 15Ch2NMFA is susceptible to stress corrosion cracking. The stress corrosion crack initiation and propagation was noticed along the whole fracture surface. We managed to determine the threshold intensity factor $K_{ISCC} = 63MPa\text{-}m^{1/2.}$ Problems occurring during experiments were discussed and proposed solution will be solved in future experiments. Experiments with stainless steel AISI 316H were successful only partly. We achieved stress corrosion crack initiation in experiments with very low displacement rates. Problems appeared in Experiments with high displacement rates because of large plastic strain zone generation at the crack tip shortly after starting the experiment. Generally it appeared problems in case of AISI 316H material at the crack initiation determination by ACPD technique. We did not notice any signs of stress corrosion crack initiation in austenitic stainless steel 08Ch18N12T under our conditions.

Study of Hydrogen Embrittlement Sensibility in Low Alloyed Steels Towards Critical Tests for Classification. B. Bayle, C. Bosch, X. Longaygue, T. Magnin, Ecole de Mines de Saint-Etienne, Saint-Etienne, France

The petroleum industry, and more especially the offshore structures, are confronted with the damage phenomenon linked to the hydrogen embrittlement of pipeline used for hydrocarbon in marine medium. It derives either from H_2S containing environment or from cathodic protection, which in both circumstances leads to a SCC damage related to hydrogen embrittlement. The steels used are low alloyed and possess high mechanical characteristics. Classical C-Mn and microalloyed carbon steels are tested in such conditions.

To characterize the material resistance to the stress corrosion cracking (SCC) in H_2S medium, the standard NACE test (TM0177-96) is mainly used. It enables the determination of critical load level under which no rupture is observed. Tests are performed on smooth specimens with no surface defects except those existing after machining. Thus, crack nucleation and propagation occur on defects developed in the medium, and for which the geometry is not controlled. Nevertheless under the combined effect of stress and hydrogen promoting medium, the sensitivity to defects is an important property for steels susceptible to be used in H_2S medium. The utilization of the NACE test does not take into account such geometrical defects. New types of tests are then necessary.

The aim of this study is to develop a critical test to quantitatively determine the hydrogen embrittlement resistance of low alloyed steels, taking the defect effects into account. The proposed method consists in slow strain rate test (SSRT) or cyclic loading test near the yield strength, in these corrosion solution at different applied cathodic potentials. We use specimens with an artificial surface microdefect of controlled geometry under electrochemical and medium conditions leading to hydrogen embrittlement type damage.

The main result is to propose a new test based on local damage mechanisms and able to classify the different alloys in regard to their hydrogen embrittlement resistance.

The Interpretation of Wave Shape Effects During the Corrosion Fatigue of Anodically Polarised Steel in Sea Water. C.J. van der Wekken, M. Janssen, Delft University of Technology, Delft, The Netherlands

Environmentally induced accelerated CF crack growth in steel is generally attributed to hydrogen embrittlement of the crack tip material. Crack tip pH measurements in artificial CF cracks (in the absence of freshly exposed crack tip material) in deaerated sea water (pH~8.2), have shown that acidification of the crack tip solution (pH<7), or lowering of the pH to values close to 7, may occur under anodic polarization conditions [1]. Hydrogen ions are origination along the crack walls as a result of anodic dissolution followed by hydrolysis and hydroxide precipitation reactions. These ions mayu be transported to the crack tip as a result of the interactions of diffusion, migration, and the periodic laminar flow in the crack solution, resulting in the rapid solute transport mechanism in the crack known as Flow Enhanced Diffusion (FED) [2]. In real CF cracks the pH dependent reduction of hydrogen ions or water molecules in the crack tip region results in the adsorption of atomic hydrogen, which may be transported into the plastic zone in front of the crack tip. In the employed model the transport of hydrogen ions (or, formally, hydroxil ion vacancies where pH>7) to the crack tip is considered to be the rate determining step in the CF mechanism.

The expected effect of sinusoidal,symmetrical as well as posiive and negative sawtooth wave shapes on the CF crack growth rates under anodic polarization of steel in deaerated sea water was investigated by means of computer simulation of the transport of large numbers of hydrogen ions in order to determine the statistical probability for these ions to reach the crack tip. In the case of sinusoidal and symmetrical triangular wave shapes the assumed anodic current density distribution along the crack walls and the calculation procedures followed were similar to those described earlier for sinusoidal loading, assuming reversible laminar solution flow in the crack and in the bulk solution in front of the crack mouth (3). Particles have moved out of the crack during fatigue cycling were found to have a definite probability of rentering the crack and to still reach the crack tip. In these cases similar amounts of hydrogen ions are predicted to reach the crack tip, leading to similar crack growth rates

In the case of the asyrrnetrical sawtooth wave shapes, turbulance was assumed tooccur in front of the crack mouth during the fast parts of the cycle,causing hydrogen ions transported out of the crack to become lost in the bulk solution. Especially in the case of negative sawtooth wave shapes, only a relatively snall fraction of all hydrogen ions gmerated along the crack walls could reach the crack tiip, leading to 1ower values of the crack growth rates carpared to the symmetrical wave shapes investigated.

The correspondence between the theoretically expected behavior and experimental data reported in the literature yields further support for the employed model used earlier [3] under sinusoidal loading conditions to successfully predict behavior of the CF crack growth rate as a function of the loading frequency and the stress intensity rate ΔK.

[1] P. C. H. Ament, Ph.D. thesis Delft University of Technology, Delft, the Netherlands, 1998.
[2] C. J. van der Wekken, Proc. UK Corrosion and Eurocorr 94 Conference, Bournemouth, UK, vol.4, 1994, pp. 29-40.
[4] C.J. van der Wekken, Proc. Int. Conf. on Environmental Degradation of Engineering Materials - EDEM '99, Gdansk-Jurata, Poland, A. Zielinski, D.Desjardins, J.Labanowski, J. Cwiek Eds, Gdansk Scientific Society, Gdansk, 1999,Vol.1, pp 83 - 93

Hydrogen Cracking and Stress Corrosion Cracking of Pipeline Steels. D. Le Friant, Société du Pipeline Méditerranéenne Rhône, Villette de Vienne, France and B. Bayle, T. Magnin, Ecole de Mines de Saint-Etienne, Saint-Etienne, France

This work is based on the study of the cracking of a French oil transmission pipeline protected by a cathodic protection system. The objective is to identify field parameters, which contribute to crack propagation, and to assess changes in the operating conditions that could lead to a mitigation of the phenomenon. We have focused on the study of the micro-mechanisms by means of slow strain rate tests. In addition, cyclic loading tests were carried out to investigate cracks propagation mechanisms. Smooth and pre-notched specimens were tested at free and cathodic potential.

Hydrogen is responsible for crack advance through changes in the local steel properties. Such effects take place when two phenomenons occur: favourable conditions for hydrogen entry, i.e. a localisation of hydrogen and its effects. In particular, we have shown the essential role of a dynamic loading in promoting hydrogen entry (especially at the very crack tip) into the steel. At cathodic potential, hydrogen-related effects are strongly promoted by the presence of MnS inclusions which leads to the initiation of internal cracks (HIC) and to a SOHIC-like crack morphology. At free potential, the lesser amount of available hydrogen gives localisation-related effects a greater importance. Cracking is then related to a hydrogen-induced SCC mechanism.

Three parameters are involved in the field cracking: operating pressures variations, period of over-protection and a sensitive steels microstructure (MnS). Cathodic protection appears to be the most efficient field parameter to mitigate the phenomenon: it requires a better control of the polarisation level. Finally, a ranking test is outlined from the study of the cracking mechanisms.

Tensile Behavior of Austenitic Stainless Steels in Hydrogen Atmosphere at Low Temperatures. S. Fukuyama, D. Sun, L. Zhang, M. Wen, K. Yokogawa, National Institute of Advanced Industria, Hiroshima, Japan

Austenitic stainless steels have been widely used in hydrogen service at present and expected to be used in fuel cell vehicles for future. Thus, the materials performance should be guaranteed in

hydrogen atmosphere in the wide temperature range. However, the materials are sensitive to hydrogen environment embrittlement (HEE), especially below room temperature. In this study, the tensile behavior of the austenitic stainless steels, type 304, 304L, 316, 316LN, 316L, F316LN and 310S, was examined at the temperature range from 300 to 80 K.

Commercially available type 304, 304L, 316, 316L, 316LN, F316LN and 310S austenitic stainless steels were used. The materials were machined into cylindrical smooth tensile specimens with a gauge length of 20 mm and diameter of 4 mm and the tensile direction of the specimen was parallel to the rolling direction of the materials. Two types of heat-treatment, solution-annealed and sensitized heat-treatments were applied to types 304 and 316 specimens. The tensile testing equipment in hydrogen atmosphere at low temperatures was originally developed by the authors. The equipment was composed of a pressure vessel to hold a specimen in hydrogen atmosphere, which was cooled down by liquid nitrogen. Tensile load was applied by the pull rod connected with the hydraulic actuator through the pressure vessel wall. As HEE occurred on the strain-induced martensite, the magnetic property of the fractured specimen was examined to identify the strain-induced martensite. Fracture surfaces of the specimens were observed by a scanning electron microscope.

Hydrogen showed marked effect on the tensile properties of type 304, 304L, 316, 316L, 316LN and F316LN stainless steels, and no effect on those of type 310S stainless steel. The order of HEE was observed as 304>304L>316>316LN>316L>F316LN>310S. HEE of the materials increased with decreasing temperature, reached a maximum at around 200 K and decreased rapidly with decreasing temperature down to 80 K. HEE of the materials also increased with increasing hydrogen pressure. Sensitization of type 304 and 316 stainless steels increased the susceptibility and decreased the minimum HEE temperature. Brittle fracture along the strain-induced martensite lath was observed in the soluted specimen, while grain boundary fracture was found in the sensitized specimen. The formation of the strain-induced martensite increased with decreasing temperature and Ms decreased with increasing Ni equivalent of the specimen. It was discussed that HEE of the materials from room temperature to the maximum HEE temperature depended on the transformation of strain-induced martensite and the behavior below the maximum HEE temperature depended on the diffusion of hydrogen. It was also discussed that the effect of strain-induced martensite on HEE of the materials.

The Influence of the Surface layer of the Carbon Steel While Its Cycle Deforming on the Hydrogen Absorption and Fatigue Strength. V.A. Slezhkin, S.M. Beloglazov, University of Kaliningrad, Kaliningrad, Russia

The greater part of electroplating is determined for corrosion protection of steel. But the mechanical properties of base material impaired by any electrochemical process with hydrogen evolution that absorbs by steel and deposited metal. Especially this phenomenon is characteristic for nickel coatings. In particular, the nickel plating reduce very strong fatigue failure resistance of high-strength steels due to hydrogen and high tension residual stresses in the coating.

The present paper is dedicated to studying fatigue resistance high-strength spring steel (composition, %: 0,62 C; 0,98 Mn; 0,32 Si and 0,2 Cr) deteriorated by hydrogen absorption in chemical and electrochemical nickel plating processes and forming of residual stresses in coating and role of these factors in decreasing fatigue strength of steel.

Electrochemical deposition of a nickel was performed from sulphate bath, modified with organic components, with composition, g/*l*: $NiSO_4 \cdot 7H_2O$ - 140; $Na_2SO_4 \cdot 10H_2O$ - 40; $MgSO_4$ - 25; H_3BO_3

-20; NaCI - 5; pH=4.8 to 5.0 T = (293 to 353) K. A chemical nickel plating was performed in the following solution, g/*l*: $NiCI_2$ - 30; NaH_2PO_2 -15; CH_3CONa - 15; pH= 4.to 5.0; T=(360 to 365) K. Hydrogen concentration in steel was measured by anodic-photometric method. Residual stresses were measured by a method of a flat strip cathode that bends by action of residual stresses in the coating with automatic registration of steel strip deformation by use of differential-tranformer bridge. The fatigue multicyclic tests were performed by use of flat steel specimens with electrocmemical or chemical deposited Ni- coating with electromagnetic excitation at the basic frequency of 90 Hz. Wöhler curves were obtained.

The following results were received: Both chemical and electrochemical nickel plating processes produce an irregular steel saturation by hydrogen. The basic contents of hydrogen comes in the surface layer with the thickness 40 to 50 μm. The most intensive steel saturation with hydrogen takes place at an electrochemical nickel plating. The concentration of hydrogen in a near-surface layer with the thickness 10 μm at an electrochemical nickel plating is approximately in 3 times higher, than at a chemical nickel plating. The residual stresses in nickel coatings formed both in chemical and in electrochemical processes and reach accordingly 280 and 420 MPa. The decrease of fatigue resistance of steel is caused basically by absorption of hydrogen by the steel base. Ours investigations demonstrated that tensile stress in nickel coating causes its fissure, that reduce fatigue resistance of plated steel to a lesser degree, than hydrogen.

Heat treatment of nickel-plated specimens, as a rule, brings about on increase of fatigue resistance of specimens with electrochemical coating and strength decrease of chemical plated specimens. The hydrogen absorption by steel base in electrochemical nickel plating can be essentially reduced by the introducing in an electrolyte benzyltributylammonium chloride. The fatigue resistance of plated steel specimens increases by 23 % as contrasted to that by nickel plating in an electrolyte without the additives.

Fatigue Behavior of the High Strength Steel SE702 in Vacuum, Air and NaCl Solution. B. Huneau, J. Mendez, LMPM-ENSMA, Futuroscope Chasseneuil, France

High strength steels are known to exhibit a higher susceptibility to hydrogen embrittlement than conventional construction steels. It is therefore of great importance to study their fatigue resistance in different environments, in order to understand the interactions between a mechanical loading and an aggressive environment.

In the last twenty years, interactions between deformation and hydrogen effects have been particularly investigated and several models have been proposed. Experimentally, the effects of corrosive environments are frequently characterized by comparison with fatigue results obtained in air. However, it is well-known that fatigue lives of most metals tested in air are considerably reduced when compared to tests performed in vacuum or in inert gases. This reduction is attributed to hydrogen embrittlement due to the water vapor dissociation. A high vacuum or an inert atmosphere must therefore be used to characterize the intrinsic behavior of materials.

This paper reports results of fatigue damage mechanisms of the high strength steel SE702 (A517 type) in vacuum (10^{-4} Pa), ambient air and in a 3.5% NaCl solution under a cathodic potential (-1050 mV/SCE). These aqueous environment conditions are defined according to the use of the SE702 in offshore platforms which are cathodically protected.

The effects of the environment were studied through the effects on the fatigue resistance: cylindrical specimens were tested at two load ratios (R=0.1 and R=-1) for two frequencies (20Hz

and 0.17Hz). Particular attention was given to the frequency effect in air. The resulting S-N curves show a strong influence of environment for the two load ratios: fatigue lives in air are strongly reduced compared to the vacuum and the fatigue results in NaCl solution also show a reduction compared to results obtained in air. This reduction is less pronounced than between air and vacuum, that means that ambient air is a particularly aggressive environment for this steel.

The initiation conditions have also been established as well as the crack growth rate of self initiated cracks. The relative influence of the three environmental conditions on the initiation stage, surface crack density and propagation rate have been quantified. The roles of the different environments are analyzed through the fracture surface morphologies. Depending on the test conditions (environment, applied stress, frequency), cracking mechanisms appear to be very different: transgranular, intergranular or quasi-cleavage cracking modes have been observed. Some specific experiments are also performed, in the NaCl solution, to separate the effect of internal hydrogen in the bulk material and external hydrogen at the crack tip. Finally the role of the oxide layer on specimens tested in air is discussed, by comparison with specimens tested in NaCl solution in which the oxide layer is reduced by the cathodic protection.

Moisture-Induced Embrittlement of B2-type CoTi Ordered Intermetallics. Y. Kaneno, T. Takasugi, Osaka Prefecture University, Osaka, Japan

At room temperature, the moisture-induced embrittlement of B2-type CoTi ordered intermetallics, which show excellent mechanical properties at high temperature as well as chemical properties at ambient temperature, was investigated on hot-rolled and annealed materials. Tensile tests were performed as functions of testing atmosphere (vacuum and air) and strain rate, and also SEM fractography was investigated. It was observed that the tensile elongation and UTS depended upon the environmental media. Higher elongation and UTS values were observed in the materials deformed in vacuum than the materials deformed in air, indicating that moisture-induced embrittlement occurred in CoTi ordered intermetallics. CoTi ordered intermetallics contain Ti as reactive element by which H_2O in air can be decomposed into atomic hydrogen according to a reaction Ti + $2H_2O$ E. TiO_2 + 4H. Thereby, atomic hydrogen can be released into material interior. It is suggested that the subsequent micro-processes of permeation, migration and condensation of atomic hydrogen to grain boundaries or lattices result in the reduced tensile elongation and UTS.

Evaluation of Electrolytic Hydrogenation Influence on Fatigue Crack Growth Resistance of High-Strength Steels. .I. Balitskii, V.I. Pokhmurskii, O.O. Krohmalny, National Academy of sciences of the Ukraine, Lviv, Ukraine

It has been earlier investigated, that hydrogenation from gas phase involves significant reduction of 8Mn8Ni4Cr steel time to failure in constant load tests. At the same time it has been established low influence of contact with gas hydrogen on static and cyclic crack resistance of high-nitrogen 18Mn18Cr type of steel. In practice take the place electrolytic hydrogenation of steels due to excess of cathodic protection, increase of solution acidity in crevices and pores, contact with more electronegative materials.

Wohler's S-N curves were obtained on the bar-type specimens with a gage diameter 5 mm and length 10 mm, tested in air and 26% H_2SO_4 solution during electrolytic hydrogenation by cathodic current density 100 A/m^2.

The fatigue strengths of 18Mn18Cr and 8Mn8Ni4Cr steels reduce accordingly to 168 and 127 MPa comparatively to the tested in air accordingly 436 and 218 Mpa. Ratios of media influence equal 6.5 and 41.7% of steels 18Mn18Cr and 8Mn8Ni4Cr. It shows that electrolytic hydrogenation exerts more influence on fatigue resistance of 18Mn18Cr than 8Mn8Ni4Cr steel. It is well known that hydrogen makes heavier the elastic sliding in metal by increasing of strains of initial stage of elastic deformation. Atoms of hydrogen diffuse to active sliding planes (it is more advantageously thermodynamically), prevent from dislocation motion and lead to yield stress increasing. Difficulties for elastic sliding in the materials due to hydrogen presence cause initiating critical dislocation density on more early stages of deformation than without hydrogen. It involves crack initiating at lower external stresses. Increasing chromium-manganese steels resistances to tangential stresses action under hydrogen influence prevent from dulling of crack tip during its growth.

On macrogeometry of fracture surfaces of the specimens some steps typical for hydrogen embrittlement of materials with high elasticity reserve are obvious. Fatigue crack starts from superficial metal layers embrittled by hydrogen. Finale stage of destruction (in the specimen core) happens under tangential stresses action at angle of 45° to normal stresses direction. Electrolytic hydrogenation enhances the range of microbrittle fracture of chromium-manganese steels. High-nitrogen 18Mn18Cr steel shows transgranular fracture and 8Mn8Ni4Cr steel shows a mixed fracture character with transgranular domination.

Prevention of Hydrogen Embrittlement and Corrosion of Steels in Aqueous Salt Media with SRB by Industrial Organic Additives. S.M. Beloglasov, A.A. Myamina, E.M. Kondrasheva, University of Kaliningrad, Kaliningrad, Russia

The hydrogen absorption (HA) by mild steel (ca. 0.1%C), ferritic-pearlitic steel with 0.8% C, 0.3% Mn and 0.2% Si and two kinds of stainless steels-martensitic (ca. 13%Cr, 2%Ni and 0.25%C) and austenitic X5CRNI 18.10 in corrosion processes in standardised microbiological Postgate B medium ($g \cdot L^{-1}$: NaCl 7.5; $MgSO_4$ 1.0; Na_2SO_4 2.0; Na_2CO_3 1.0; NaH_2PO_4 0.5, calcium lactate 2.0) with sulfate reducing bacteria (SRB) are studied. The SRB develop rapidly in anaerobic situations, covering steel with insoluble FeS and depolarising the cathodes of local corrosion cells on the steel surface by involving H_{ad} in their metabolism for catalytic interaction with sulfate ions: $10\ H + SO_4^{2-} = H_2S + 4H_2O$. In our study Desulfovibrio Desuluricans was isolated from river sediments by repeated subculturing in Postgate B medium.

Hydrogen sulfide acts as a strong stimulator of HA by steel surface layer that results in considerable loss of mechanical properties of the metal. In this work the HA by corroded steel was studied with the aid of an anodic dissolution technique. This permits the hydrogen content in steel to be obtained as a function of depth in the metal. In this work the anodic dissolution of steel after exposure in corrosion media at 310 K was made in small steps by ca. 10 μm of dissoluted steel layer with absorption-spectrometric determination of H, evolved from steel.

Despite the thick deposit of iron sulfides covering the steel, the hydrogen came from the cathodic corrosion reaction and appeared at the steel surface as H_{ad}. A large quantity of H_{ad} is absorbed by steel subsurface layer. The HC of the 25 μm subsurface layer the all tested steel runs to 40 ppm after corrosion 200 h in specified above medium. The experimental evidence points to the fact that existence of H_2 traps in the subsurface steel layer prevents the deeper penetration of H diffusing into the steel. Molecularisation of H atoms on the trap surface results in a increase of p_{H2} in them. Further H diffusion into the steel depth then has to take place through the stressed and

strained metal around the traps and goes slightly. But the strenght-related properties of metals are determined by the relative thin subs-urface layer.

Hydrogen absorption by steel with a cold worked ferritic-pearlitic structure produced considerable decay of steel plasticity (testing by torsion twisting of wire samples Ø 1.0 mm from carbon steel of type 8A). Both the stainless steels undergo the deterioration of endurance limit by dead load to 75 or 90% from limited loading. It is found that the integral hydrogen content of steel (IHC) is linearly proportional to the corrosion rate K and quantity of bacterial cells N in the corrosion medium. The IHC of the steel subsurface layers was less in specimens, corroded in aqueous salt medium containing special organic compounds with inhibiting corrosion and HA efficiency. The graphs IHC-K and IHC-N made for each inhibitor in conc. range 1.to 15 mM, have a different slope to K and N axis because the compounds efficiency as corrosion inhibitor, HA inhibitor and biocide on SRB varies greatly with molecular structure of organic compounds. The most effective compounds are patented by us for use as corrosion and HA-inhibitor with biocide action.

Thursday Evening, September 26, 2002
Session IX: High Temperature Stress Corrosion Cracking

Interactions of Hydrogen with Moving Dislocations in Nickel and Nickel Base Alloys-Consequences on the Intergranular Rupture. J. Chêne, A.M. Brass, Université Paris-Sud, Orsay, France

The kinetics of hydrogen assisted crack initiation and growth has been often related to a deformation assisted transport of hydrogen to critical failure sites in the material. The hydrogen enrichment of critical sites is alternatively considered to be a consequence of the interaction of hydrogen with elastic stress fields or of hydrogen-dislocation interactions in the plastic zone. The later have been recently shown to play an important role in the environmental degradation of numerous engineering materials. Dislocation sweeping of hydrogen and the stripping of solutes from moving dislocations by traps and by the annihilation of hydrogen containing dislocations have been proposed for a long time as a mechanism controlling the hydrogen enrichment. More recently hydrogen atmospheres have been shown to play a determinant role on the motion of dislocations and their interaction with other defects. Whereas numerous studies support the existence of hydrogen-dislocation interactions very few experimental data are available to characterize both the long range dislocation transport of hydrogen and the effect of hydrogen on the dislocation motion. Such data are missing for any predictive analysis of the hydrogen assisted crack growth rate in engineering materials.

This paper will review recent experimental studies of the interaction of hydrogen with mobile dislocations in fcc materials (nickel and Ni base alloys).The monitoring of tritium desorption from tritiated single crystals during tensile straining gives direct evidence of hydrogen accelerated transport by moving dislocations and allows to get quantitative data on this long range transport mechanism and on a possible local supersaturation. The effect of hydrogen concentration on the mechanical behavior (planar glide, critical resolved shear stress,...) has been investigated simultaneously. Similar measurements performed on polycrystals together with investigations of the effect of temperature, strain rate, and grain boundaries disorientation on H induced intergranular cracking allow to evidence the effect of hydrogen transport by dislocations to grain boundaries on the intergranular rupture.

These experimental results are compared with computed values used to define the temperature and strain rate ranges over which dislocation transport may be efficient in nickel base alloys. Some conclusions can be drawn about the role of transient effects associated with dislocation transport on the hydrogen embrittlement and stress corrosion cracking susceptibilities of Ni base alloys.

The Effect of Hydrogen on Creep in High Purity Ni-16Cr-9Fe Alloys at 360°C. D.J. Paraventi, General Electric Corporate Research and Development Center, Schenectady, NY, USA, T.M. Angelius, G.S. Was, University of Michigan, Ann Arbor, MI, USA

Environmentally assisted cracking involves synergistic interactions between corrosion and deformation processes. This study focused on providing insight into the influence of environment on time dependent deformation of Ni-16Cr-9Fe in argon, dissociated hydrogen, and primary water environments at 360°C. Results from experiments conducted in dissociated hydrogen or primary water showed enhancements in both primary and secondary creep over those conducted in argon. Experiments begun in argon gas exhibited positive strain transients when dissociated hydrogen gas was introduced during steady state creep. These results indicate a strong effect of hydrogen on the primary and transient creep behavior of this alloy at 360°C. The environmentally enhanced creep is attributed to a mechanism involving the collapse of dislocation pileups due to the presence of hydrogen. The mechanism is supported by detailed experiments that revealed lower internal stresses and activation areas in primary water than in argon. Changes in the primary creep behavior due to hydrogen are consistent with a change in the work hardening behavior observed in similar alloys. An increase in the steady state creep rate is likely due to a combination of mechanisms that involve hydrogen.

Constituitive Deformation Model for Analysis of Stress Corrosion Crack Tip Strain Rates in Ni-Cr-Fe Alloy 600. M.M. Hall, Jr, D.M. Symons, Bettis Atomic Power Laboratory, West Mifflin, PA.

There is general consensus that stress corrosion crack growth rate (SCCGR) is fundamentally related to crack tip strain rate. However, little has been written on how a material's deformation rate behavior may influence the stress and temperature sensitivities of the SCCGR. In two previous papers we developed a Hydrogen Assisted Creep Fracture (HACF) model for low potential stress corrosion cracking of nickel base alloys in an aqueous environment. This phenomenological model was developed using a constitutive equation for plasticity that was developed by Kocks et al. to describe deformation due to the thermally activated glide of dislocations. With this constitutive equation, the effects of yield stress and strain hardening on the SCCGR stress and temperature sensitivities were modeled. As predicted by the model and observed in the data, 1) the stress sensitivity of the SCCGR decreases with both increasing yield stress and increasing temperature and 2) the apparent thermal activation energy for the SCCGR decreases with both increasing applied stress intensity factor and increasing yield stress. These results were found to hold for cracks that propagate on planes that lie parallel to the principal metal working direction for cold worked Alloy 600. Data obtained on specimens having cracks growing perpendicular to the principal metal working direction show significantly different stress and temperature sensitivities of the SCCGR, which was identified as an area for additional development of the HACF model.

In this paper we extend the constitutive equation for plasticity to include the effects of orientation and dynamic strain aging on the crack tip strain rate. The resulting deformation rate equation is used to extend the HACF model to account for the effects of crack orientation and dynamic strain aging on the stress and temperature sensitivities of the SCCGR. Tensile flow stress data obtained

for two orientations of cold worked Ni-Cr-Fe Alloy 600 are presented showing the effects of orientation and level of cold work, carbon concentration and temperature on the strain aging response. These deformation data and the extended HACF model are used to correlate SCCGR data obtained on cold worked Alloy 600 having a range of yield stresses, carbon concentrations and for crack growth orientations that are both parallel and perpendicular to the principal metal working direction. The results show that orientation-dependent strain aging effects on the crack tip strain rate can account for the effects of orientation on the stress and temperature sensitivities of the SCCGR.

Some Uses of Slow Strain Rate Testing Under Applied Potential Control in Studying SCC of Materials Used in Nuclear Power Plant. J. Congleton, E.A. Charles,University of Newcastle, Newcastle upon Tyne, United Kingdom

Work performed at Newcastle has shown that the stress corrosion cracking of iron base alloys, stainless steels and nickel based alloys exposed to high temperature water environments is influenced by the electrode potential existing at the specimen surface. In nuclear coolant environments under free corrosion conditions this is strongly influenced by the dissolved oxygen content of the water. However, a range of water chemistry conditions can be modeled in the laboratory by utilising small static or refreshed autoclave systems and potentiostatic control of the specimens. Rector pressure vessel steels crack during slow strain rate tests in simulated light water reactor environments, but only if the conditions generate high (anodic) potentials or if such potentials are applied by some external means. SCC during slow strain rate testing can be induced in pure iron and a wide range of iron base alloys by testing under applied potential control. Susceptibility to cracking is influenced by water temperature, the inclusion content of the steel, the electrode potential, the applied strain and the crack-tip strain rate. Cracks often initiate at sulphide inclusions but can also be initiated at slip-steps and/or corrosion pits. Sulphate contamination of the water enhances cracking for low sulphur content alloys but has little effect if the alloy already contains many sulphide inclusions. Data has been obtained showing that the SCC of various stainless steels, alloy 600 and alloy 690 is also influenced by the electrode potential of the samples. The usefulness of such experiments for providing a semi-quantitative measure of safety and for studying the mechanism of cracking will be discussed.

Hydrogen Dislocation Interactions During Cyclic Plastic Deformation and Static Strain Ageing Tests in Single Crystals and Polycristals of Ni and Its Alloys. C. Bosch, G. Girardin, D. Delafosse, T. Magnin, Ecole National Supérieure des Mines de Saint-Etienne, Saint-Etienne, France

Among the numerous modeling and experimental studies of hydrogen effects in engineering systems, many recent contributions point out a mechanism of “enhanced” and “localised” plastic deformation caused by the screening of stress centres by segregation of solute hydrogen. Numerical studies of this mechanism are limited so far to elementary configurations of parallel edge dislocations en 2 dimensions. The well established HELP model and CEPM which is particularly adapted for quantitative description of SCC and CF of materials, take into account these hydrogen dislocation interactions. On the other hand, several experimental observations of a localisation of plastic deformation associated to hydrogen diffusion were recently performed and have nourished an already debate on the “softening” versus “hardening” of metals by hydrogen. Experimental studies on this issue are indeed mainly focussed on fcc metals or alloys, where the macroscopic flow stress is governed by collective behaviour of dislocations, and where “two-dislocations” mechanisms have a very indirect influence on the tensile behaviour. Such mechanisms not only involve elastic pair interactions, but also “reactions” between dislocations such as multiplication, annihilation and cross-slip.

This paper presents two experimental studies specifically aimed at investigating the effect of precharged hydrogen on the collective behaviour of dislocations in fcc nickel and its alloys. The first is based on the particular microstructure of deformation, well defined and characterised, obtained in cyclic plastic deformation of nickel single crystals oriented for single slip. A decrease of the cross slip ability in presence of hydrogen leads to different cyclic stress-strain curves according to the hydrogen content. In the low strain amplitude domain, saturation stress is reached faster in presence of hydrogen. Such effect results from a new equilibrium between bundles and mobile screw segments between the veins, which leads to a lower value of the saturation stress. In the plateau region when PSB are formed, a softening effect due to hydrogen is observed whatever the applied strain amplitude. It can be explained in terms of decrease of the internal shear stress in PSB walls, which induces a decrease of the saturation stress.

The second explores the phenomenon of static and dynamic strain ageing in polycrystalline Ni and Ni-16%Cr like a marker of hydrogen dislocation interactions. The careful comparison of experimental stress transients obtained after static ageing at low temperature with the most recent models based on the evolution of mobile and forest dislocation densities allows for an evaluation of the role of hydrogen on different mechanisms influencing the tensile flow stress at room temperature. The respective contributions of solute dragging, increased multiplication of mobile dislocations, and forest density evolution are quantitatively reviewed. Conclusions may be drawn concerning the role of hydrogen on the plastic behaviour of fcc alloys.

Oxidation Induced Intergranular Cracking in Nickel Base Alloys in the Temperature Range 400°C to 600°C. L. Fournier, B. Capell, G.S. Was, University of Michigan, Ann Arbor, MI, USA, and T. Magnin, Ecole Nationale Supérieure des Mines de Saint-Etienne, Saint-Etienne, France

It is well established that nickel base alloys experience intergranular stress corrosion cracking (IGSCC) in hot water such as in the primary water of pressurized light water reactors. However, the mechanisms that control this process are not clearly understood. Recent observations that nickel base alloys are also sensitive to IGSCC in supercritical water (T>374°C and P>22.1 MPa), i.e. in an environment where the corrosion process is controlled by oxidation rather than by ionic mechanisms (coupled cathodic and anodic reactions) suggest that an oxidation-induced intergranular cracking process may be responsible for IGSCC of nickel base alloys in hot water around its critical point.

At temperature typically higher than 1000°C, the oxidation-induced intergranular cracking behavior of nickel and its alloys is well documented. Grain boundary penetration by oxygen is known to be responsible for the embrittlement effect. At lower temperature, nickel base alloys are also sensitive to oxidation-induced intergranular cracking but very little is known about the cracking process. The objective of this study was therefore to gain a better understanding of the mechanisms that may control the oxidation-induced intergranular cracking process in nickel base alloys in the temperature range 400ºC to 650ºC.

Two different types of experiments were performed. First, the possible continuity in the oxidation-induced intergranular cracking mechanism of nickel base alloys was examined over a wide range of temperatures. Constant extension rate tensile (CERT) tests were carried out at $5x10^{-7}$ s^{-1} in air and under vacuum ($2x10^{-9}$ MPa) on nickel base superalloy 718 in the temperature range 400°C to 650°C. Above 500°C, oxidation-induced intergranular cracking resulted in an important loss of ductility in air in comparison to vacuum, as well as in a transition from intergranular cracking in air to transgranular cracking under vacuum. Below 470°C, the Portevin-

Le Chatelier effect occurred, leading to shear fracture and the disappearance of the environmental effect.

In parallel, the oxidation-induced intergranular cracking behavior of ultra high purity Ni-xCr-9Fe-C alloys was investigated in controlled oxygen partial pressure steam environment. CERT tests were performed at 3 x 10^{-7} s^{-1} in hydrogenated steam at atmospheric pressure, and at H_2/H_2O ratios that result in free energies above and below the Ni/NiO equilibrium at 360°C, 400°C and 550°C. Results at 550°C show a significant decrease of the fracture strain of the Ni-16Cr-9Fe-C alloy tested in the NiO stable region, in comparison to the same alloy strained in the Ni stable region. These results are in good agreement with those obtained on nickel base superalloy 718. CERT tests in hydrogenated steam at 360°C and 400°C are being currently performed.

Author Index

Aaltonen, P. 2
Abramov, E. 41
Adams, D.P. 56
Aguilar, A. 58
Akid, R. 29
Albarran, J.L. 26,27,37,57,58
Alexandreanu, B. 30
Al-Faqeer, F.M. 22
Alyferenko, T.D. 8
Angelius, T.M. 68
Anteri, G. 44
Aravas, N. 53
Archakov, Yu I. 3
Artchakov, I.Yu. 8
Atrens, A. 36

Bach, H. 33
Bahr, D.F. 4, 54
Bajaj, R. 5
Balitskii, A.I. 65
Barker, J. 54
Baskes, M.I. 32
Bastasz, R. 17
Bates, D.W. 47
Bayle, B. 23,28,37,60,62
Beduli, E. 42
Beloglasov, S.M. 63,66
Betakova, P. 45
Bhat, B.N. 38
Boellinghaus, T. 52
Bosch, C. 28,60,69
Bouzina, A. 40
Braham, C. 40
Brass, A.M. 15,20,58,67
Bridges, R.L. 54
Brooks, J.A. 56
Bruzzoni, P. 44
Bullock, J.S. 54

Cadden, C.H. 36
Capell, B. 70
Casales, M. 37
Castello" P. 4
Causey, R.A. 9,54
Chapman, G.K. 5
Charles, E.A. 69
Chateau, J.P. 37
Chêne, J. 15,58,67
Chiba, Y. 11
Christ, H.-J. 51
Congleton, J. 69
Cordoba, R.J. 44
Cowgill, D.F. 55

Dagbert, C. 45
Danielson, M.J. 22
Daugela, A. 57
Daum, R.S. 47
Dauskardt, R.H. 24
Deakin, J. 30
Decker, M. 51
Delafosse, D. 28,37,69
Dickson, J.I. 1
Dietzel, W. 12,26
Dornheim, M. 15

El-Amoush, A.S. 46
Eliaz, N. 11,42,49
Eliezer, D. 10,11,41,42,49

Field, D.P. 4
Floro, J. 56
Fournier, L. 70
Froes, F.H. 41,49
Fuks, D. 11
Fukuyama, S. 43,62

Gadgil, V.J. 40
Galland, J. 45
Gamboa, E. 36
Gangloff, R.P. 21,50
Gelles, D.S. 5
Gentz, S. 36
Gerberich, W.W. 53,54,57
Girardin, G. 69
Gonzalez, G. 26
Gonzalez-Rodriguez, J.G. 37
Goods, S.H. 55
Grethlein, C.E. 38
Gross, K.J. 55
Guthrie, S.E. 42
Gutmanas, E.Y. 41

Habashi, M. 7
Hall, M.M. 68
Han, E-H. 18
Hanninen, H. 2,4,39,51,
Hanrahan, R.J. 47
Hazarabedian, A. 44
Hoagland, R.G. 32
Hu, H. 29
Huneau, B. 64
Hurless, B. 36
Hyspecka, L. 45

Ichitani, K. 12

Jackson, M. 36
Janssen, M. 61
Jiang, C.B. 9
Jones, R.H. 22
Juilfs, G.G. 12,26
Jung, P. 34
Jungk, J. 53,57

Kaneno, Y. 65
Kanno, M. 12,25
Katz, Y. 57
Ke, W. 18
Kefferstein, R. 37
Khachaturyan, A.G. 32
Kharin, V. 27
Kim, I.S. 38
Kirchheim, R. 15,20
Kofmann, B. 41
Kolman, D.G 21
Konakov, V.G. 8
Kondrasheva, E.M. 66
Koss, D.A. 47
Köster, U. 42
Krohmalny, O.O. 65
Kulkarni, S.D. 40
Kuramoto, S. 12,25

Lalonde' S. 1
Lang, D.M. 41
Lédion, J. 40
Lee, J.A. 8
Lee, S.G. 38
LeFriant, D. 62
Leinonen, H. 39
Leitch, B.W. 47
Lensing, C. 13
Li, H. 9

Liang, Y. 53
Liu, C. 34
Liu, Z. 59
Longaygue, X. 60
Lopez, H.F. 27,57,58
Louthan, M.R. 6
Lucas, J.P. 59
Ludtka, G.M. 54
Luo, X.-H. 7
Luppo, M.I. 44
Lynch, B. 30
Lynch, S.P. 1

Magnin, T. 23,28,37,60,62,69,70
Majzoub, E.H. 55
Malhotra, S.N. 40
Malyshev, L.G. 46,58
Maroef, I. 13
Martinez, L. 26,27,3757,58
McPherson, W.B. 38
Mehboob, A. 27
Meletis, E.I. 19
Mendez, J. 64
Meyer, B. 32
Mingol, N. 44
Moody, N.R. 54,56
Morasch, K.R. 4
Moreno, D. 10
Morgan, M.J. 5
Motta, A.T. 47
Myamina, A.A. 66

Nagumo, M. 24
Newman, G.W. 48
Newman, R.C. 30
Nguyen, D.C. 5
Novotny, R. 8,60
Nozue, A. 11,15

Ohno, T. 35
Okahana, J. 25
Olson, D. 13,41,49
Ortiz, M. 44
Ovejero, E. 27
Ovejero-Garcia, J. 44

Paraventi, D.J. 68
Patankar, S.N. 41
Patu, S. 9
Petrov, A.S. 14
Pevzner, B.Z. 8
Pfuff, M. 12,26
Pickering, H.W. 22
Pokhmurskii, V.I. 65
Politi, A. 44
Pound, B. 23
Powell, G.L. 54
Prüßner, K. 51
Puls, M.P. 47
Pundt, A. 15

Qazi, J.I. 41,49

Rahim, J. 41
Raja, V.S. 40
Raman, R. 40
Ricker, R.E. 1931
Risson, E. 37
Roberge, R. 1
Robertson, I.M. 24,53
Robinson, S.L. 36
Rodriguez, M. 56
Romero, J.A. 56
Rosanvallon, S. 15

Sagat, S. 48
Sajdl, P. 8,60
Salinas-Bravo, V.M. 37
Scarth, D.A. 48
Schindler, I. 45
Schlogl, S.M. 33
Schneeweiss, O. 8
Schosger, J.-P. 4
Schwarz, R.B. 32,33
Scully, J.R. 17,21,50
Senemmar, A. 51
Senkov, O.N. 41,49
Serna, S. 26
Shamruk, V.G. 46,58
Shi, S.-Q. 47
Shipilov, S.A. 29
Shuai, M.B. 41
Skryabina, N.E. 14
Skrypnyk, I. 16
Slezhkin, V.A. 63
Smugeresky, J.E. 56
Snead, L.L. 9
Sofronis, P. 53
Sojka, J. 45
Soman, S.N. 40
Somerday, B.P. 36,55,56
Sozanska, M. 45
Spivak, L.V. 14
Spooner, S. 54
Su, Y.J. 41
Sugawara, T. 24
Suh, D. 24
Sun, D. 62
Symons, D.M. 68

Takai, K. 11,15
Takasugi, T. 65
Tamaoki, T. 24
Tanguy, D. 23
Tarasenko, O. 2,4,51
Tateyama, Y. 35
Teter, D.F. 47,53
Teysseyre, S. 37
Thompson, A.W. 1,5
Toribio, J. 27
Tosten, M.H. 5
Tuggle, D. 33
Tvrdy, M. 45
Tymiak, N.I. 53,57

Vander Giessen, E. 33
Vander Wekken, C.J. 61
Vasudevan, A.K. 19
Venhaus, T.J. 9
Venkatramanian, A. 59
Verniquet, É. 1
Vesely, E.J. 38
Vigna, G. 44
Virkkunen, I. 39
Vosta, J. 8,60
Wampler, W.R. 9
Wang, Z.H. 41

Was, G.S. 30,68,70
Watwood, M. 36
Wei, R.P. 25
Wen, M. 43,62
West, S.L. 5
Wetteland, C.J. 47
Whaley, J.A. 17
Wilson, K.L. 54
Wolfer, W.G. 32,42
Woodcock, C.L. 4
Wu, S. 41
Wu, S.D. 9
Wyrobek, T. 53

Xu, X. 43

Yagodzinskyy, Y. 2,4,51
Yamada, D. 15
Yao, Z. 34
Yokogama, K. 43,62
Young, G.A. 17,21
Young, L.M. 21

Zander, D. 41,42,49
Zhang, , B. 18
Zhang, L. 62
Zhang, Z.G. 18
Zhao, P.J. 41

NOTES

NOTES

NOTES

NOTES

NOTES